การพัฒนาอุปกรณ์วิเคราะห์ของไหลจุลภาคสำหรับการตรวจวัดโลหะหนัก

นายสุดเขต ไชโย

วิทยานิพนธ์นี้เป็นส่วนหนึ่งของการศึกษาตามหลักสูตรปริญญาวิทยาศาสตรดุษฎีบัณฑิต
สาขาวิชาเคมี ภาควิชาเคมี
คณะวิทยาศาสตร์ จุฬาลงกรณ์มหาวิทยาลัย
ปีการศึกษา 2558

DEVELOPMENT OF MICROFLUIDIC ANALYTICAL DEVICE FOR DETERMINATION OF HEAVY METALS

Mr. Sudkate Chaiyo

A Dissertation Submitted in Partial Fulfillment of the Requirements
for the Degree of Doctor of Philosophy Program in Chemistry
Department of Chemistry
Faculty of Science
Chulalongkorn University
Academic Year 2015

Thesis Title	DEVELOPMENT OF MICROFLUIDIC ANALYTICAL DEVICE FOR DETERMINATION OF HEAVY METALS
By	Mr. Sudkate Chaiyo
Field of Study	Chemistry
Thesis Advisor	Professor Orawon Chailapakul, Ph.D.
Thesis Co-Advisor	Associate Professor Weena Siangproh, Ph.D. Amara Apilux, Ph.D.

Accepted by the Faculty of Science, Chulalongkorn University in Partial Fulfillment of the Requirements for the Doctoral Degree

.....Dean of the Faculty of Science
(Associate Professor Polkit Sangvanich, Ph.D.)

THESIS COMMITTEE

.....Chairman
(Associate Professor Vudhichai Parasuk, Ph.D.)

.....Thesis Advisor
(Professor Orawon Chailapakul, Ph.D.)

.....Thesis Co-Advisor
(Associate Professor Weena Siangproh, Ph.D.)

.....Thesis Co-Advisor
(Amara Apilux, Ph.D.)

.....Examiner
(Assistant Professor Suchada Chuanuwatanakul, Ph.D.)

.....Examiner
(Associate Professor Nattaya Ngamrojanavanich, Ph.D.)

.....External Examiner
(Associate Professor Pornpimol Muangthai, Ph.D.)

สุดเขต ไชโย : การพัฒนาอุปกรณ์วิเคราะห์ของไหลจุลภาคสำหรับการตรวจวัดโลหะหนัก (DEVELOPMENT OF MICROFLUIDIC ANALYTICAL DEVICE FOR DETERMINATION OF HEAVY METALS) อ.ที่ปรึกษาวิทยานิพนธ์หลัก: ศ. ดร.อรวรรณ ชัยลภากุล, อ.ที่ปรึกษาวิทยานิพนธ์ร่วม: รศ. ดร.วีณา เสียงเพราะ, ดร.อมรา อภิลักษณ์, 112 หน้า.

งานวิจัยนี้มีจุดมุ่งหมายเพื่อพัฒนาอุปกรณ์วิเคราะห์ของไหลจุลภาคสำหรับการตรวจวัดโลหะหนัก ซึ่งสามารถแบ่งออกเป็น 3 ส่วน โดยส่วนแรกคือ การพัฒนาอุปกรณ์วิเคราะห์ของไหลจุลภาคบนฐานกระดาษเชิงสีโดยอาศัยการเร่งการสลายของไทโอซัลเฟตกับนาโนเพลตของเงินสำหรับการวิเคราะห์ทองแดง ซึ่งอุปกรณ์ชนิดนี้มีความไวและมีความจำเพาะเจาะจงสูงในการวิเคราะห์ทองแดงมากกว่าไอออนโลหะอื่น ๆ รวมไปถึงสามารถเห็นการเปลี่ยนแปลงสีด้วยตาเปล่า ซึ่งมีขีดจำกัดในการวิเคราะห์ในระดับ 0.3 นาโนกรัมต่อมิลลิลิตรและมีช่วงความเป็นเส้นตรงคือ 0.5 - 200.0 นาโนกรัมต่อมิลลิลิตรโดยการวิเคราะห์ด้วยโปรแกรมอิมเมจเจ ส่วนที่สองคือ การวิเคราะห์ตะกั่ว แคดเมียมและทองแดงในคราวเดียวกันโดยใช้อุปกรณ์วิเคราะห์ของไหลจุลภาคบนฐานกระดาษเชิงเคมีไฟฟ้าและเชิงสี ซึ่งการตรวจวัดเชิงเคมีไฟฟ้าใช้สำหรับการวิเคราะห์ตะกั่วและแคดเมียมโดยใช้ขั้วไฟฟ้าเพชรเจือโบรอนที่ดัดแปรด้วยฟิล์มของบิสมัท สำหรับการวิเคราะห์ทองแดงใช้การตรวจวัดเชิงสีของการเร่งการกัดกร่อนของนาโนเพลตของเงินด้วยไทโอซัลเฟต ภายใต้ภาวะที่เหมาะสมช่วงความเป็นเส้นตรงของการวิเคราะห์โลหะหนักด้วยอุปกรณ์นี้คือ 0.5 - 70 นาโนกรัมต่อมิลลิลิตรสำหรับตะกั่วและแคดเมียมและ 10 - 350 นาโนกรัมต่อมิลลิลิตรสำหรับทองแดง และมีขีดจำกัดในการวิเคราะห์คือ 0.1 นาโนกรัมต่อมิลลิลิตรสำหรับตะกั่วและแคดเมียมและ 5.0 นาโนกรัมต่อมิลลิลิตรสำหรับทองแดง ส่วนสุดท้ายคือ การพัฒนาวิธีการวิเคราะห์ของโลหะหนักโดยใช้ขั้วไฟฟ้าพิมพ์สกรีนที่ดัดแปรด้วยคอมโพสิตของแนฟฟีออน/ของเหลวของไอออนิก/กราฟฟีน ซึ่งคอมโพสิตที่ใช้ดัดแปรขั้วไฟฟ้าชนิดนี้มีความไวสูงต่อการวิเคราะห์ สังกะสี แคดเมียมและตะกั่วในคราวเดียวกัน โดยที่มีขีดจำกัดของการวิเคราะห์พร้อมกันคือ 0.09, 0.06 และ 0.08 นาโนกรัมต่อมิลลิลิตร ตามลำดับ ซึ่งคอมโพสิตชนิดนี้ได้รับความสนใจที่จะนำไปใช้ร่วมกับอุปกรณ์วิเคราะห์ของไหลจุลภาคสำหรับการวิเคราะห์โลหะหนักต่อไปในอนาคต นอกจากนี้อุปกรณ์ที่เสนอมาทั้งหมดนี้ยังสามารถประยุกต์ใช้ในการวิเคราะห์หาปริมาณโลหะหนักในตัวอย่างจริงได้อีกด้วย (เช่น ตัวอย่างทางด้านอาหาร สิ่งแวดล้อมและคลินิก) ซึ่งผลที่ได้สองคล้องกับผลการทดลองที่ได้จากวิธีมาตรฐาน

ภาควิชา เคมี	ลายมือชื่อนิสิต .....
สาขาวิชา เคมี	ลายมือชื่อ อ.ที่ปรึกษาหลัก .....
ปีการศึกษา 2558	ลายมือชื่อ อ.ที่ปรึกษาร่วม .....
	ลายมือชื่อ อ.ที่ปรึกษาร่วม .....

5572884123 : MAJOR CHEMISTRY
KEYWORDS: MICROFLUIDIC ANALYTICAL DEVICE / ELECTROCHEMICAL DETECTION / COLORIMETRIC DETECTION / HEAVY METAL IONS

SUDKATE CHAIYO: DEVELOPMENT OF MICROFLUIDIC ANALYTICAL DEVICE FOR DETERMINATION OF HEAVY METALS. ADVISOR: PROF. ORAWON CHAILAPAKUL, Ph.D., CO-ADVISOR: ASSOC. PROF. WEENA SIANGPROH, Ph.D., AMARA APILUX, Ph.D., 112 pp.

This research aimed to develop a microfluidic analytical device for determination of heavy metals, which can be divided into 3 parts. The first part is the development of microfluidic paper-based colorimetric device using thiosulfate catalytic etching of silver nanoplates for determination of copper. This device offers high sensitivity and selectivity for determination of copper over other metal ions. The color change can be monitored by the naked eye. The limit of detection was found to be 0.3 ng mL^{-1} and the relevant calibration curves was linear in the range of 0.5 - 200.0 ng mL^{-1} by ImageJ analysis. The second part is simultaneous determination of lead, cadmium and copper using microfluidic paper-based analytical device with dual electrochemical and colorimetric detection. Electrochemical detection was applied for determination of lead and cadmium using a bismuth film modified boron-doped diamond electrodes (Bi-BDDE). For the copper assay, the concentration of copper was measured by colorimetric detection based on the catalytic etching of silver nanoplates by thiosulfate. Under optimized conditions, the linear range obtained was found to be 0.5 - 70 ng mL^{-1} for lead and cadmium, 10 - 350 ng mL^{-1} for copper, and the detection limits were 0.1 ng mL^{-1} for lead and cadmium, and 5.0 ng mL^{-1} for copper. The final part is development of analytical method for the determination of heavy metal using a nafion/ionic liquid/graphene composite modified screen-printed carbon electrode. The composite-modified electrode was fabricated and evaluated for the highly sensitive simultaneous determination of zinc, cadmium and lead, which the detection limits of the simultaneous analyses were 0.09 ng mL^{-1}, 0.06 ng mL^{-1} and 0.08 ng mL^{-1}, respectively. This composite-modified electrode can be a candidate working electrode used in a microfluidic analytical device for determination of heavy metals in the future. Moreover, all proposed assays were applied to detect heavy metals in real samples (e.g. food, environmental and clinical samples), which the results were in good agreement with obtained from those of the standard methods.

Department:	Chemistry	Student's Signature	.....
Field of Study:	Chemistry	Advisor's Signature	.....
Academic Year:	2015	Co-Advisor's Signature	.....
		Co-Advisor's Signature	.....

ACKNOWLEDGEMENTS

First and foremost, I would like to express my sincere gratitude to my advisor Professor Dr. Orawon Chailapakul for the continuous support of my Ph.D study and research, for her patience, motivation, enthusiasm, and immense knowledge. Her guidance helped me in all the time of research and writing of this thesis. I hope that one day I would become as good an advisor to my students as my advisor has been to me.

A special thanks goes to my co-advisor, Associate Professor Dr. Weena Siangproh, who is most responsible for helping me to complete the writing of this dissertation as well as the challenging research that lies behind it. She trained me how to write academic papers, had confidence in me when I doubted myself, and brought out the good ideas to me. She constantly provided contribution and excellent advice with kindness and enthusiasm from time to time. And, Dr. Amara Apilux, has been always there to listen and to give the advice. I am also thankful to her for encouragement the use of correct grammar in my writings and for carefully reading and commenting on countless revisions of my manuscript.

l wounld to take this opportunity to thank to Professor Dr. Kurt Kalcher from Karl Franzens Universität Graz, I am extremely grateful for his kind supports and affectionate encouragement throughout my 8 months in Austria.

Besides my advisors, I would like to thank the rest of my thesis committee: Associate Professor Dr. Vudhichai Parasuk, Assistance Professor Dr. Suchada Chuanuwatanakul, Associate Professor Dr. Nattaya Ngamrojanavanich and Associate Professor Dr. Pornpimol Muangthai, for their encouragement, questions, and insightful comments.

I gratefully acknowledges the financial supports from Thailand Research Fund (TRF) through the Royal Golden Jubilee Ph.D. program (Grant number PHD/0127/2556).

I would like to thank all the members of Electrochemistry and Optical Spectroscopy Research Unit (EOSRU) for providing necessary supports and helpful advice during difficult time. We were not only able to support each other by deliberating over our problems and findings, but also happness by talking about things other than just our papers.

Last but not the least, I would like to thank the important persons in my life. Without Pra Chaiyo, Somdath Chaiyo, Mali Kladphet, Chaiyachet Chaiyo, Nantanit Numjaiyen and Chutinan Chaiyo, I would not have been accomplished anything in my life. I always treasure your benediction, encouragement and unconditional love.

CONTENTS

Page

Page

Page

Page

Page

LIST OF TABLES

LIST OF FIGURES

LIST OF ABBREVIATIONS

μPAD	Microfluidic paper-based analytical devices
CV	Cyclic voltammetry
SWASV	Square wave anodic stripping voltammetry
E_{pa}	Pack anodic potential
E_{pc}	Pack cathodic potential
E°	Standard reduction potential
ΔE_p	The difference between pack anodic potential and pack cathodic potential
E_s	Potential step
E_p	Potential pulse
I_{pa}	Pack anodic current
I_{pc}	Pack cathodic current
n	Number of electrons transferred in the redox
R	Gas constant
T	Temperature
F	Faraday constant
A	Area of the working electrode
C	Concentration
D	The diffusion coefficient of the electroactive species
ν	Scan rate
mol	Molarity
cm^3	Cubic centimeter

cm^2	Square centimeter
AgNPls	Silver nanoplates
AuNPs	Gold nanoparticles
AgNPs	Silver nanoparticles
$S_2O_3^{2-}$	Thiosulfate
CTAB	Hexadecyltrimethylammonium bromide
ΔI	The difference in the color intensity values
I_{blank}	The color intensity values of blank
I_{sample}	The color intensity values of sample
LOQ	Limit of Quantitation
LOD	Limit of detection
R^2	Coefficient of determination
$\bar{X}$	Arithmetic Mean
SD	Standard deviation
RSD	The relative standard deviation
ND	Not detection
N.M.	Not Measured
µL	Microliter
mL	Milliliter
ng mL^{-1}	Nanogram per milliliter
µg mL^{-1}	Microgram per milliliter
rpm	Revolutions per minute
v/v	Volume per volume
°C	Degree celsius

g	Gram
μm	micrometer
λ_{max}	Wavelength maximum
SEM	Scanning electron microscopy
TEM	Transmission electron microscopy
SPCE	Screen printing carbon electrode
BDDE	Boron-doped diamond electrode
GCE	Glassy carbon electrode
N	Nafion
IL	Ionic liquid
G	Graphene

CHAPTER I

INTRODUCTION

1.1 Introduction

The contamination caused by toxic heavy metals such as copper (Cu(II)), lead (Pb(II)), cadmium (Cd(II)), and zinc (Zn(II)) has drawn extensive attention worldwide. A small concentrations of toxic heavy metal ions can cause serious health problems and damage ecosystem. Actually, an increasing number of regulations such as those set by the US Environmental Protection Agency (EPA), the World Health Organization (WHO), and the pollutant control department of Thailand, include heavy metals in the list of priority substances which are examined [1-4]. In addition, maximum concentration levels, guideline values or acceptable concentrations in water have to be set in order to control the environmental quality following the requirement of environmental quality standards (EQS). Therefore, it is necessary to develop highly sensitive, rapid, and simple methods for the detection of these contaminants. Various techniques have been developed for determination of heavy metals, such as colorimetric analysis [5], UV-vis spectrometry [6], surface enhanced raman spectrometry (SERS) [7], atomic absorption spectrometry (AAS) [8], atomic fluorescence spectrometry [9], ion chromatography [10], inductively coupled plasma mass spectrometry (ICP-MS) [11] and inductively coupled plasma optical emission spectrometry (ICP-OES) [12], but these methods are still expensive and require complicated instrumentation, large sample volume and can generally perform only in the laboratory.

To overcome these problems, microfluidic systems have been utilized for determination of heavy metals [13]. Utilizing the benefits from micron-scale systems, microfluidic devices offer a number of advantages including requirement of small samples and reagents volume, fast analysis time, high analytical performance,

portability and possibility for high-throughput analysis [13, 14]. Recently, the microfluidic paper-based analytical devices (μPADs) have been first developed for the application in biological assays [15]. μPADs are very attractive due to their portability, ease of use, small sample volume requirement, and inexpensiveness [16].

Normally, Colorimetry [17], electrochemical [18], fluorescence [19], chemiluminescence [20], electrochemiluminescence [21] and electrical methods [22] were proposed as the detectors of μPADs. In this research, colorimetric and electrochemical detection were developed for determination of heavy metal ions. Colorimetric sensor provides a high selectivity, rapidity and simplicity, and can produce semi-quantitative [23]. Moreover, electrochemical technique has attracted extensive attention for determination of heavy metals. It acts as an alternative choice to spectroscopic techniques because it offers advantages of high sensitivity, fast analysis, and simple equipment [24, 25].

In this work, μPADs combined with colorimetric and/or electrochemical detection were successfully used for sensitive and selective determination of heavy metals. The development of μPADs in this research consists of 2 parts which are; 1.) Highly selective and sensitive paper-based colorimetric sensor using thiosulfate catalytic etching of silver nanoplates for trace determination of copper ions, and 2.) High sensitivity and specificity for simultaneous determination of lead, cadmium and copper using μPAD with dual electrochemical and colorimetric detection.

In addition, the last past is the development of electrochemical sensors using a nafion/ionic liquid/graphene composite modified screen-printed carbon electrode. This sensor developed was successfully applied to sensitively simultaneous determination of zinc, cadmium and lead. In this part, it demonstrated that the proposed electrode is a new sensor which can be combined to microfluidic analytical system for simultaneous determination of heavy metal ions in the future.

These developed sensors were used to determine heavy metals with high sensitivity and selectivity. Under the optimal condition, it showed the excellent analytical performance. In addition, the developed sensors displayed a good

repeatability and reproducibility. Finally, this research had demonstrated the ability of these proposed assays for determination of target analytes in real samples (e.g. food, environmental and clinical samples).

1.2 Objectives of the research

This research consists of three goals for development and improvement:

1. To develop microfluidic analytical device for determination of heavy metal ions.

2. To develop the highly sensitive and selective sensors for determination of heavy metal ions.

3. To apply the developed microfluidic analytical devices and/or developed sensors for determination of heavy metal ions in food or environment.

1.3 Scope of the research

The microfluidic analytical devices were designed to obtain the suitable platform for the determination of heavy metal ions (Cu(II), Pb(II), Cd(II) and Zn(II)). The influences of experimental variables on the sensitivity of the proposed method were investigated. Under the optimal conditions, the analytical performance of the proposed methods were studied, including range of linearity, limits of detection and quantification, repeatability and reproducibility. The selectivity for the determination of heavy metal ions was studied using various interfering species. Finally, the proposed methods were applied to detect heavy metal ions contaminated in food or environment with high sensitivity, accuracy and precision.

CHAPTER II

THEORY

2.1 Heavy metals

Heavy metals are assigned as metallic elements that have a high atomic weight, rather high density and are toxic at low concentrations. Heavy metal contamination in natural environments is an urgent problem due to the increasing industrial activities. Normally, metal ions can be separated into essential and nonessential ions. Nonessential heavy metals, such as cadmium (Cd(II)), mercury (Hg(III)), arsenic (As(III)) and lead (Pb(II)), even at trace amount exposure, are highly toxic and carcinogenic [26, 27]. Although essential metals (copper (Cu(II)) and zinc (Zn(II)) are required to support biological activities. However, these essential metals are toxic when their presence in excess. Furthermore, both of them can pose a severe threat to human health and environment due to their non-biodegradable nature and accumulation in the food chain [28]. Therefore, it is necessary to quantify not only essential but also nonessential heavey metals at trace level in the environment, food and drinking water.

In this dissertation, copper (Cu(II)) cadmium (Cd(II)), lead (Pb(II)) and zinc (Zn(II) were selected as represent ions for essential and nonessential ions in order to develop the high performance method to determine them in the environment, food and clinical samples at trace level amount.

2.2 Microfluidic analytical system

Microfluidics deal with the flow of liquid inside micrometer size channels. At least one dimension of the channel is in the order of a micrometer or tens of micrometers in order to consider it as microfluidics. First publication concerning the construction of microfluidic separation device based on miniaturized gas

chromatography and integrated circuit processing technology was first published in 1975 [29]. It consisted of a 5-cm-diameter silicon wafer with an open-tubular capillary column, two sample injection valves and a thermal conductivity detector. This separation device was able to separate a simple mixture of compounds in a matter of seconds [29, 30]. Then, No. further research on given miniaturized gas chromatography was developed continuously until the 1990s. The first response of the scientific community to this was silicon chip device. It may be concerned the lack of technological experience and the most research work focused on the fabrication of the key components such as micropumps, microvalves and chemical sensors [31]. In 1990, Manz and co-workers described a miniaturized open-tubular liquid chromatograph using silicon chip technology [32]. Manz also proposed the concept of "miniaturized total chemical analysis system" or μTAS [33]. In his article, he proposed the use of silicon chip analyzers incorporating sample pretreatment, separation, and detection and also disclosed the ideas of integrating a capillary electrophoresis setting onto a chip. Thus, in the last two decades, the development of new microfabrication techniques and materials as well as separation and detection methods used in μTAS devices are grown very fast and it was widely used in various applications [34, 35].

2.3 Microfluidic paper-based analytical device

Microfluidic paper-based analytical device (μPAD), as a growing research field with its beginning in 2007 [15], provides a novel system for fluid handling and fluid analysis for a variety of applications including food analysis, environmental monitoring, and clinical diagnosis. This sensor shows various advantages including ease of use, high throughput analysis, portability, small sample and reagent requirement, and inexpensiveness. The hydrophilic microchannel inside μPADs was fabricated by creating the hydrophobic wall using photolithography [15, 36, 37].

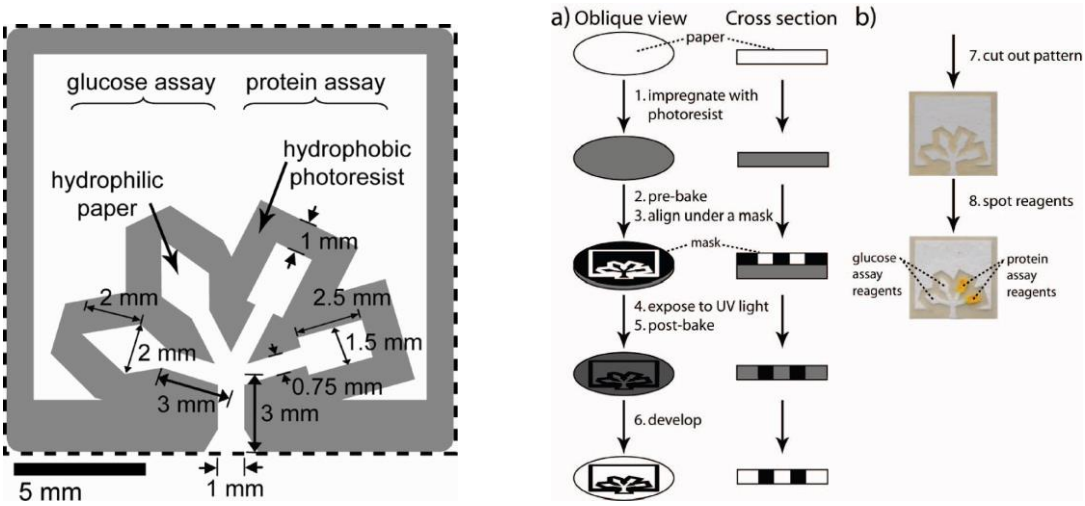

Figure 2.1 Design of the μPAD for determination of two analytes and schematic of the photolithography method for fabricating μPAD [15].

2.3.1 Fabrication method

In fabricating μPAD, the criteria for selection the methods and materials depended on low cost, simplicity and efficient production process. There are several techniques and processes involving chemical modification and/or physical deposition that could be used to adjust the properties of the paper such that it becomes available for further modification or direct usage in a range of applications [38]. Various techniques were proposed to fabricate these devices, include photolithography, analogue plotting, screen printing, plasma treatment, paper cutting, ink jet etching, ink jet printing, flexography printing, laser treatment, and wax printing. The advantages and limitations of each fabrication system are exhibited in Table 2.1 [39].

Table 2.1 Comparison of the main advantages and disadvantages for different fabrication methods of μPAD

Fabrication methods	Advantages	Disadvantages
Photolithography	- High resolution	- Requires high cost tools - Requires an further washing step to eliminate uncross-linked polymer
Plotting	- PDMS is inexpensive - Sensors are flexible	- Cannot be used to high throughput production
Ink jet etching	- Involves only a single printing machine	- Difficult for customization of the printer
Plasma treatment	- Agent (AKD) and the material are very cheap	- Uses different masks for creating different μPAD
Ink jet printing	- Uses very cheap AKD - Fast and simply	- Requires an very heating step for melt AKD - Requires modified ink jet printers
Flexography printing	- Allows direct roll-to-roll production in present printing houses - Escapes the heat treatment of printed patterns	- Requires two prints of polystyrene solution - Requires different printing plates
Screen printing	- Simple for creation process	- Low resolution - Requires different printing screens for creating different patterns

Table 2.1 Comparison of the main advantages and disadvantages for different fabrication methods of μPAD (continuous)

Fabrication methods	Advantages	Disadvantages
Screen printing	- Simple for creation process	- Low resolution - Requires different printing screens for creating different patterns
Laser treatment	- High resolution	- Microfluidic channels do not allow lateral flow of fluids - Requires extra coating for liquid flow
Wax printing	- Simple and reduce time for fabrication procedure	- Requires expensive wax printers; - Requires heating to wax at all times

In this research, wax printing was chosen for fabrication of μPADs because this method is low cost, fast, simple, and no mask required, while it needs only computer-designed pattern. Solid wax patterns can be printed onto the surface of paper followed by the use of heat source such as an oven, hot plate or heat gun to melt the wax as shown in Figure 2.2. This method is also better for the fabrication of large quantities of sensors because less steps are involved in forming the hydrophobic wall compared to other methods. The heating process allows wax to penetrate within the paper medium. Dispersion of the wax vertically through the paper will effectively confine the solution flow to the desired regions of the paper. However, due to the nature of the fiber matrix, the paper tends to align the wax in a horizontal rather than vertical direction [40]. The wax spreads faster in the horizontal direction causing a wider line compared to the original width of the applied wax [40]. Therefore, the

reproducibility of the fabrication method is highly dependent on the width of the wax line and the heating temperature. μPADs offer the possibility for users to produce a simple and mass-scalable devices at an affordable cost.

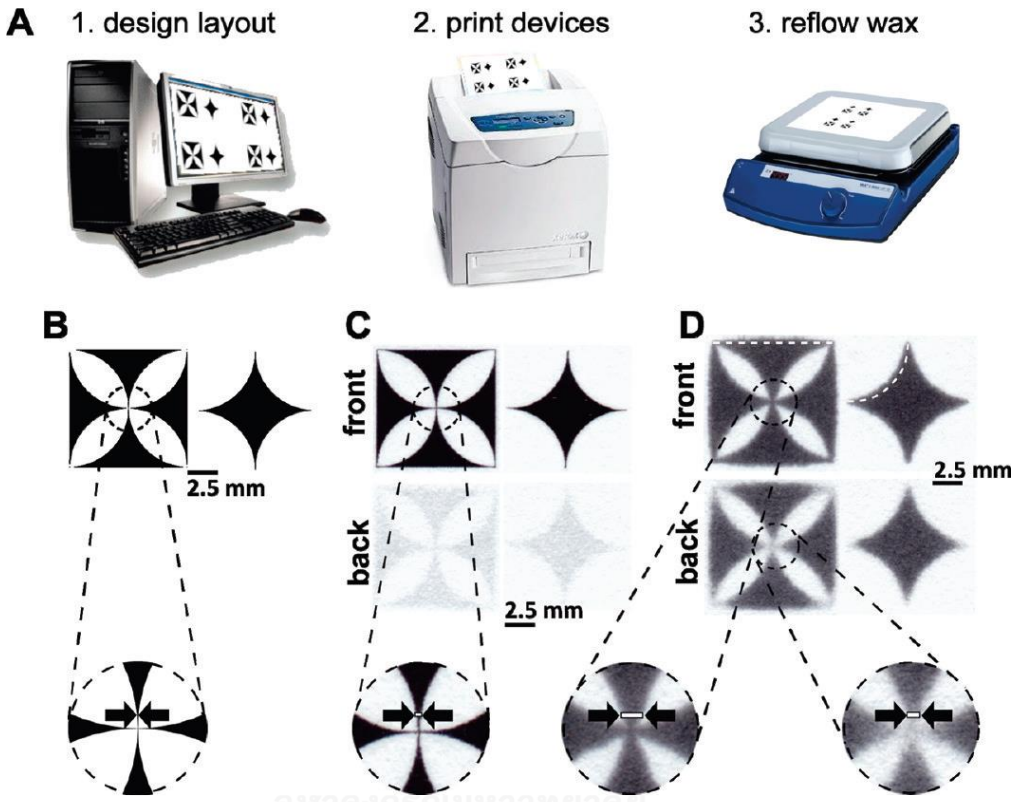

Figure 2.2 Wax printing techniques for the fabrication of μPAD [40].

2.3.2 Detectors for μPAD

As mentioned, μPAD offer the opportunity for users to produce a simple, mass-scalable devices at an affordable cost. However, in order to create an analytical device, suitable transduction methods are necessary which may require the additional reagents, materials and instrumentation leading to the further cost and complexity. There are five most commonly reported techniques used for quantitative analysis on paper including colorimetric [41], electrochemical [18, 42], fluorescent [43], chemiluminescence [44, 45], electrochemiluminescence [46] and electrical

conductivity [47]. However, in order to maintain simplicity, affordability and portability, low power techniques such as optical and electrochemical methods are well suited as transducers on μPADs. Therefore, in this dissertation, two of these techniques are focused on the use as detector for μPADs.

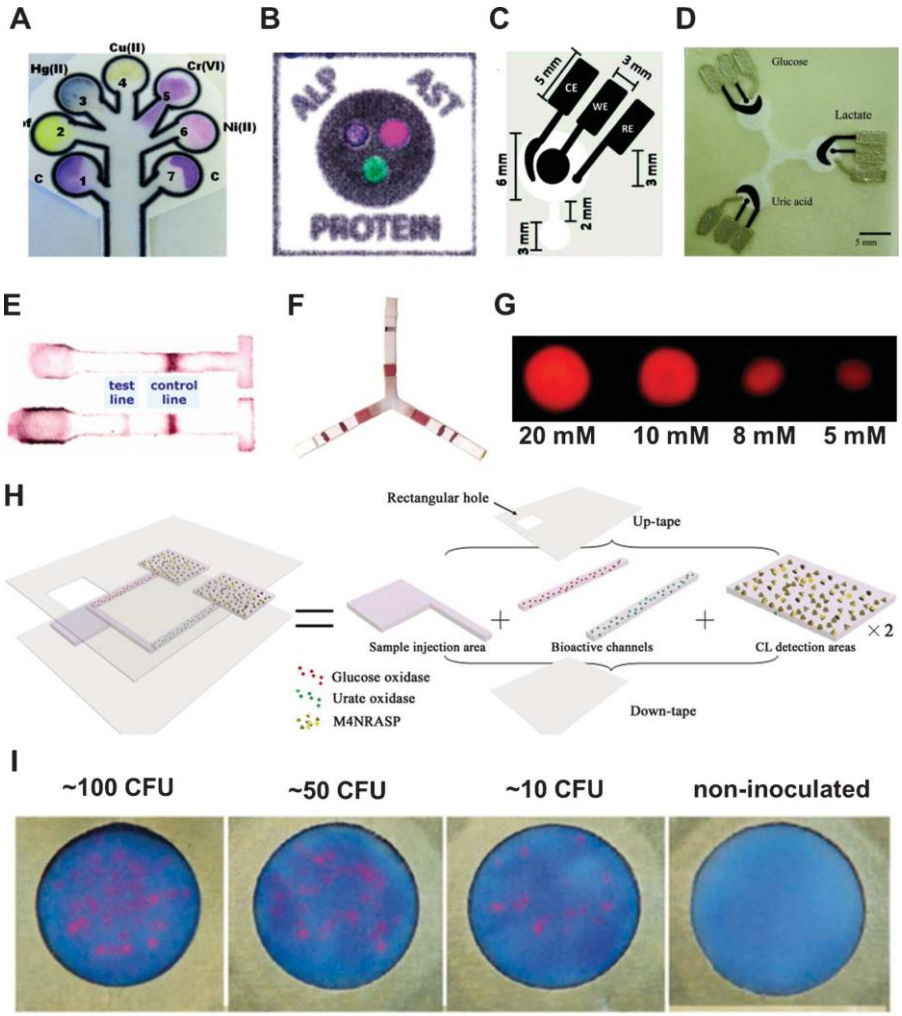

Figure 2.3 Illustrations of difference detectors for μPAD. (A, B) Colorimetric detection, (C) Dual electrochemical/colorimetric determination, (D) Electrochemical detection, (E, F) Antibody conjugated gold nanoparticle detection, (G) electrochemiluminescence detection (H) chemiluminescence detection and (I) Fluorescent detection.

2.3.3.1 Electrochemical method

Electrochemical method has been widely used in μPAD because of its fast sensor response, lower detection limits, quantitative results, and ability for external electronics to be miniaturized [48]. The most significant electrochemical techniques are divided into five major groups: potentiometry, voltammetry, coulometry, conductometry, and dielectrometry [49]. In this research, voltammetry was utilized as an electrochemical detection technique, especially cyclic voltammetry and stripping square-wave voltammetry are in focus.

2.3.3.1.1 Voltammetry

Voltammetry is a collection of techniques in which rely on the relation between current and potential. The current observed during electrochemical processes are based on the applied potential. The plot between current and working electrode potential is called a voltammogram. Voltammetry can be applied to examine the electrochemical property of electroactive species that can be oxidized or reduced at the working electrode [50]. For example, the voltammogram in Figure 2.4 shows a graph of current versus working electrode potential for a mixture of ferricyanide ($Fe(CN)_6^{3-}$) and ferrocyanide ($Fe(CN)_6^{4-}$). The diffusion current for oxidation of $Fe(CN)_6^{4-}$ is observed at a potential about +0.5 V (vs SCE.) [51].

$$Fe(CN)_6^{4-} \longrightarrow Fe(CN)_6^{3-} + e^- \quad \text{.....eq. 2.1}$$

In this region, current is governed by the rate at which $Fe(CN)_6^{4-}$ diffuses to the electrode. Figure 2.4 shows that this current is proportional to concentration of $Fe(CN)_6^{4-}$ in bulk solution. Below 0 V, there is another plateau corresponding to the diffusion current for reduction of $Fe(CN)_6^{3-}$ whose concentration is constant in all the solutions. The voltammetric techniques including cyclic voltammetry and stripping

square-wave voltammetry were used in this research for characterization the electrochemical property and quantity of target analyte.

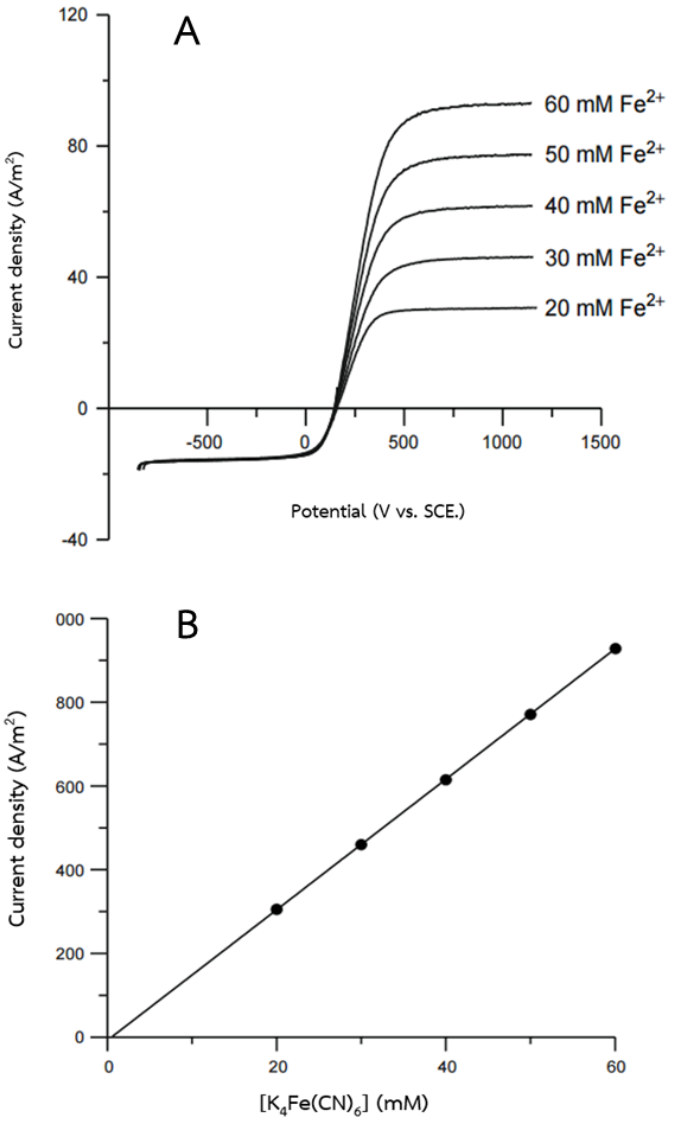

Figure 2.4 (A) Voltammogram for mixture of ferricyanide $(Fe(CN)_6^{3-})$ and (B) ferrocyanide $(Fe(CN)_6^{4-})$ and Plot of current density of mixture vs concentration of mixture from the curves in Figure 2.4 A [51].

2.3.3.1.2 Cyclic voltammetry

Cyclic voltammetry (CV) has become an important and widely used electrochemical technique in many areas of chemistry to characterize the electrochemical property of target analyte. In cyclic voltammetry, Figure 2.5 shows the triangular waveform applied to the working electrode. After the application of a linear voltage slope between times t_0 and t_1, the slope is reversed to bring the potential back to its initial value at time t_2. The cycle can be repeated many times [52].

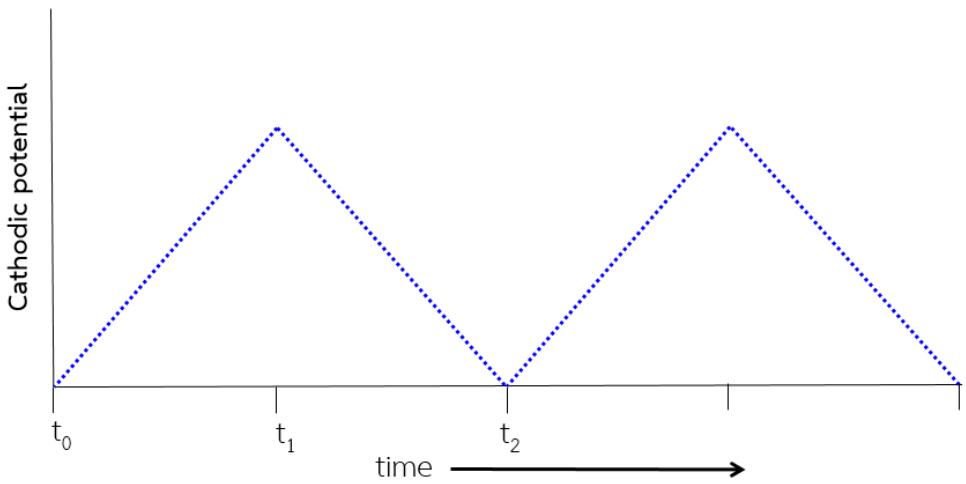

Figure 2.5 Cyclic voltammetry waveform

The initial portion of the cyclic voltammogram as shown in Figure 2.6, beginning at displays a cathodic wave. Instead of leveling off at the top of the wave, current decreases at more negative potential because analyte becomes depleted near the electrode. Diffusion is too slow to replenish analyte near the electrode. At the time of peak potential (t_1) in the Figure, the cathodic current has decayed to a small value. After t_1 the potential is reversed and, eventually, reduced product near the electrode is oxidized, thereby giving rise to an anodic wave. Finally, as the reduced product is depleted, the anodic current decays back toward its initial value at t_2.

Figure 2.6 demonstrates a reversible reaction that is fast enough to maintain equilibrium concentrations of reactant and product at the electrode surface. The anodic peak and cathodic peak currents have equal magnitudes in a reversible process, and

$$E_{pa} - E_{pc} = 22.2RF/nF = 57.0/n \text{ (mV)} \quad \text{(at 25 °C)}.....\text{eq. 2.2}$$

Where:

E_{pa} = peak anodic currents

E_{pc} = peak cathodic currents

n = number of electrons transferred in the redox event (usually 1)

R = gas constant in VC K^{-1} mol^{-1}

T = temperature in K

F = faraday constant in 96487 C mol^{-1}

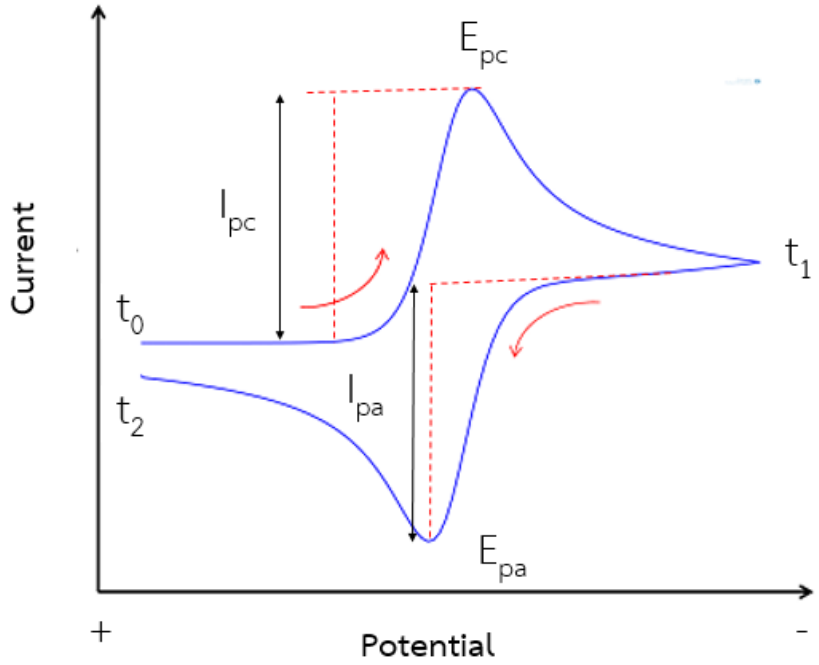

Figure 2.6 Typical cyclic voltammogram where I_{pc} and I_{pa} show the peak cathodic and anodic current respectively for a reversible reaction.

For a reversible reaction, the peak current for the forward scan of the first cycle is proportional to the concentration of analyte and the square root of scan rate.

$$I_{pc} = (2.69 \times 10^{8})\, n^{3/2}\, ACD^{1/2}\, \nu^{1/2} \quad \text{.....eq. 2.3}$$

Where:

I_{pc}	=	current maximum in amps
n	=	number of electrons transferred in the redox event (usually 1)
A	=	area of the working electrode in m^2
C	=	concentration in mol L^{-1}
D	=	the diffusion coefficient of the electroactive species in $m^2\ s^{-1}$
ν	=	scan rate in V s^{-1}

The use of faster scan rate, the greater of the current are obtained during the reaction remains reversible. If the electroactive species is adsorbed on the electrode, the peak current is proportional to ν rather than the square root of ν.

For an irreversible reaction, the cathodic and anodic peaks are drawn out and more separated. At the limit of irreversibility, where the oxidation is very slow, no anodic peak is noticed as shown in Figure 2.7.

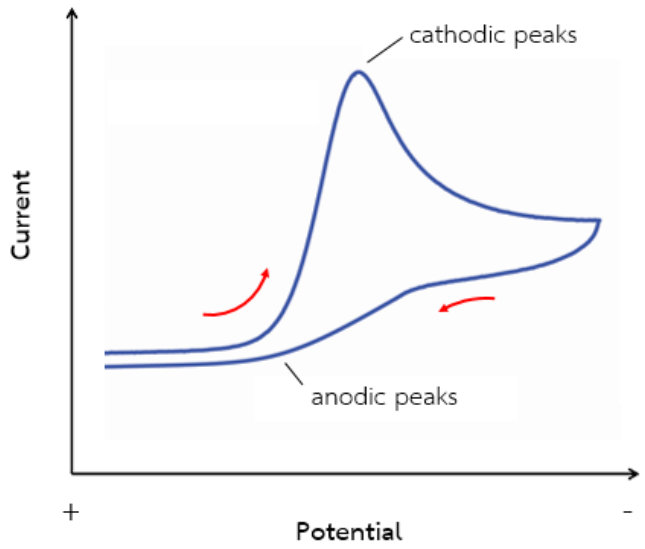

Figure 2.7 Typical cyclic voltammogram show the peak cathodic and anodic current respectively for an irreversible reaction.

2.3.3.1.3 Square-wave anodic stripping voltammetry

Square-wave anodic stripping voltammetry is a very sensitive method for quantitative determination of electroactive species. This method combines the advantages of square-wave voltammetry and anodic stripping voltammetry. Square-wave voltammetric method have proved to be a very sensitive for the direct evaluation of concentrations. It can be widely used and popular for the trace analysis. The waveform of square wave voltammetry was showed in Figure 2.8. It can be observed that a square wave was applied on a staircase. During each cathodic pulse, there is a rush of analyte to be reduced at the electrode surface. During the anodic

pulse, analyte that was just reduced is reoxidized. The square wave voltammogram is the difference in current intervals of cathodic and anodic measurement. The two currents have opposite signs, their difference is larger than either current alone. When the difference in current is plotted, the shape of the square wave volrammogram is obtained as shown in Figure 2.9 which is essentially derivative of the sample current voltammogram. Therefore, the square wave voltammetric method offered the advantages in term of high sensitivity for the trace analysis [53].

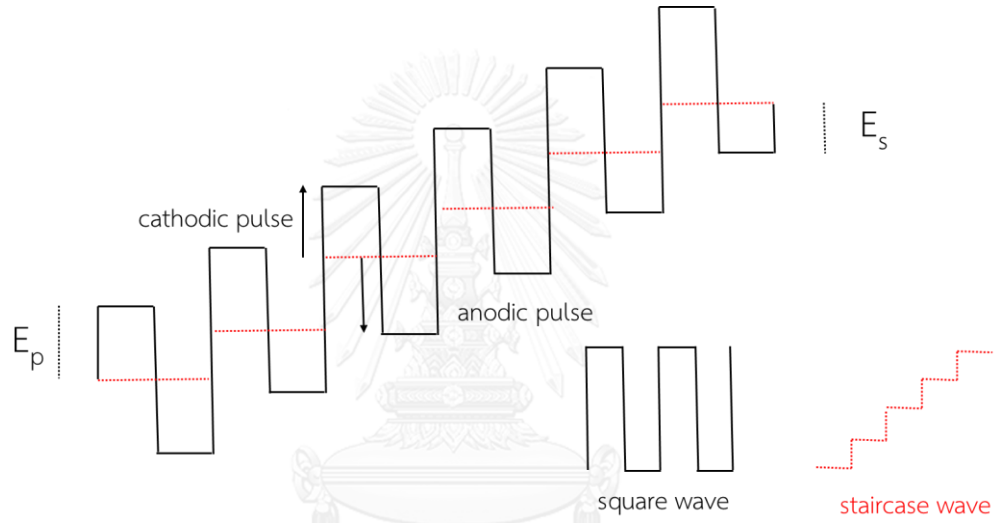

Figure 2.8 Waveform for square wave voltammetry,

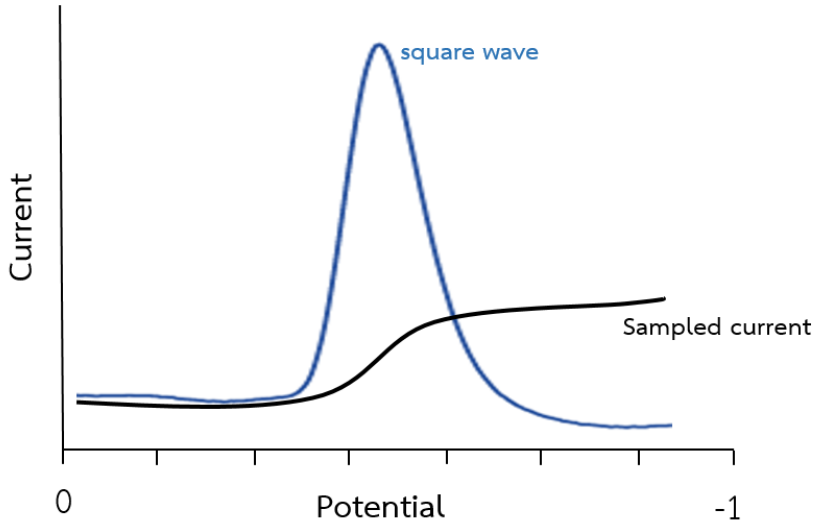

Figure 2.9 Comparison between (a) sample current voltammogram and (b) square wave voltammogram.

For stripping mode of square wave voltammetric analysis. Normally, anodic stripping voltammetry consists of two steps [54]. The first step, the target analyte from a dilute solution is deposited onto the electrode surface; usually by electroreduction at an appropriately cathodic potential. For example, the deposition reaction of M^{2+} is

$$M^{2+} + 2e^- \longrightarrow M^0 \text{ (onto surface electrode)} \quad \text{.....(eq. 2.3)}$$

After the deposition time, the accumulated species is then stripped from the electrode surface by reversing the direction of the square-wave potential sweep. Monitoring the current through the stripping step provides the peak shaped voltammogram, as shown in Figure 2.10. Hence, this method offers a very high sensitivity for the analysis of trace and ultra-trace concentrations of target analyte in real sample.

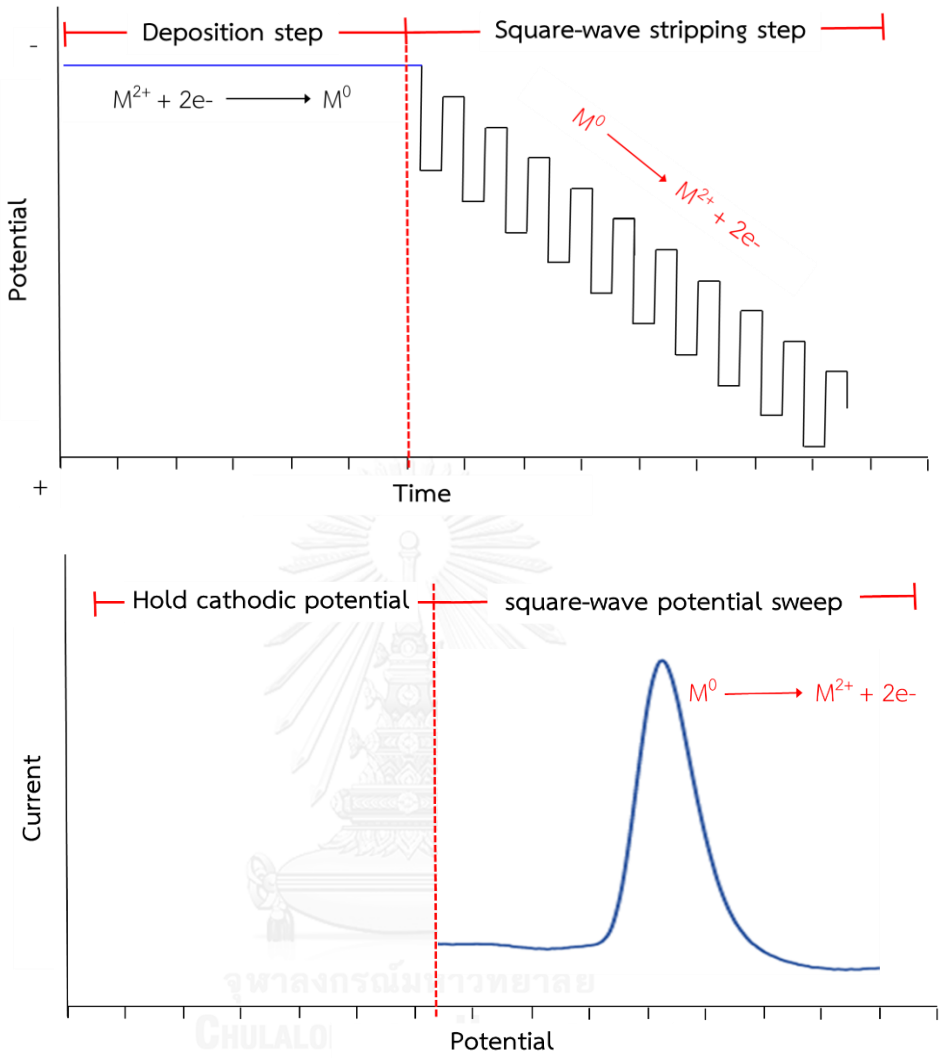

Figure 2.10 Potential waveform for square-wave anodic stripping voltammetry

2.2.3.2 Colorimetric method

Presently, colorimetric detection coupled with μPAD has been widely used for the qualitative analysis of multiplex analytes in target samples. This detection can be examined by visually observing the change in color, intensity, or brightness caused by the presence of the analyte. The quantify changes in color was monitored by digital camera or scanners or by measuring the amount of light reflected from a surface where an assay has occurred. In 2008, Martinez et al. [15] first proposed the colorimetric

detection coupled with μPADs for determination of glucose and protein. The investigation is based on a change color from chemical reaction between reagents and analytes. The signal of photograph of the color product were detected by Adobe Photoshop software to obtain the calibration curve for glucose and protein

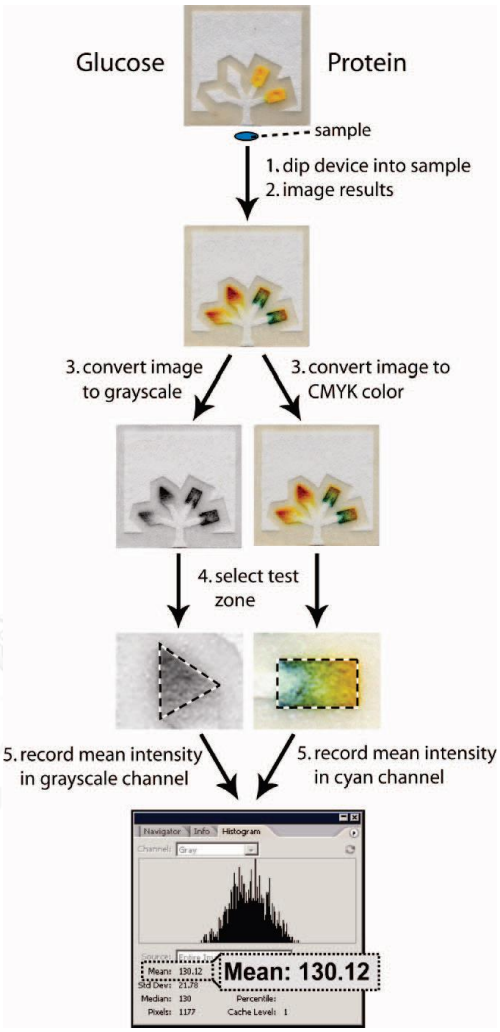

Figure 2.11 Procedure for quantifying the levels of glucose and protein in urine using image Adobe Photoshop software [15].

CHAPTER III

DEVELOPMENT OF MICROFLUIDIC PAPER-BASED ANALYTICAL DEVICES FOR TRACE DETERMINATION OF HEAVY METALS

There are two parts for this chapter. Past I presents highly selective and sensitive paper-based colorimetric microfluidic sensor using of silver nanoplates with thiosulfate for trace determination of copper. Past II reports high sensitivity and specificity simultaneous determination of lead, cadmium and copper using microfluidic paper-based device with dual electrochemical and colorimetric detection.

Parts I:

Highly selective and sensitive paper-based colorimetric sensor using thiosulfate catalytic etching of silver nanoplates for trace determination of copper ions

Sudkate Chaiyo[a], Weena Siangproh[b], Amara Apilux[c]*, Orawon Chailapakul[a, d]**

[a] Electrochemistry and Optical Spectroscopy Research Unit, Department of Chemistry, Faculty of Science, Chulalongkorn University, 254 Phayathai Road, Pathumwan, Bangkok 10330, Thailand

[b] Department of Chemistry, Faculty of Science, Srinakharinwirot University, Sukhumvit 23, Wattanna, Bangkok 10110, Thailand

[c] Center for Innovation Development and Technology Transfer, Faculty of Medical Technology, Mahidol University, 999 Phuttamonthon 4 Road, Salaya, Nakhon Pathom 73170, Thailand

[d] Center for Petroleum, Petrochemicals and Advanced Materials, Chulalongkorn University, 254 Phayathai Road, Pathumwan, Bangkok 10330, Thailand

** Corresponding author

* Co-corresponding author

Analytica Chimica Acta 866 (2015): 75-83

Abstract

A novel, highly selective and sensitive paper-based colorimetric sensor for trace determination of copper (Cu(II)) ions was developed. The measurement is based on the catalytic etching of silver nanoplates (AgNPls) by thiosulfate ($S_2O_3^{2-}$). Upon the addition of Cu(II) to the ammonium buffer at pH 11, the absorption peak intensity of AuNPls/$S_2O_3^{2-}$ at 522 nm decreased and the pinkish violet AuNPls became clear in color as visible to the naked eye. This assay provides highly sensitive and selective detection of Cu(II) over other metal ions (K^+, Cr^{3+}, Cd^{2+}, Zn^{2+}, As^{3+}, Mn^{2+} Co^{2+}, Pb^{2+}, Al^{3+}, Ni^{2+}, Fe^{3+}, Mg^{2+}, Hg^{2+} and Bi^{3+}). A paper-based colorimetric sensor was then developed for the simple and rapid determination of Cu(II) using the catalytic etching of AgNPls. Under optimized conditions, the modified AgNPls coated at the test zone of the devices immediately changes in color in the presence of Cu(II). The limit of detection (LOD) was found to be 1.0 ng mL^{-1} by visual detection. For semi-quantitative measurement with image processing, the method detected Cu(II) in the range of 0.5–200 ng mL^{-1} (R^2=0.9974) with an LOD of 0.3 ng mL^{-1}. The proposed method was successfully applied to detect Cu(II) in the wide range of real samples including water, food, and blood. The results were in good agreement according to a paired t-test with results from inductively coupled plasma–optical emission spectrometry (ICP-OES).

Keywords: copper ions, colorimetric detection, paper-based sensor, silver nanoplates, thiosulfate

3.1 Introduction

Copper ions (Cu(II)) are an essential trace element for life. Cupric ions play an important role in many body functions as an enzyme co-factor and are involved in the formation of red blood cells [55]. However, an excessive uptake of Cu(II) can cause serious health problems, including ischemic heart disease, kidney disease, neurodegenerative disease, anemia and bone disorders [56]. Because of their toxicity, the maximum contamination value of Cu(II) in the environment and in food was set by several organizations throughout the world to protect human health. For example, the United States Environmental Protection Agency (USEPA) issued the maximum contamination level of Cu(II) in drinking water at 1.30 mg L^{-1} [1]. In Thailand, the pollutant control organization permitted a Cu(II) concentration of 2.00 mg L^{-1} in surface water [3]. In addition, the concentration limit of Cu(II) for exposure from foods is in the range of 1.2-4.2 mg copper/day as set by The European Food Safety Authority (EFSA) [57]. Therefore, the monitoring of Cu(II) contaminants in water, food and the environment is necessary.

Conventional methods for the measurement of Cu(II) include atomic absorption spectrometry (AAS) [58], inductively coupled plasma atomic emission spectrometry (ICP-AES) [59], inductively coupled plasma mass spectrometry (ICP-MS) [60], voltammetry [61] and fluorescence spectrometry [62]. Although these methods provide high sensitivity and selectivity, they require expensive instrumentation, laboratory setup, and high operating cost, which makes these methods unsuitable for field monitoring. Therefore, there is an increasing interest in the development of simple and low-cost sensors for the highly sensitive and selective detection of Cu(II) that can allow reliable on-site real time detection.

Recently, colorimetric sensors based on noble metal nanoparticles such as gold nanoparticles (AuNPs) [63] or silver nanoparticles (AgNPs) [64] for the visual determination of Cu(II) have gained increased attention. AgNPs is particularly of interest because it has a higher extinction coefficient compared to AuNPs of the same size and a lower cost compared to AuNPs [65]. Zhou and coworkers reported on the colorimetric detection of Cu(II) by using 4-mercaptobenzoic acid (4-MBA) modified

AgNPs. The measurement was based on the aggregation of 4-MBA-AgNPs in the presence of Cu(II) via ion-templated chelation [64]. Miao and coworkers proposed a colorimetric detection method of Cu(II) with high sensitivity and selectivity by utilizing the redox reaction between starch-stabilized AgNPs and Cu(II) [66]. Ratnarathorn and coworkers presented the colorimetric measurement on μPAD by using the homocysteine (Hcy) and dithiothreitol (DTT) modified AgNP surface that is able to induce the aggregation of AgNPs in the presence of Cu(II) [67]. In addition, a sensitive and selective colorimetric method was developed based on catalytic thiosulfate leaching of nanoparticles including silver coated gold nanoparticles (Ag/Au NPs) [68] or AuNPs [69] by Cu(II). Cu(II) can accelerate the leaching rate of NPs and leads to a dramatic decrease in its surface plasmon resonance (SPR) absorption because the nanoparticles size is decreased. Although these assays provided high sensitivity, they are time-consuming (25-60 min) and large volumes of solution are required.

A paper-based sensor or microfluidic paper-based analytical devices (μPADs) are a new alternative methodology of a micro total analytical system (μTAS) applied to food analysis, environmental monitoring, and clinical diagnosis. They provide several advantages such as ease of use, high throughput, disposability, low sample and reagents consumption, low expense, and portability [18, 70, 71]. The μPADs were first introduced by Whitesides and coworkers, where the hydrophilic microchannels on devices were fabricated by creating a hydrophobic wall using photolithography [15]. To date, several methods were proposed to fabricate these devices, including inkjet-printing [72], plotting [73], wax-printing [40], plasma treatment [74], and screen printing [75]. Herein, the wax printing method, which is easy and is a quick fabrication process, was applied to create paper-based devices. This paper-based colorimetric sensor is based on the catalytic etching of silver nanoplates (AgNPls) with thiosulfate ($S2O_3^{2-}$) and is developed for the highly selective and sensitive detection of trace Cu(II).

3.2 Experimental

3.2.1 Chemicals and materials

Copper sulfate ($CuSO_4$) and ammonium hydroxide (NH_4OH) were purchased from BDH (England). Sodium thiosulfate, hexadecyltrimethylammonium bromide (CTAB), magnesium sulfate ($MgSO_4$), manganese chloride ($MnCl_2$) and ammonium dichromate ($(NH_4)_2Cr_2O_7$) were obtained from Sigma-Aldrich (Missouri). Ammonium chloride (NH_4Cl) was obtained from Ajax (NSW, Australia). Standard solutions of 1000 µg mL-1 Hg(II), Bi(III), As(III), Pb(II), Co(II), Cd(II) and Zn(II) were purchased from Spectrosol (Poole, UK), and standard solutions of 1000 µg mL^{-1} Ni(II) and Al(III) were purchased from Merck (Darmstadt, Germany). The following chemicals were used as received: iron chloride hexahydrate ($FeCl_3.6H_2O$) (Merck, Darmstadt, Germany) and potassium chloride (KCl) (Univar, Redmond, WA). All chemicals were analytical-grade. All reagents were prepared with 18 MΩ.cm resistance in deionized water (obtained from a Millipore Milli-Q purification system)

3.2.2 Instrumentation

The absorbance measurement was carried out by a UV–visible spectrophotometer (HP HEWLETT PACKARD 8453, UK) using a 1.0 cm path length quartz cell. The modified surface morphology of the paper-based device was characterized by scanning electron microscopy (SEM) (JEOL, Ltd., Japan). Transmission electron microscopy (TEM) was recorded by a H-7650 transmission electron microscope (Hitachi Model, Japan). The levels of Cu(II) in real samples were analyzed by inductively coupled plasma optical emission spectrometry (ICP-OES) (CAP 6000 series ICP-OES, Thermo Scientific, USA).

3.2.3 Synthesis of the modified AgNPls

AgNPls [76] were obtained from the Sensor Research Unit at the Department of Chemistry, Faculty of Science, Chulalongkorn University. Briefly, the AgNPls were

synthesized by reduction of $AgNO_3$ using $NaBH_4$ and the shape transformation using a 30% H_2O_2 solution [76]. First, the $NaBH_4$ was added into the $AgNO_3$ under vigorously magnetic stirring. The solution turned light yellow, indicating the formation of NPs. The shape transformation reaction was done by an injection of the 30% H_2O_2 solution at the rate of 13.45 mL min^{-1} into AgNs. After the complete addition of the H_2O_2 solution, the colloid was further stirred for 10 min to complete the shape conversation process. The solution turned color from light yellow to the blue of AgNPls. For the modification of AgNPls, hexadecyltrimethylammonium bromide (CTAB) capped AgNPls were prepared by the dilution of AgNPls to 200 μg mL^{-1} in a total final volume of 1000 μL with a 0.1 M ammonia buffer at pH 11. Then, 10 μL of 0.1 M CTAB was added to produce the CTAB-capped AgNPls. Sequentially, 5 μL of 1.0 M $Na_2S_2O_3$ was added to the CTAB-capped AgNPls followed by incubation of the mixture for 5 min at room temperature.

3.2.4 Device design and fabrication

In order to obtain highly reproducible measurements, the dendritic hydrophilic channel terminated in the eight detection zone to enable repeating eight measurements at the same time, and in the four circular area of the control zone that was designed on the paper-based sensor using Adobe illustrator CS4. The wax printing method was used to pattern the resulting design. The fabrication process includes two steps: 1. printing of the wax pattern on the surface of the filter paper (Whatman no. 1) by using the wax printer (Xerox Color Qube 8570, Japan) and 2; melting the wax-printed paper on a hot plate at 175 °C for 40 s. The wax covered area was hydrophobic, while the area without wax was hydrophilic. These processes can be finished within 2 minutes.

3.2.5 Colorimetric assay of Cu(II) on paper based devices

The modified AgNPls at 0.8 μL were dropped onto the detection zone and control zone, and allowed to dry. For Cu(II) measurement, 20 μL of the

standard/sample solutions was added to the sample application zone and then the solution flowed into the detection zone. The color change at the test zone can be observed within 2 mins. For quantitative analysis, the photograph of the results on the paper-based sensor was recorded by a digital camera (Cannon EOS 1000 D1, Japan) in a light control box. Then, color intensity of the testing area on the device was measured using ImageJ 1.45s (National Institutes of Health, USA). Finally, the color intensity values were used to obtain a calibration curve.

3.2.6 Analysis of Cu(II) in real world samples

3.2.6.1 Mineral water and groundwater

The mineral water samples were purchased from a local supermarket. The groundwater samples were obtained from the paddy field of the Suphanburi province, Thailand. All of the water samples were filtered using 0.45 μm member filters before testing.

3.2.6.2 Tomato juices

The tomato juices were purchased from a local supermarket. A 1.5 mL aliquot of the juices was centrifuged for 40 min at 6000 rpm [77]. The centrifuged juice samples were then filtered using cotton and a 0.45 μm membrane filter.

3.2.6.3 Rice

The rice sample was obtained from a Surin Provincial source, Thailand. The samples were digested by an acid digestion method [78]. A 0.5 g of rice sample was added in the mixing between concentrated nitric acid and concentrated perchloric acid in the ratio 1:1 (v/v) and heated to 150 °C and stirred for 4 h. The solution was evaporated to less than 2 mL of volume. Sequentially, the concentrated hydrogen peroxide was added dropwise under heating until the solution was colorless after the

solution was evaporated. Finally, the sample solution was filtered through a 0.45 μm membrane filter.

3.2.6.4 Blood

The leftover blood samples were obtained from the local hospital. The whole blood samples (1 mL) were added to 4 mL of the mixture solution of concentrated nitric acid and concentrated perchloric acid (3:1 v/v) [79] and heated to near dryness. The sample solution was then filtered using a 0.45 μm member filter.

For all cases, the filtered solution was diluted with 0.1 M ammonia buffer at pH 11 before measurement. Fortunately, after preparation of the real samples, the solution obtained was colorless. Therefore, there was no interference effect from color of sample.

3.3 Results and discussion

3.3.1 UV-visible absorption spectra and mechanism of AgNPls the presence of Cu(II)

To understand the mechanism of the catalytic etching of AgNPls by $S_2O_3^{2-}$ for the measurement of Cu(II), the SPR absorption was investigated as shown in Figure 3.1. The CTAB/AgNPls in 0.1 M ammonia buffer at pH 11 exhibited an absorption maximum (λmax) of 563 nm (curve a). After the addition of 1 M $Na_2S_2O_3$ at 1.5 μL in 3 mL of CTAB/AgNPls, the λmax of the CTAB/AgNPls was decreased (curve b) and blue shifted to 522 nm. This is due to the decreased AuNPls size through oxidation of AgNPls with oxygen (O_2). By the addition of Cu(II), the color of the solutions changed from violet-red to colorless within 5 min. The absorbance peak at 522 nm decreased with an increase in concentration of Cu(II) from 50 to 200 ng mL^{-1} (curve c, d and e). The insets of Figure 3.1 show the color change of CTAB/AgNPls caused by the catalytic etching of CTAB/AgNPls by $S_2O_3^{2-}$ in the presence of Cu(II).

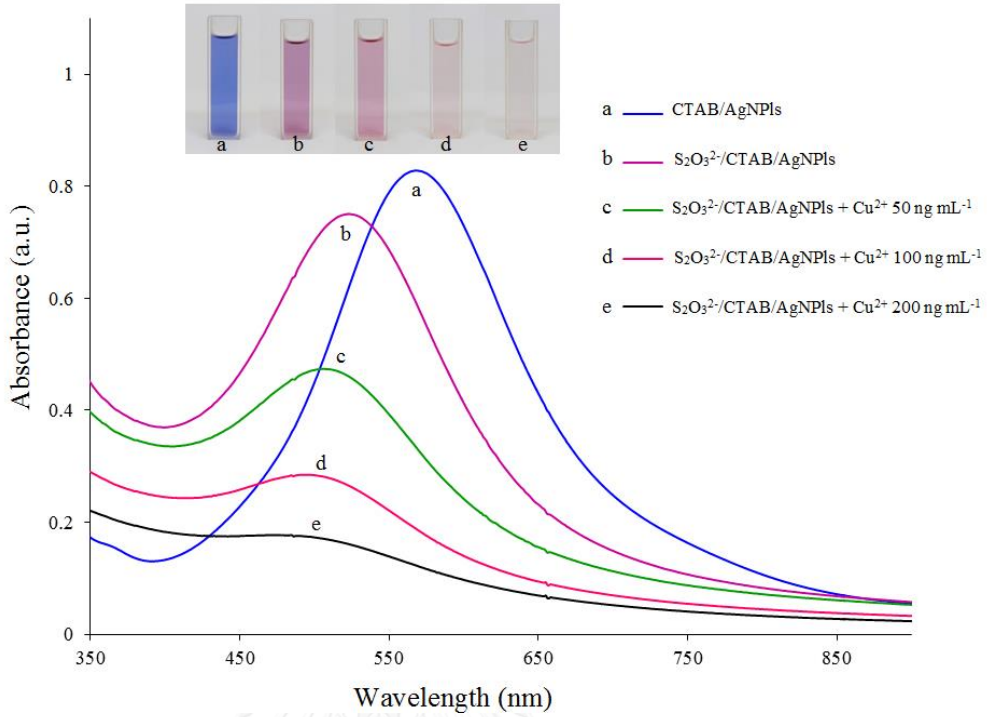

Figure 3.1 The absorption spectra of AgNPls (a) CTAB/AgNPls (max = 563 nm, A = 0.827); (b) $S_2O_3^{2-}$/CTAB/AgNPls (λmax = 522 nm, A = 0.749); (c) $S_2O_3^{2-}$/CTAB/AgNPls + 50 ng mL^{-1} of Cu(II) (A = 0.473); (d) $S_2O_3^{2-}$/CTAB/AgNPls + 100 ng mL^{-1} of Cu(II) (A = 0.284); (e) $S_2O_3^{2-}$/CTAB/AgNPls + 200 ng mL^{-1} of Cu(II) (A = 0.174). The experiment was carried out at room temperature in 0.1 M ammonia buffer pH 11, The UV-vis spectra was investigated after 5 min. (Inset: The color product of the catalytic etching of modified CTAB/AgNPls with $S_2O_3^{2-}$ for measurement of Cu(II)).

Upon the addition of $S_2O_3^{2-}$ ions to CTAB/AgNPls, the AgNPls can be oxidized by dissolved O_2 leading to reduction of the particle size of AgNPls (Figure 3.2). However, it was found that this reaction is very slow because the $Ag(S_2O_3)_2^{3-}$ complexes immediately generated a passive layer on the surface AgNPls. By adding Cu(II), the Cu(II) in the 0.1 M ammonia buffer at pH 11 forms the $Cu(NH_3)_4^{2+}$ complex and the standard potential of $Cu(NH_3)_4^{2+}$/Cu(II) in the presence of $S_2O_3^{2-}$ was increased (eq.

3.2). The Cu(II) could accelerate the etching rate of the AgNPls by forming $Cu(S_2O_3)_3^{5-}$ and the complexes could also be oxidized to Cu(II) by dissolved oxygen (eq. 3.3). The etching of $S_2O_3^{2-}$/CTAB/AgNPls increased with increasing concentration of Cu(II). As a result, the color solution changes from violet-red to colorless. Therefore, the colorimetric detection based on the catalytic etching of modified AgNPls provides a simple and sensitive method for the measurement of trace Cu(II)

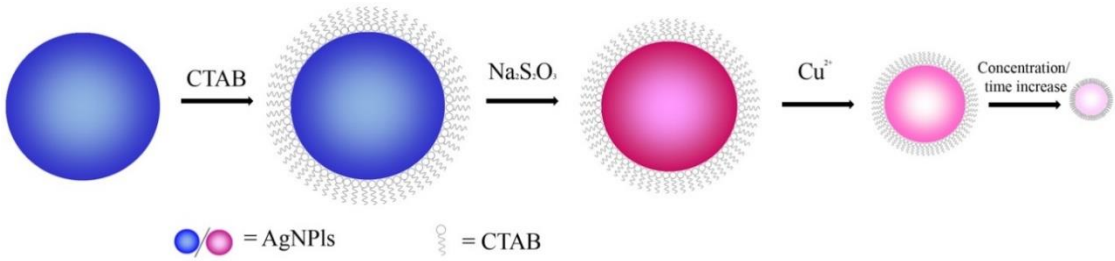

Figure 3.2 The catalytic etching mechanism of the CTAB/AgNPls by $S_2O_3^{2-}$ for Cu(II) measurement

$$Ag(S_2O_3)_2^{3-} + e^- \longrightarrow Ag^0 + 2S_2O_3^{2-} \qquad E^\circ = 0.01\ V \qquad (3.1)$$

$$Cu(NH_3)_4^{2+} + 2e^- \longrightarrow Cu^0 + 4NH_3 \qquad E^\circ = -0.04\ V \qquad (3.2)$$

$$Cu(NH_3)_4^{2+} + 3S_2O_3^{2-} + e^- \longrightarrow Cu(S_2O_3)_3^{5-} + 4NH_3 \qquad E^\circ = 0.22\ V \qquad (3.3)$$

$$Ag^0 + 5S_2O_3^{2-} + Cu(II) \longrightarrow Cu(S_2O_3)_3^{5-} + Ag(S_2O_3)_2^{3-}$$

O_2

3.3.2 Paper-based sensor for tract determination of Cu(II)

To improve the colorimetric determination of Cu(II) for rapid on-site screening applications, the developed approach using a paper-based sensor was applied. The $S_2O_3^{2-}$/CTAB/AgNPls was pre-prepared with the test zone and control zone on the paper-based sensor as fabricated by wax printing method (Figure 3.3a). For Cu(II)

measurement, the sample solution at 20 µL was applied at the sample zone and then the solution flowed outward via capillary forces to the eight detection zones. In the absence of Cu(II), the color results at the detection zone were not changed (Figure 3.1.3b). However, in the presence of Cu(II), the color at the detection zones changed from violet-red to colorless with increasing Cu(II) concentration, which can be monitored by the naked eye after 120 s (Figure 3.3c and d). The SEM image of the paper based-sensor at the detection zone was shown in Figure 3.3 both (e) without and (f) with AgNPls, and (g) AgNPls in the presence of Cu(II). The results indicated that the modified AgNPls were etched by Cu(II). Additionally, the TEM image (Figure 3.3h) clearly shows that the $S_2O_3^{2-}$/CTAB/AgNPls was well dispersed in the aqueous solution. The average size of $S_2O_3^{2-}$/CTAB/AgNPls was approximately 30 nm. After the addition of Cu(II) (Figure 3.3i), the $S_2O_3^{2-}$/CTAB/AgNPls would be catalytically oxidized and etched into the solution. The average size of $S_2O_3^{2-}$/CTAB/AgNPls were decreased after incubation for 5 min at room temperature.

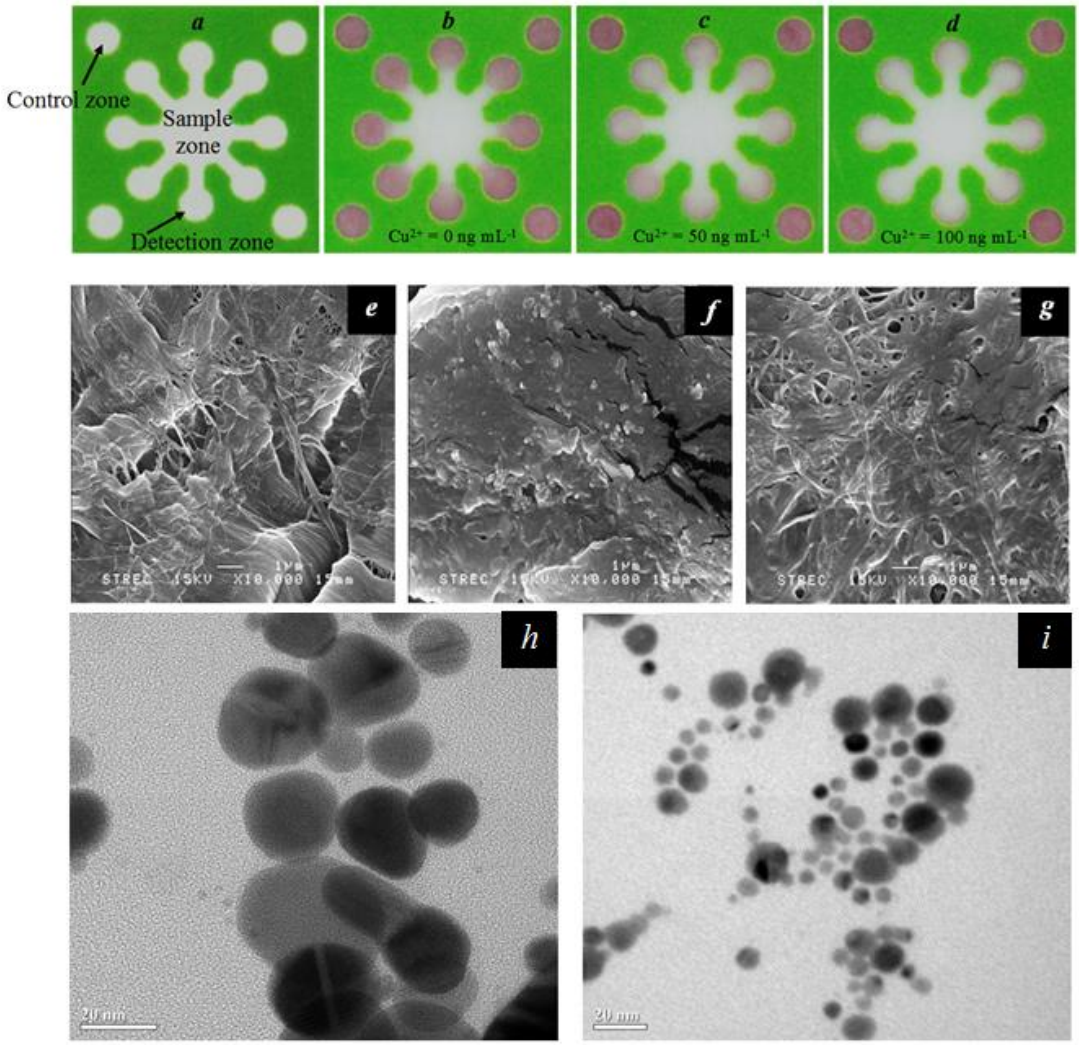

Figure 3.3 Paper-based colorimetric sensor based on the catalytic etching mechanism of the CTAB/AgNPls with $S_2O_3^{2-}$ for measurement of Cu(II) at (a) image of paper-based deviecs; image of paper-based devices after measurement of Cu(II) (b) 0 ng mL^{-1}, (c) 50 ng mL^{-1} and (d) 100 ng mL^{-1} of Cu(II); the SEM images of paper-based sensor at the detection zone (e) without CTAB/AgNPls (f) with CTAB/AgNPls (g) CTAB/AgNPls in the presence of 100 ng mL^{-1} Cu(II); the TEM images of $S_2O_3^{2-}$/CTAB/AgNPls without Cu(II) (h) and with 100 ng mL^{-1} of Cu(II) (i).

3.3.3 Optimization of the detection conditions

The sensitivity of the paper-based colorimetric sensors containing the modified AgNPls for Cu(II) detection is related to various factors including, pH of buffer solutions, concentrations of AgNPls and $S_2O_3^{2-}$ and incubation time. Therefore, these parameters were optimized by using 100 ng mL^{-1} of Cu(II). The difference in the color intensity values of the AgNPls before and after the addition of Cu(II) ($\Delta I = I_{sample} - I_{blank}$) was determined.

3.3.3.1 Effect of the pH of the ammonia buffer

The influence of the pH on this system was investigated in pH range of 6.0-11.0 (Figure 3.4a). At pH lower than 8, the ΔI decreased because the $S_2O_3^{2-}$ was not stable and broke down into sulfate, sulfide, sulfite tetrathionate, trithionate, polythionates and polysulfides [80]. However, in the pH range of 9-12, the complex $Cu(NH_3)_4^{2+}$ concentration increased with increasing NH_3 concentration, enabling the oxidation of AgNPls by $Cu(NH_3)_4^{2+}$. The intensity color of modified AgNPls was almost constant above pH 11 in the presence Cu(II). Therefore, pH 11 was selected as the optimal value for all experiment.

3.3.3.2 Effect of the concentration of AgNPls

The effect of AgNPls concentration was investigated in the range of 40-360 μg mL^{-1}. As the results show in Figure 3.4b, ΔI increased with increasing AgNPls concentration and tends to be stable above 200 μg mL^{-1}. Therefore, 0.8 μL of 200 μg mL^{-1} AgNPls was used to prepare the detection and control zone on the paper-based sensor in future experiments.

3.3.3.3 Effect of the concentration of $S_2O_3^{2-}$ and the incubation time

The concentration of $S_2O_3^{2-}$ and the incubation time have influences on the detection of Cu(II)$^{-}$. The effect of the $S_2O_3^{2-}$ concentration was examined in range of 1.0-9.0 mM (Figure 3.4c). The ΔI value increased with increasing $S_2O_3^{2-}$ concentration and slightly decreased above 5.0 mM. Therefore, the concentration of 5.0 mM $S_2O_3^{2-}$ was selected as the optimized concentration. Furthermore, the effect of incubation time on the Cu(II) detection was studied. The ΔI increased with increasing incubation time and remains constant above 120 sec (Figure 3.4d). This indicated that the developed method provides a rapid measurement of Cu(II).

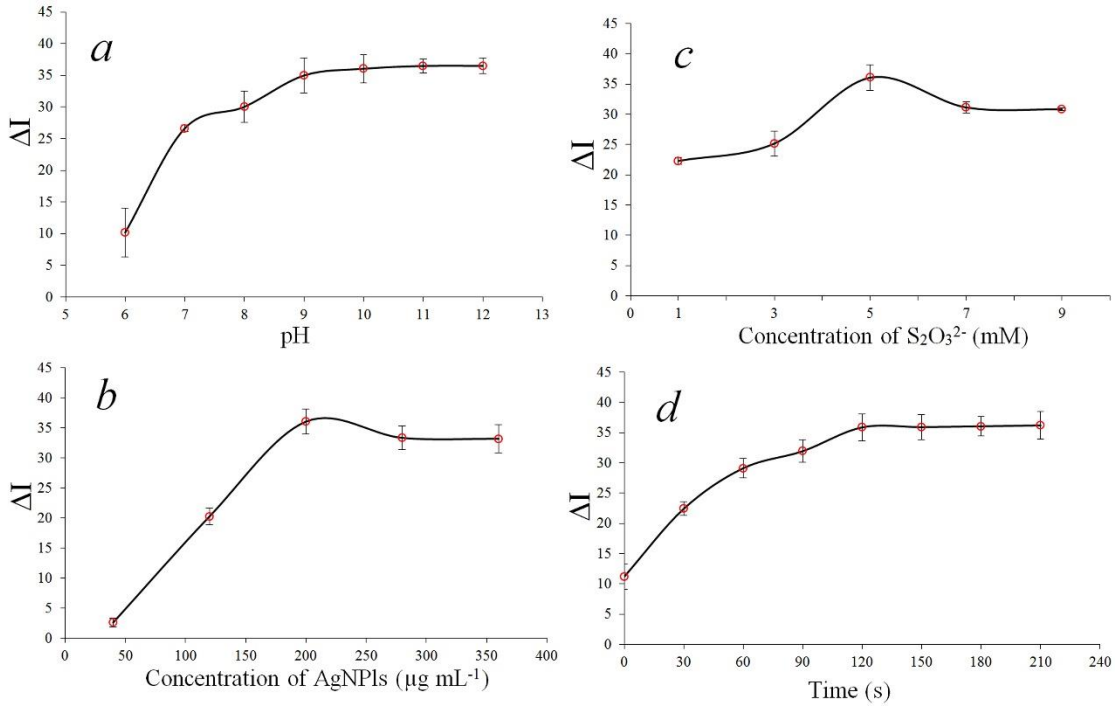

Figure 3.4 Effect of experimental conditions for Cu(II) measurement on paper-based sensor; (a) pH of ammonia buffer, (b) concentration of AgNPls, (c) concentration of $S_2O_3^{2-}$ and (d) incubation time.

3.3.4 Selectivity of the modified AgNPls for the determination of Cu(II)

In order to evaluate the selectivity of the colorimetric assay for the determination of Cu(II), the other environmentally relevant metallic ions including K^{+}, Cr^{3+}, Cd^{2+}, Zn^{2+}, As^{3+}, Mn^{2+}, Co^{2+}, Pb^{2+}, Al^{3+}, Ni^{2+}, Fe^{3+}, Mg^{2+}, Hg^{2+} and Bi^{3+} were investigated under optimized conditions. The metal ions were prepared in 0.1 M ammonia buffer at pH 11 at concentration of 100 times higher than Cu(II). The plots of the mean color intensity as determined by NIH ImageJ analysis of the results image versus the concentration of metal ions are shown in Figure 3.5. As a result, only Cu(II) can oxidize modified AgNPls, causing the color change of the modified AgNPls from violet-red to colorless, and this change can be monitored by the naked eye.

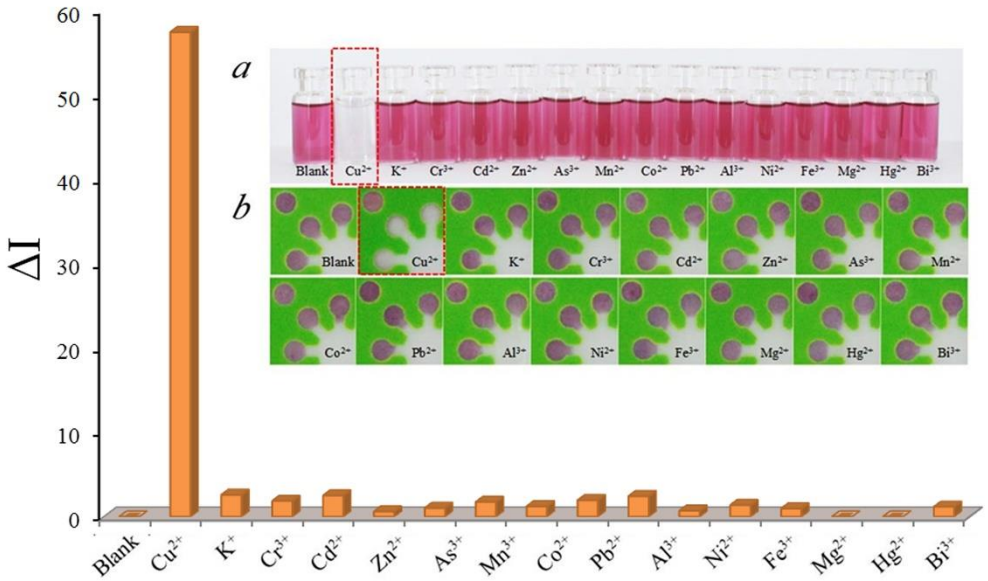

Figure 3.5 The mean color intensity values of the modified AgNPls on paper-based sensor after addition of different metal ions at concentration of 100 ng mL^{-1} Cu(II)and 10 µg mL^{-1} others metals. Inset: The photographic images results of colorimetric determination of metal ions (a) in solution (b) on paper-based devices.

In order to study the influence of other ions on the catalytic etching of AgNPls induced by Cu(II), competitive experiments were carried out in the presence of 100 ng mL^{-1} Cu(II) and 10 µg mL^{-1} of other metal ions including K^{+}, Cr^{3+}, Cd^{2+}, Zn^{2+}, As^{3+}, Mn^{2+} Co^{2+}, Pb^{2+}, Al^{3+}, Ni^{2+}, Fe^{3+}, Mg^{2+}, Hg^{2+}, Bi^{3+}, SO_4^{2-}, NO^{3-} and Cl^{-}. The results obtained by measurement of the mixture solution of Cu(II) and a common ion were not different from Cu(II) alone (Figure 3.6). This indicates that the proposed method offers a high selectivity for the determination of Cu(II).

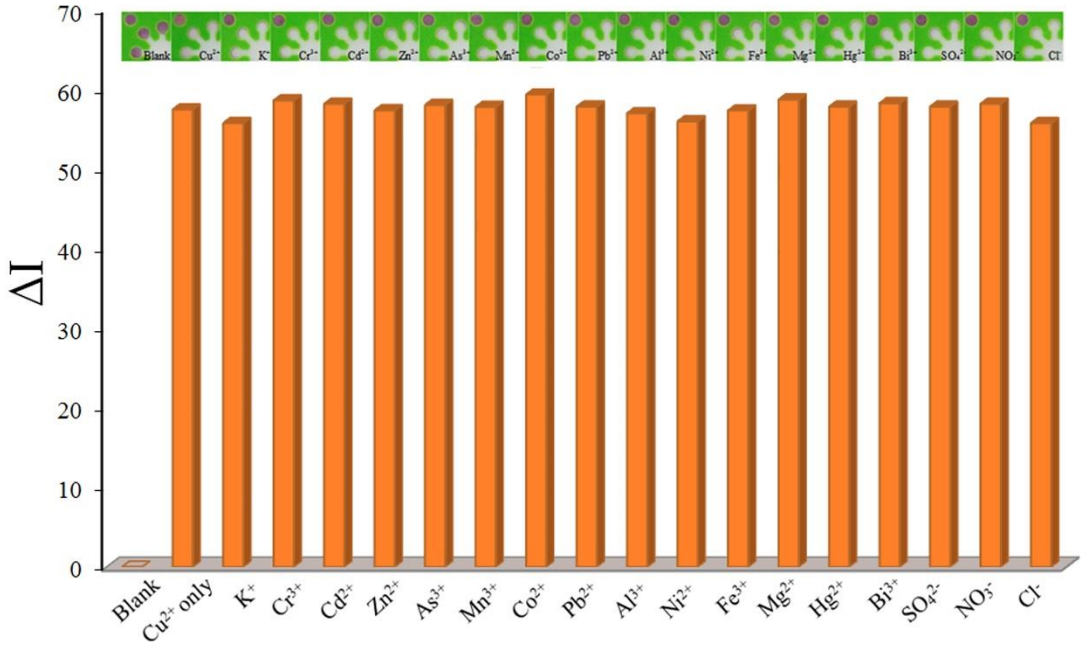

Figure 3.6 Effect of other common ions (10 µg mL^{-1}) on the determination of 100 ng mL^{-1} Cu(II). Inset: corresponding photographs of the paper-based sensor at the detection zone after addition of Cu(II) and Cu(II) with various other common ions.

3.3.5 Analytical performance

The performance of the developed method was evaluated for the quantitative detection of Cu(II). Under the optimized conditions, the color intensity values of modified AuNPls at the detection zone on paper-based devices were examined at room temperature in the presence of Cu(II) in rage of 0-350 ng mL^{-1}. The pinkest of

the violet colors at the test zone changed to colorless after adding Cu(II) to over 0.1 ng mL^{-1}, and these results can easily be distinguished by the naked eye as shown in Figure 3.7a. The plots of the mean intensity and concentration of Cu(II) show a reasonable linearity in the range of 0.5-200 ng mL^{-1} (R^2 = 0.9974), with a LOD and LOQ of 0.35 and 1.16 ng mL^{-1}, respectively (Figure 3.7b), which is lower than that obtained from the other nanoparticles. (Table 3.1). The obtained LOQ values are lower than the maximum allowable levels of 1.30 µg mL^{-1} in the United States for drinking water (3], and ~2.00 µg mL^{-1} in Thailand for surface water (4]

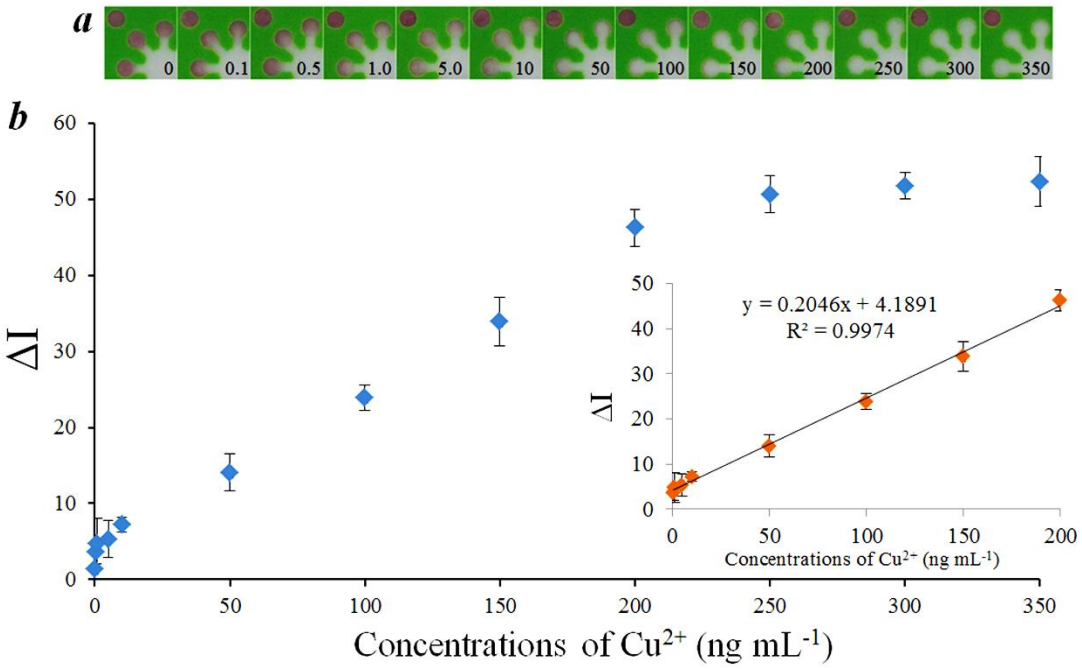

Figure 3.7 (a) Corresponding photographs of the paper-based sensor at detection zone for detection of Cu(II)at various concentrations. (b) The plot of the mean intensity of the AgNPls color determined by photograph analysis using NIH ImageJ vs. Cu(II) concentration (0-350 ng mL^{-1}). Inset: linear regression analysis and best fit line in the concentration range of 0.5-200 ng mL^{-1} Cu(II).

Table 3.1 Comparison of the performance of different nanoparticles for the detection of Cu(II)

Nanoparticles	Method	LOD (ng mL^{-1})	Linearity range (ng mL^{-1})	Incubation time (min)	Ref.
Starch-stabilized silver nanoparticles	Colorimetric assay	31.75	6.35 to 63.5	10	[66]
D-penicillamine/gold nanoparticles	Colorimetric assay	1.9	3.17 to 117.47	12	[81]
CTAB/thiosulfate/gold nanoparticles	Colorimetric assay	0.32	0.63 to 5.08	25	[69]
4-mercaptobenzoic acid/silver nanoparticles	Colorimetric assay	1.58	6.35 to 6350	30	[64]
Gold nanorods	Colorimetric assay	13.97	5.08 to 304.8	25	[82]
NaSCN /H_2O_2/Gold nanorods	Colorimetric assay	0.65	0.65 to 19.05	17	[83]
ZnO@ZnS core–shell nanoparticles	Colorimetric paper assay	952.5	952.5 to 95250	20	[84]
Homocysteine/dithiothreitol /silver nanoparticles	Colorimetric paper assay	0.5	0.5 to 3.98	5	[67]
CTAB/thiosulfate/ silver nanoplates	Colorimetric paper assay	0.3	0.5 to 200	2	In this work

3.3.6 Semi-quantitative determination of Cu(II) in real samples

To demonstrate the utility of our approach, the developed devices were evaluated for detecting Cu(II) in real samples, including mineral water, groundwater, tomato, rice and blood samples. Cu(II) was spiked into the samples at concentration levels of 10, 50 and 100 ng mL^{-1} and was measured using the developed devices. The recovery results are shown in Table 3.2, the recoveries and %RSDs of Cu(II) were found in the range of 92.60-119.01 % and 0.87-9.16 %, respectively, which suggests that this method is reliable. In addition, the unknown samples were then determined by both the developed method and the standard method, i.e., inductively coupled plasma optical emission spectrometry (ICP – OES) (Table 3.3). The results from the developed method were in good agreement with those from the ICP – OES method (paired t-test at the 95% confidence level gave $t_{calculated}$ (1.346) below $t_{critical}$ at t = 2.776 with 4 degrees of freedom). These results indicate that the developed paper-based colorimetric sensor that is based on the thiosulfate catalytic etching of AgNPls is applicable for Cu(II) detection in real samples.

Table 3.2 Recovery tests of the proposed method and standard method for the determination of Cu(II) in real samples (n=3)

Sample	Proposed method				Standard method [a]			
	Cu (II) (ng mL^{-1})		%Recovery	%RSD	Cu (II) (ng mL^{-1})		%Recovery	%RSD
	Added	Found			Added	Found		
Drinking water	10.00	9.89 ± 1.77	98.95	7.91	10.00	9.98 ± 0.43	99.80	4.31
	50.00	49.95 ± 3.26	99.89	6.52	50.00	50.64 ± 1.03	101.28	2.03
	100.0	98.06 ± 0.96	98.06	0.9	100.0	100.23 ± 0.84	100.23	0.84
Groundwater	10.00	10.20 ± 0.69	101.99	6.78	10.00	10.11 ± 0.20	101.10	1.98
	50.00	53.27 ± 1.25	106.57	2.35	50.00	50.71 ± 1.19	101.42	2.35
	100.0	95.23 ± 0.83	95.23	0.87	100.0	98.92 ± 0.39	98.92	0.39
Tomato	10.00	11.90 ± 0.41	119.01	3.41	10.00	10.78 ± 0.12	107.80	1.11
	50.00	48.88 ± 0.97	97.76	1.99	50.00	50.21 ± 0.43	100.42	0.86
	100.0	102.36 ± 0.93	102.36	0.91	100.0	99.21 ± 0.53	99.21	0.53
Rice	10.00	9.90 ± 0.76	99.01	7.71	10.00	10.12 ± 0.22	101.20	2.17
	50.00	46.30 ± 3.44	92.60	7.44	50.00	46.30 ± 1.24	92.60	2.68
	100.0	99.04 ± 2.15	99.04	2.17	100.0	98.21 ± 1.50	98.21	1.53
Blood	10.00	10.40 ± 0.95	103.98	9.16	10.00	11.02 ± 0.53	110.20	4.81
	50.00	52.90 ± 3.23	105.80	6.11	50.00	50.01 ± 1.66	100.02	3.32
	100.0	98.06 ±1.83	98.06	1.87	100.0	100.61 ± 0.98	100.61	0.97

[a] Inductively coupled plasma optical emission spectrometry (ICP-OES)

Table 3.3 Determination of Cu(II) in real samples using paper-based b colorimetric sensor based on thiosulfate catalytic etching of AgNPls at room temperature

Sample	Proposed method (n=8)	Standard method [a] (n=3)
Drinking water	14.26 ± 0.92 ng mL^{-1}	13.75 ± 0.39 ng mL^{-1}
Groundwater	30.93 ± 1.56 ng mL^{-1}	29.48 ± 0.18 ng mL^{-1}
Blood	34.27 ± 1.72 ng mL^{-1}	27.10 ± 0.08 ng mL^{-1}
Tomato	2.10 ± 0.47 ng mg^{-1}	2.18 ± 0.14 ng mg^{-1}
Rice	4.37 ± 1.08 ng mg^{-1}	4.13 ± 0.09 ng mg^{-1}

[a] Inductively coupled plasma optical emission spectrometry (ICP-OES)

3.4 Conclusion

A paper-based device with a highly sensitive and selective colorimetric assay that is based on the catalytic etching of modified AgNPls by thiosulfate was developed for the rapid detection of Cu(II). The developed sensor was easily fabricated by a wax screen printing method. In the presence of Cu(II), the color of modified AgNPls changed from pinkish-violet to colorless at the detection zone and the change can be easily detected by the naked eye. The approach demonstrated good selectivity for Cu(II) against other metal ions. For semi-quantitative analysis, the color intensity values of the paper-based sensor photograph were digitized by NIH ImageJ software to obtain the calibration curve. The color intensity values are linear with the concentration of Cu(II) ranging from 0.5-200 ng mL^{-1} with a coefficient of 0.9974, and shows good sensitivity with a LOD = 0.35 ng mL^{-1}. Furthermore, this method was successfully used for the determination of Cu(II) in real samples (mineral water, groundwater, tomato, rice and blood). The developed paper-based colorimetric sensor that is based on the thiosulfate etching of silver nanoplates has great potential for the low-cost, rapid, simple, portable, highly sensitive and selective determination of Cu(II) levels.

Parts II:

High sensitivity and specificity simultaneous determination of lead, cadmium and copper using microfluidic paper-based analytical device with dual electrochemical and colorimetric detection

Sudkate Chaiyo[a], Amara Apilux[b], Weena Siangproh[c]*, Orawon Chailapakul[a, d]**

[a] Electrochemistry and Optical Spectroscopy Research Unit, Department of Chemistry, Faculty of Science, Chulalongkorn University, 254 Phayathai Road, Pathumwan, Bangkok 10330, Thailand

[b] Center for Innovation Development and Technology Transfer, Faculty of Medical Technology, Mahidol University, 999 Phuttamonthon 4 Road, Salaya, Nakhon Pathom 73170, Thailand

[c] Department of Chemistry, Faculty of Science, Srinakharinwirot University, Sukhumvit 23, Wattanna, Bangkok 10110, Thailand

[d] Center for Petroleum, Petrochemicals and Advanced Materials, Chulalongkorn University, 254 Phayathai Road, Pathumwan, Bangkok 10330, Thailand

** Corresponding author

* Co-corresponding author

Sensors and Actuators B: Chemical 233 (2016): 540-549.

Abstract

A bismuth-modified electrode can increase the sensitivity of lead and cadmium detection. However, use of a bismuth-modified electrode in the detection of copper remains limited because the bismuth signal overlaps with the signal for copper. In this study, a new microfluidic paper-based analytical device (μPAD) coupled with dual electrochemical and colorimetric detection was developed to obtain high sensitivity and specificity for the simultaneous determination of lead, cadmium and copper. The μPAD is divided into two parts. The first part is electrochemical detection for the determination of lead and cadmium using a bismuth-modified, boron-doped diamond electrode (Bi-BDDE). The limit of detection was 0.1 ng mL^{-1} (for both metals). The second part is colorimetric detection for the determination of copper based on the catalytic etching of silver nanoplates (AgNPls) by thiosulfate ($S_2O_3^{2-}$). The color of AgNPls on μPAD changed from pinkish violet to colorless after the addition of copper; this change can be monitored by naked eyes and its detection limit was 5.0 ng mL^{-1} by the Image J analysis. The proposed method was applied for the simultaneous determination of these three metals in real samples and no significant differences in accuracy and precision were observed compared to the standard method.

Keywords: lead, cadmium, copper, microfluidic paper-based analytical device, dual detection

3.5 Introduction

Heavy metal ions are hazardous pollutants to living organisms that can accumulate in the human body via the food chain and cause adverse effects on the immune, central nervous and reproductive systems [85]. Metal ions such as lead (Pb(II)), cadmium (Cd(II)), copper (Cu(II)), mercury (Hg(II)), and zinc (Zn(II)) are serious hazards that cannot be degraded in the environment. Therefore, a rapid, sensitive, and simple method for the determination of these trace heavy metal ions is critically important.

Several techniques for the determination of trace heavy metal ions, including atomic absorption spectroscopy (AAS) [86], inductively coupled plasma-mass spectrometry (ICP-MS) [87] and inductively coupled plasma optical emission spectrometry (ICP-OES) [88], are available. However, these techniques have some drawbacks; they are time-consuming, costly and require complex and expensive instrumentation. Therefore, they are unsuitable for field analysis. Currently, electrochemical detection has attracted extensive attention due to their intrinsic advantages of simplicity, portability, low cost, high sensitivity, and excellent selectivity [89]. Early electroanalytical methods were frequently conducted with hanging mercury drop electrodes [90] and mercury-film working electrodes [91]. However, the toxicity of mercury and mercury salt for humans and the environment has significantly hindered the use of this electrode. Currently, the bismuth-modified electrode has attracted considerable interest because its behavior is similar to the behavior of a mercury-film electrode and presents significantly low toxicity [92]. Bismuth film electrodes, formed by electrochemical deposition on substrates, including glassy carbon electrodes [93], screen-printed carbon electrodes (SPCEs) [94], carbon paste electrode (CPEs) [95] and boron doped diamond electrodes (BDDEs) [96]. Among these electrode substrates, the BDDEs offers the most favorable electroanalytical properties. These beneficial properties include a wide potential window, a low background current, chemical inertness, and the readily renewable surface of the BDDEs [97]. Therefore, the BDDEs is a potentially ideal substrate electrode for the application of a bismuth- modified electrode.

Cu(II) is commonly detected in environmental samples, which poses a problem for the environmental analysis of a trace heavy metal. The use of a bismuth-modified electrode for the detection of Cu(II) remains limited because the signal of stripping bismuth overlaps with the signal of Cu(II) [98, 99]. Therefore, the simultaneous determination of Cu(II) in samples with other trace heavy metals is important and challenging. Based on this problem, the development of a simple colorimetric detection to the simultaneous determination of Cu(II) with trace heavy metals (Pb(II) and the detection of Cd(II)) using a bismuth-modified boron doped diamond electrode (Bi-BDDE) is our primary objective.

In 2007, the concept of a microfluidic paper-based analytical device (μPAD) was developed by the Whitesides group [15]. The μPAD is a new alternative device that can be applied to food analysis, environmental monitoring, and clinical diagnosis due to their advantages of simplicity, high throughput, disposability, low sample and reagent consumption, low cost, and portability [18, 20, 41, 100]. Several detectors of μPADs are proposed: for example, colorimetry [41], electrochemical [18], chemiluminescence [100], electrochemiluminescence [20] and electrical [47] methods. These techniques have advantages and disadvantages in terms of sensitivity, simplicity and cost-effectiveness. Recently, an interesting sensing approach for μPADs involved the realization of a dual-detection device. The first hybrid paper-based device, which consisted of colorimetric and electrochemical detection, was proposed for the simultaneous detection of Au(III) and Fe(III) in industrial waste solutions [71]. Although hybrid detection instruments are a feasible alternative to single-type sensing assays, they require multiple readout mechanisms.

The objective of this study is to develop μPADs combined with dual electrochemical and colorimetric detection for high sensitivity, specificity, rapidity, simplicity, portability, and the simultaneous determination of Pb(II), Cd(II) and Cu(II). Electrochemical detection with bismuth-modified boron doped diamond electrodes (Bi-BDDEs) was employed to measure Pb(II) and Cd(II), whereas colorimetric detection for the determination of Cu(II) based on the catalytic etching of silver nanoplates (AgNPls) by thiosulfate ($S_2O_3^{2-}$) [101] was proposed. In the presence of Cu(II), the catalytic etching system induced a distinct decrease in the size of the AgNPls and

concomitantly produced a red-shift with a pinkish violet to colorless change. The proposed devices were successfully applied to the simultaneous determination of Pb(II), Cd(II) and Cu(II) in real samples.

3.6 Experimental

3.6.1 Reagents and apparatus

Standard solutions of 1000 μg mL^{-1} Pb(II), Cd(II), Hg(II), Bi(III), As(III), Co(II) and Zn(II) were purchased from Spectrosol (Poole, UK), and standard solutions of 1000 μg mL^{-1} Ni(II) and Al(III) were purchased from Merck (Darmstadt, Germany). Copper sulfate ($CuSO_4$, BDH, UK), ammonium hydroxide (NH_4OH, BDH, England), sodium thiosulfate ($Na_2S_2O_3$, Sigma-Aldrich, Missouri), hexadecyltrimethylammonium bromide (CTAB, Sigma-Aldrich, Missouri), magnesium sulfate ($MgSO_4$, Sigma-Aldrich, Missouri), manganese chloride ($MnCl_2$, Sigma-Aldrich, Missouri), ammonium dichromate ($(NH_4)_2Cr_2O_7$, Sigma-Aldrich, Missouri), ammonium chloride (NH_4Cl, Ajax, Australia), iron chloride hexahydrate ($FeCl_3.6H_2O$, Merck, Germany), sodium chloride (NaCl, Univar, Redmond, WA) and potassium chloride (KCl, Univar, Redmond, WA) were used as received. All chemicals were analytical-grade chemicals. Ultrapure water (resistivity ≥ 18.2 MΩ.cm at 25 °C) was used to prepare all aqueous solutions (obtained from a Millipore Milli-Q purification system).

Electrochemical measurements were performed using a model—the PGSTAT 101 Autolab Electrochemical System—controlled with the NOVA software package (Kanaalweg 29-G 3526 KM Utrecht, The Netherlands). A three-electrode system, in which a silver/silver chloride paste 70/30 (Gwent Electronic Materials Ltd., UK) served as the reference electrode, a carbon ink (Acheson, California, USA) served as the auxiliary electrode and BDDE served as working electrode, was employed. The screen-printed block was fabricated by Chaiyaboon Co. Ltd. (Bangkok, Thailand). The absorbance measurement was conducted by a UV–visible spectrophotometer (HP HEWLETT PACKARD 8453, UK) using a 1.0 cm path length quartz cell. Transmission electron microscopy (TEM) was recorded by an H-7650 transmission electron microscope (Hitachi Model, Japan).

3.6.2 Design and fabrication of the μPAD

The design of the wax-patterned paper, including the electrochemical detection zone (cycle, diameter = 1 cm), the colorimetric detection zone (cycle, diameter = 3 mm), the channel connection among the electrochemical detection zone, the colorimetric detection zone (channel, 1 x 1 mm) and the reference color zone (cycle, diameter = 3 mm), as defined in Figure 3.8a, was created using Adobe Illustrator software (Adobe Systems, Inc.). The wax-pattern was printed onto Whatman grade 1 filter paper using a solid-wax printer (Xerox Color Qube 8570, Japan). After printing the wax pattern, the printed paper is placed on a hot plate and the wax on the filter paper is melted and spread throughout the thickness of the filter paper. The wax-covered area was hydrophobic, whereas the area without wax was hydrophilic. For the electrochemical detection zone, the two electrodes were fabricated on wax-patterned paper using the screen-printing method, carbon ink served as the counter electrode and silver/silver chloride ink served as the reference electrode (Figure 3.8a). After each printing step, the wax-patterned paper was cured in the oven at 65 °C for 30 min. The finished product is shown in Figure 3.8a. To complete the device, a BDD electrode was attached to the wax-patterned paper using 8 mm-punched double-sided adhesive tape, and the modified AgNPls at 0.8 μL were dropped onto the colorimetric detection zone and the reference color zone. All fabrication procedures of the μPAD are shown in Figure 3.8b.

3.6.3 Electrochemical detection of Pb(II) and Cd(II)

Anodic stripping voltammetry (ASV) was chosen for the determination of trace heavy metals due to its high sensitivity, simplicity, speed, low cost and low detection limits [102]. ASV measurements were performed with *in situ* bismuth film preparation. For the analytical procedures, 50 μL of the mixture between 2 μg mL^{-1} Bi(III) and appropriate amounts of Pb(II) and Cd(II) in 0.2 M NaCl solutions (pH 6.0) was added to the electrochemical detection zone of μPAD, which caused the solution flows through the channels to the colorimetric detection zones, whereas the solution covered the three electrodes. A preconcentration was performed at -1.2 V for 120 s, where Bi(III) and the target metals were simultaneously deposited on the surface of the electrode.

After the accumulation time, the voltammogram was recorded between -1.2 V and 0.2 V (Figure 3.8c). All experiments were conducted at room temperature (25 °C).

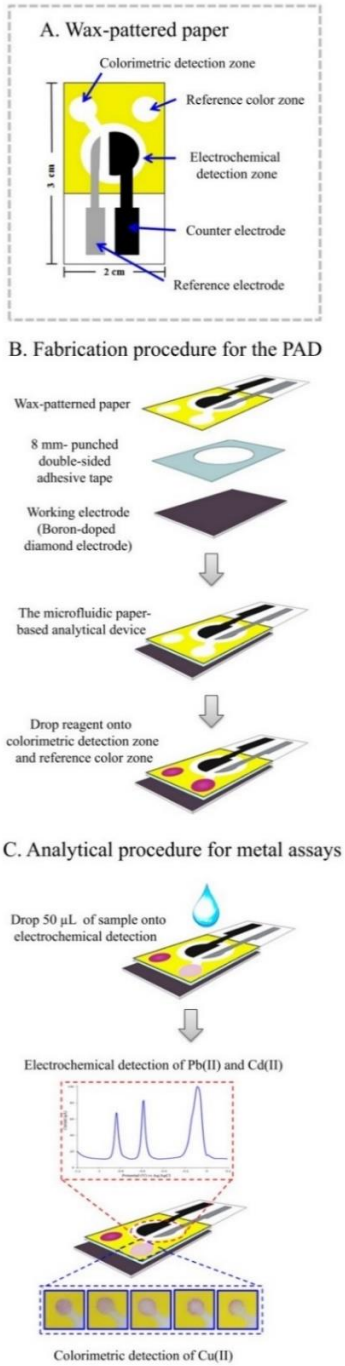

Figure 3.8 Drawings of µPAD coupled the dual electrochemical/colorimetric detection (a). Schematics of the fabrication procedure for a µPAD (b). Analytical procedures for the simultaneous determination of Pb(II), Cd(II) and Cu(II) (c).

3.6.4 Colorimetric detection of Cu(II)

AgNPls were synthesized by the reported procedure using the chemical reduction process [76]. Sodium borohydride and methyl cellulose solution served as the reducing agent and the stabilizer, respectively, and the shape transformation was achieved using a 30% H_2O_2 solution. AgNPls solutions were obtained from the Sensor Research Unit at the Department of Chemistry, Faculty of Science, Chulalongkorn University. For the modification of AgNPls, 200 μg mL^{-1} AgNPls solution was prepared from the dilution of 1000 μg mL^{-1} AgNPls stock solution with 0.1 M ammonia buffer at pH 11. Subsequently, 10 μL of 0.1 M CTAB was added to 1 mL of 200 μg mL^{-1} AgNPls. Sequentially, 5 μL of 1.0 M $Na_2S_2O_3$ were added to the CTAB-capped AgNPls followed by incubation of the mixture for 5 min at room temperature. To complete the measurement, 0.8 μL of modified AgNPls solution was added to the colorimetric detection zone, and 50 μL of standard/sample solution were added to the electrochemical detection zone of μPAD; the solution flowed into the colorimetric detection zone by capillary force. The color change in the test zone was observed within 120 s. A digital camera (Cannon EOS 1000 D1, Japan) was used to record a μPAD image of the colorimetric measurements. All experiments of colorimetric detection were performed in a light control box. For the quantitative analysis, the color intensity of the colorimetric detection area on a μPAD was measured using ImageJ 1.45s (National Institutes of Health, USA).

3.6.5 Simultaneous determination of Pb(II), Cd(II) and Cu(II) in real samples

3.6.5.1 Stream water and groundwater

Stream water (collected in Saen Saep stream, Bangkok, Thailand) and groundwater (collected in Suphanburi, Thailand) were filtered through a 0.45 μm membrane filter to remove suspended particles. Subsequently, 2 mL of each sample solution was transferred to a volumetric flask and diluted to 10 mL with 0.2 M NaCl.

The pH of the sample solutions was adjusted to pH 6.0 by the addition of NaOH solution prior to analysis using the proposed devices.

3.6.5.2 Rice and fish

The commercial rice and fish samples were purchased from a local market. The treatment process was performed according to published literature with slight modifications [103]. The sample (rice or fish) was grinded by a blender machine into a fine powder for the rice sample or small pieces for the fish sample. Subsequently, 0.2 g of the sample (rice or fish) was digested with 3 mL of the mixture of HNO_3 and $HClO_4$ (1:1). The samples were heated at 100 $^{\circ}$C for 4 h to digest the samples and evaporate the solvent. Then, 10 mL of 0.2 M NaCl was added and heated until a clear solution was formed (~1 h). The residue was adjusted to 10 mL with 0.2 M NaCl (pH 6.0), and the resulting mixture was filtered through a membrane with a pore size of 0.45 μm. Prior to measurement, the pH of the digest solutions was adjusted to pH = 6.0 by adding an appropriate amount of NaOH solution.

3.7 Results and discussion

3.7.1 Comparison of the electrochemical response between Bi-BDDEs and Bi-SPCEs

In previous study, the authors discussed the attractive stripping behavior of bismuth-coated electrodes for trace measurements of Pb(II) and Cd(II). Figure 3.9 shows the ASV analytical characteristics from use of a screen printing carbon electrode (SPCE) and a BDDE by *in situ* plating bismuth film on paper devices. The stripping voltammograms were recorded using 0.2 M NaCl (pH = 6.0), which contained 50 ng mL^{-1} Pb(II) and Cd(II) and 2 μg mL^{-1} Bi(III). The stripping peaks were observed at -0.85 V and -0.58 V for Cd(II) and Pb(II), respectively, at both bismuth-modified SPCE and BDDE. The bismuth-modified electrodes exhibited superior voltammetric performance, and yielded well-defined, sharp and separated stripping peaks for both Pb(II) and Cd(II). The improved stripping responses at the bismuth-modified electrodes can be

attributed to the fact that bismuth can form “fused” alloys with Pb(II) and Cd(II), which renders them ready to be reduced [104, 105]. However, the stripping peaks at the Bi-BDDE (solid line) were significantly higher than the stripping peak current that was observed on the Bi-SPCE (dotted line) by four-fold and five-fold for Pb(II) and Cd(II), respectively. This suggests that the use of a BDD electrode can enhance the sensitivity for the determination of Pb(II) and Cd(II) with the proposed μPAD.

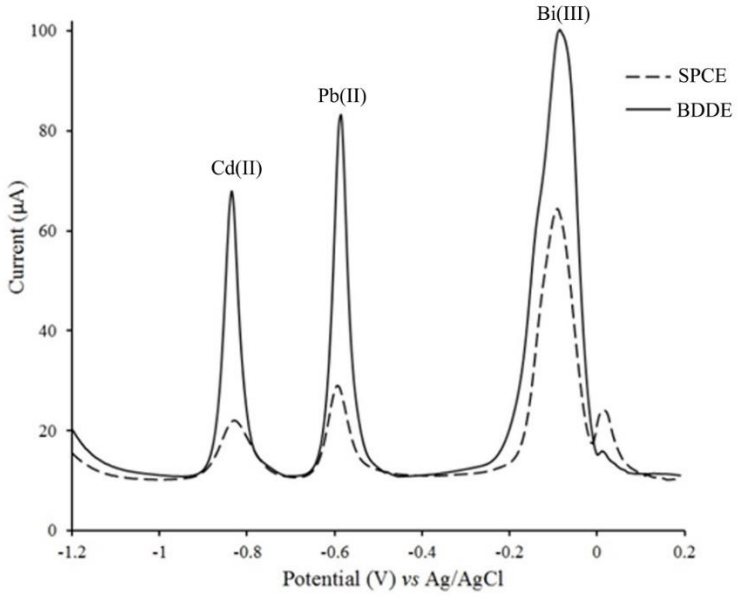

Figure 3.9 Anodic stripping voltammograms of 50 ng mL-1 for both Pb(II) and Cd(II) in 0.2 M NaCl (pH = 6.0) on Bi-SPCE (dotted line) and Bi-BDDE (solid line). The accumulation potential was -1.2 V, and the accumulation time was 120 s.

3.7.2 Colorimetric detection of Cu(II)

For the determination of Cu(II) in parallel to the electrochemical measurement, a highly selective and sensitive colorimetric sensor based on the catalytic etching of silver nanoplates (AgNPls) with thiosulfate ($S_2O_3^{2-}$) was developed. As shown in Figure 3.10a, the addition of Cu(II) and $S_2O_3^{2-}$ to AgNPls caused a reduction in the sizes of the AgNPls and a distinct change of color from pinkish violet to colorless after the addition

of Cu(II). These results explain that $S_2O_3^{2-}$ can be strongly adsorbed to the surfaces of the AgNPls to form the $Ag(S_2O_3)_2^{3-}$ complexes in the presence of dissolved oxygen and the complexes immediately generated a passive layer on the surface of AgNPls. For this reason, the etching reaction slowly occurred because the surfaces of the AgNPls was blocked by the passive layer. In the presence of Cu(II), the etching rate of this reaction can be accelerated by forming $Cu(S_2O_3)_3^{5-}$, and the complexes can also be oxidized to Cu(II) by dissolved oxygen (eq. 3.2.1). To understand the role of Cu(II) in the catalytic etching of AgNPls, the absorption spectra of AgNPls was monitored for the conditions of varying Cu(II) concentrations, as shown in Figure 3.10b. The CTAB-stabilized AuNPls (CTAB/AuNPls) in ammonia buffer exhibited the absorption spectra located at 563 nm (curve a). For the addition of $S_2O_3^{2-}$ solution, the absorption spectra of CTAB/AuNPls are blue-shifted (λ = 522 nm) and absorbance-decreased (curve b); therefore, the color of the CTAB/AuNPls solutions changed from blue to pinkish violet. In the presence of Cu(II), the absorbance at 522 nm decreased when the concentration of Cu(II) increased (curves c and d). The color of the solutions gradually changed from pinkish violet to colorless. For the detection of Cu(II) on μPAD, 0.8 μL of the modified AgNPls was added to the colorimetric detection zone. The sample solution at 50 μL was subsequently dropped on the electrochemical detection zone and the solution flowed outward via capillary forces to the colorimetric detection zones. The color at the colorimetric detection zones changed from pinkish violet to colorless as the concentration of Cu(II) increased, which could be monitored by the naked eye after 120 s.

$$Ag^0 + 5S_2O_3^{2-} + Cu^{2+} \longrightarrow Cu(S_2O_3)_3^{5-} + Ag(S_2O_3)_2^{3-} \qquad \text{eq 3.4}$$

O_2

As shown in the TEM images, the size of the initial AgNPls was ~30 nm (Figure 3.10c). The size of the AgNPls reduced to ~15 nm with the addition of Cu(II) after incubation for 5 min at room temperature (Figure 3.10d), which indicates that Cu(II) can

accelerate the etching rate of the AgNPls. The morphology and size changes of AgNPls effectively proved the sensing mechanism.

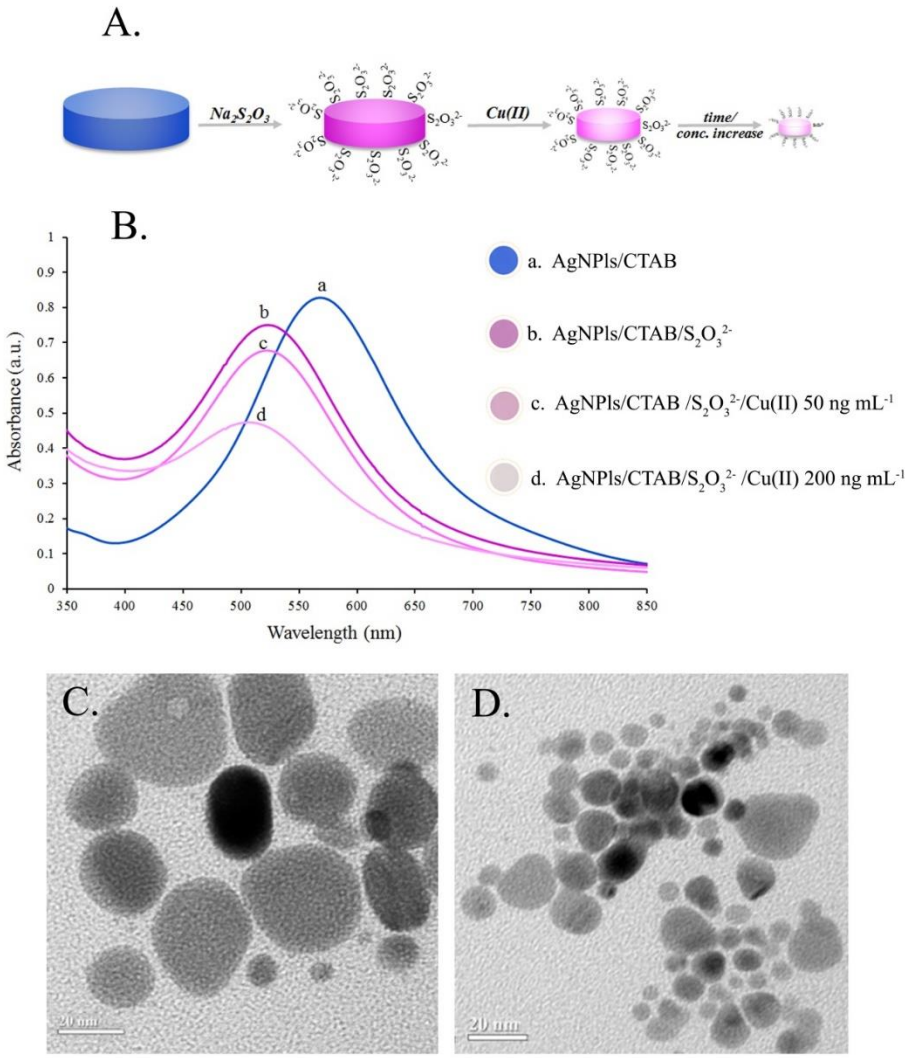

Figure 3.10 Schematic mechanism of sensing Cu(II) based on catalytic etching of silver nanoplates (AgNPls) with thiosulfate ($S_2O_3^{2-}$) (a). The absorption spectra of AgNPls CTAB/AgNPls (a), $S_2O_3^{2-}$/CTAB/AgNPls (b), $S_2O_3^{2-}$/CTAB/AgNPls + 50 ng mL^{-1} of Cu^2 (curve c) and $S_2O_3^{2-}$/CTAB/AgNPls + 200 ng mL^{-1} of Cu^{2+} (curve d) (b). The experiment was performed at room temperature, and the UV-vis spectra was *investigated after 5 min. The TEM images of $S_2O_3^{2-}$ /CTAB/AgNPls without Cu(II) (c) and with 100 ng mL^{-1} of Cu(II) (d).*

To investigate the selectivity of the modified AgNPls toward Cu(II), different common metal ions, including 10 μg mL^{-1} of K(I), Cr(III), Cd(II), Zn(II), As(III), Mn(II), Co(II), Pb(II), Al(III), Ni(II), Fe(III), Mg(II), Hg(II) and Bi(III), were tested by this method (the concentration at 10 μg mL^{-1} are excess amount of metal found in the environment). As shown in Figure 3.11, only Cu(II) (100 ng mL^{-1}) can etch the modified AgNPls and cause the color change of modified AgNPls from pinkish violet to colorless, which suggests that this detection system exhibited a high selectivity for Cu(II) [68, 69].

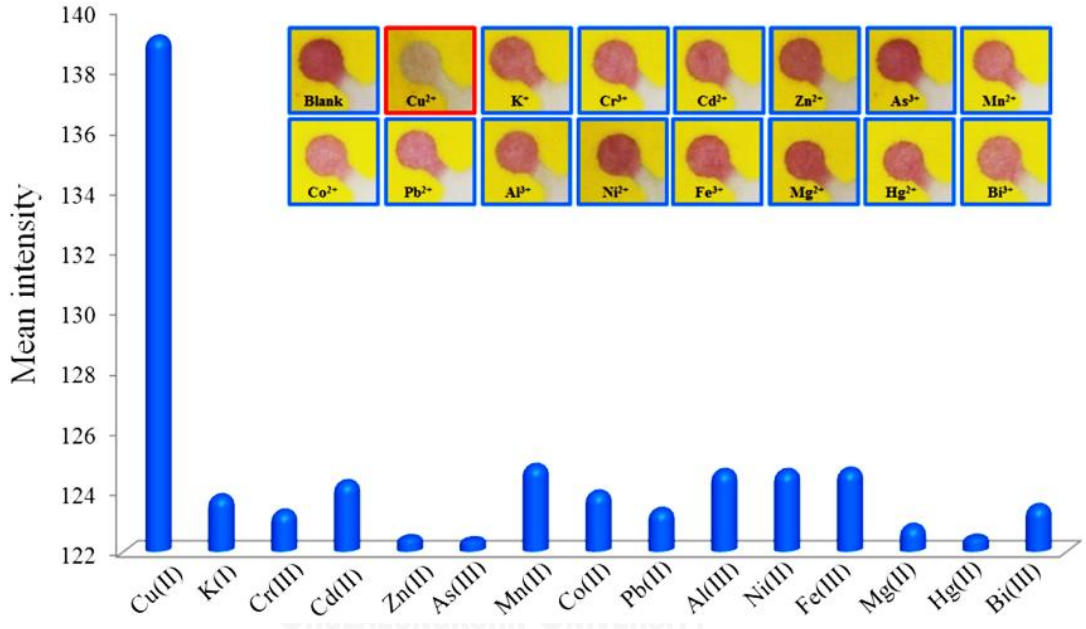

Figure 3.11 Mean color intensity values of the modified AgNPls on μPAD after the addition of different common metal ions at the concentration of 100 ng mL^{-1} Cu(II) and 10 μg mL^{-1} common metals. Inset: photographic images of the colorimetric determination of metal ions on paper-based devices.

3.7.3 Optimization of operation conditions

3.7.3.1 Optimization of the parameters for the electrochemical detection of Pb(II) and Cd(II) levels

The operating conditions and parameters of electrochemical detection, including supporting electrolyte, accumulation potential, accumulation time and concentration of Bi(III), were subsequently investigated. The supporting electrolyte can affect both the electrochemical sensor and the colorimetric sensor. The preliminary experiments were conducted with aqueous solution, including HCl, NaCl and ammonia buffer that served as the supporting electrolyte. From the results, 0.1 M HCl (pH = 2.0) provided a high sensitivity for Pb(II) and Cd(II) detection because the acidic chloride ions are a better ligand for metal ions compared with other ions [92] (as shown in Figure 3.12). Conversely, the intensity of detecting Cu(II) by colorimetry was attributed to its low sensitivity because the $S_2O_3^{2-}$ was not stable and broke down to form sulfate, sulfide, sulfite, tetrathionate, trithionate, polythionates and polysulfides [80]. For the results of ammonia buffer (pH = 9.0), the detection of Cu(II) using a colorimetric sensor provided a high-intensity color change. However, the sensitivity of Pb(II) and Cd(II) detection decreased because the OH^- may be complexed with Pb(II) or Cd(II) by forming $Pb(OH)_2$ or $Cd(OH)_2$ [106]. Thus, 0.2 M NaCl (pH = 6.0) was used throughout this study to optimize simultaneous electrochemical and colorimetric detection using the same solution because this supporting electrolyte provided not only high sensitivity of Pb(II) and Cd(II) using electrochemistry but also a high intensity of Cu(II) by colorimetry.

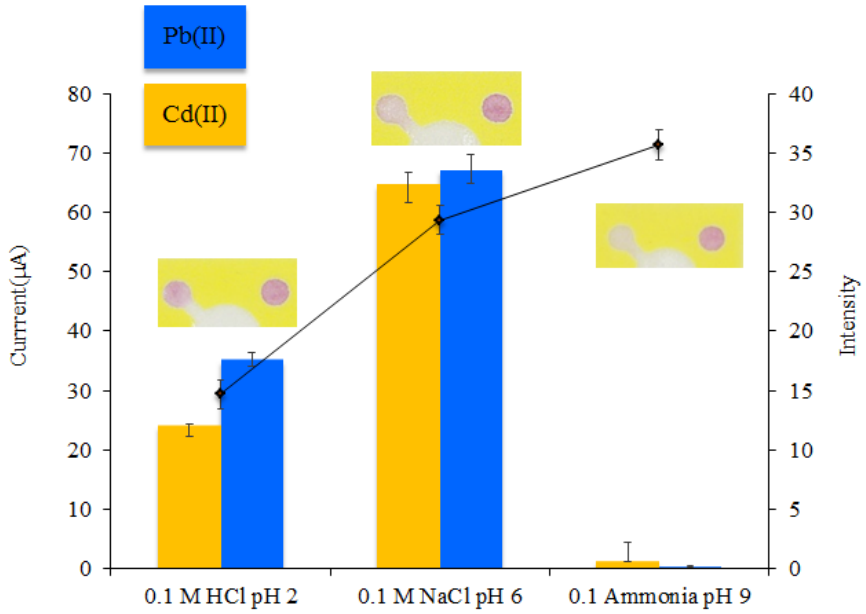

Figure 3.12 Effect of supporting electrolyte for simultaneous determination of Pb(II), Cd(II) and Cu(II).

The effect of accumulation potential on the stripping peaks current for Pb(II) and Cd(II) was individually examined over the potential range of -0.6 to -1.4 V *vs* Ag/AgCl. The accumulation potential of -1.2 V *vs*. Ag/AgCl was optimal because it yielded the highest stripping peak currents (Figure 3.13a). The effect of the accumulation potential on both electrochemical detection and colorimetric detection was examined in the range of 0-180 s. Figure 3.13b indicated that the stripping peak currents of Pb(II) and Cd(II) increased with an increase in the accumulation time. Therefore, an accumulation time of 120 s was used throughout this study. In addition, this accumulation time provides not only high sensitivity but also a short analysis time.

Next, the effect of the bismuth film was optimized by varying the concentration of the Bi(III) plating solution in the range of 0.5 to 3 μg mL^{-1}. As shown in Figure 3.13c, the stripping peak currents of the Pb(II) and Cd(II) increased with an increase in concentration of Bi(III) from 0 to 2 μg mL^{-1} and subsequently decreased at 2.5 – 3 μg mL^{-1} Bi(III) concentrations, which is probably due to the fact that the thick bismuth film might hinder the mass transfer of both metal ions during the stripping step [107].

Therefore, the Bi(III) plating solution concentration of 2 μg mL^{-1} was chosen for the determinations of Pb(II) and Cd(II).

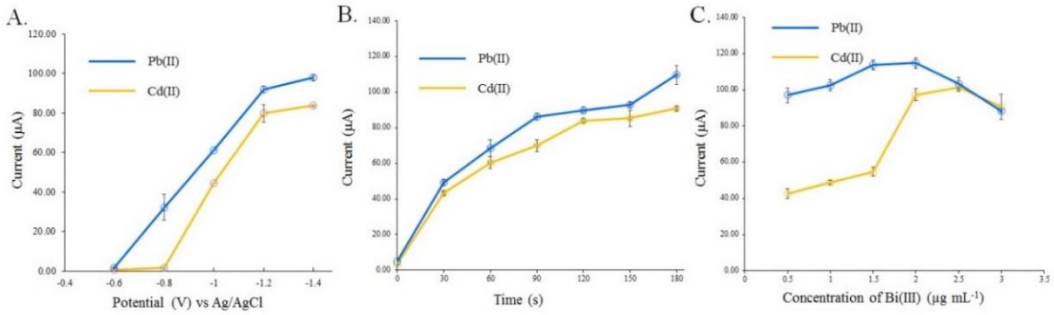

Figure 3.13 Effect of experimental conditions for Pb(II) and Cd(II) measurement on microfluidic paper-based sensor; (a) accumulation potential, (b) accumulation time and (c)concentration of Bi(III).

3.7.3.2 Optimization of the parameters for the colorimetric detection of Cu(II) levels

For the system that contains 100 ng mL^{-1} of Cu(II), a number of parameters, including the concentrations of the AgNPls, concentration of $S_2O_3^{2-}$ and incubation time were investigated. The difference in the color intensity values before and after the addition of Cu(II) ($\Delta I = I_{sample} - I_{blank}$) was considered for determining the optimal conditions. For the effect of AgNPl concentration, different concentrations of AgNPls in the range of 100 to 900 μg mL^{-1} was investigated. The best ΔI was determined at 500 μg mL^{-1}(Figure 3.14a). Thus, 500 μg mL^{-1} was used in the subsequent experiments. Then, the influence of $S_2O_3^{2-}$concentration on ΔI is examined and illustrated in Figure 3.14b. The ΔI increased with an increase in the concentration of $S_2O_3^{2-}$ and slightly decreased above 5.0 mM. Therefore, the concentration at 5.0 mM $S_2O_3^{2-}$ was selected as the optimized concentration. The effect of incubation time was investigated in the range of 0 to 210 s as shown in Figure 3.14c. The ΔI increased linearly with an increase in incubation time. Then, 120 s was selected as the optimum reaction time to obtain a distinct color difference in our paper devices. Table 3.4 summarized all optimum

experimental conditions for the simultaneous determination of Pb(II), Cd(II) and Cu(II) using the proposed μPAD.

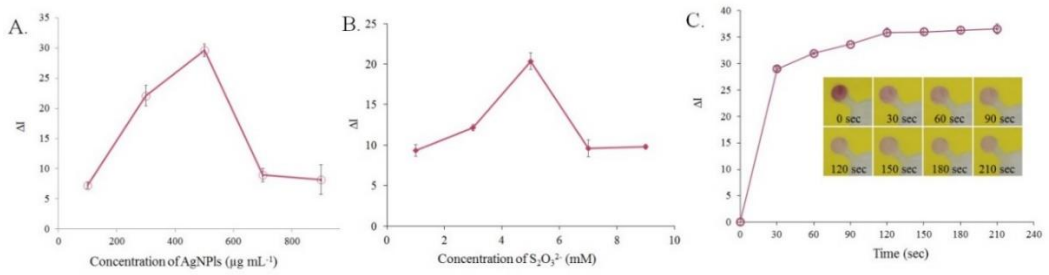

Figure 3.14 Effect of experimental conditions for Cu(II) measurement on microfluidic paper-based sensor; (a) concentration of AgNPls, (b) concentration of $S_2O_3^{2-}$ and (c) incubation time.

Table 3.4 Operating conditions and parameters for the simultaneous determination of Pb(II), Cd(II) and Cu(II).

Optimization parameter	Range of study	Selected
Supporting electrolyte	HCl, NaCl, Ammonia buffer pH 9	NaCl
Deposition potential	-0.6 to -1.4 V	-1.2 V
Deposition time or incubation time	0 to 180 s	120 s
Concentration of Bi(III)	0.5 to 3 μg mL^{-1}	2 μg mL^{-1}
Concentration of AgNPls	100 to 900 μg mL^{-1}	500 μg mL^{-1}
Concentration of $Na_2S_2O_3$	1 to 10 mM	5 mM

3.7.4 Interferences

For electrochemical detection, the interference study was performed by adding common metal ions into a standard solution that contains 50 ng L^{-1} Pb(II) and Cd(II). Using ±5.0% tolerance ratios (Figure 3.15a), the results indicated that the 1000-fold

(green-column) K(I), Mg(II), Mn(II), Al(III), 500-fold (light green-column) As(III), Fe(III), Cr(III), 400-fold (yellow-column) Zn(II), Hg(II), Co(II), Ni(II) and 200-fold (red-column) Cu(II) had no significant effect on the signals of Pb(II) and Cd(II). For colorimetric detection, the concentration of common metal ions was investigated at more than 100 times the Cu(II) concentration (100 ng L^{-1} of Cu(II) and 10 µg mL^{-1} of K(I), Cr(III), Cd(II), Zn(II), As(III), Mn(II), Co(II), Pb(II), Al(III), Ni(II), Fe(III), Mg(II), Hg(II) and Bi(III)). The results indicated that the color of solution did not change to colorless after the addition of these common metal ions, as shown in Figure 3.15b. This finding indicates that these common metal ions did not interfere in the determination of Cu(II) based on the catalytic etching of AgNPls with $S_2O_3^{2-}$ using µPAD.

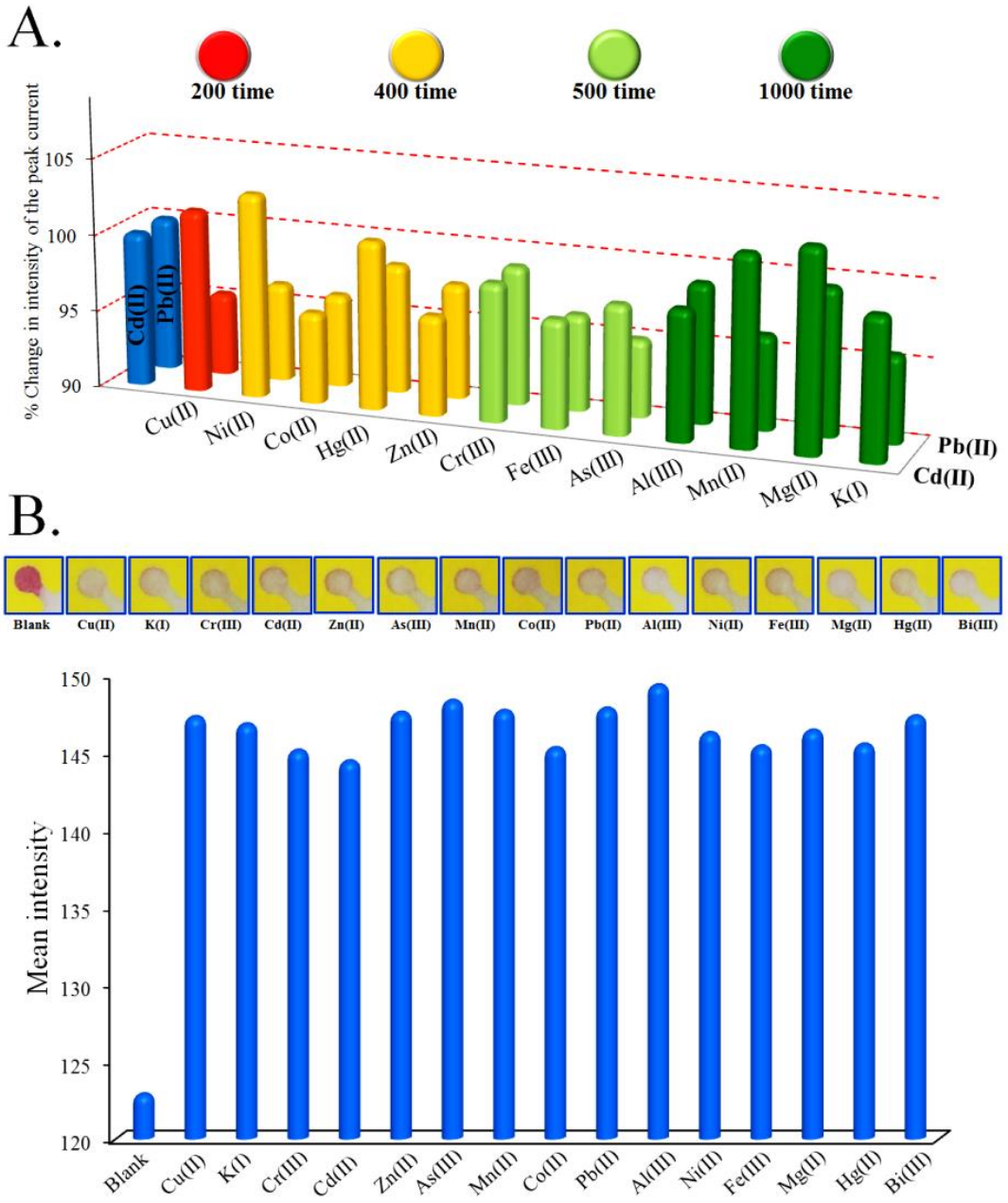

Figure 3.15 Tolerance ratio of interfering ions in the electrochemical determination of 50 ng mL^{-1} of Pb(II) and Cd(II) (a). Effect of common metal ions (10 µg mL^{-1}) in the colorimetric determination of 100 ng mL^{-1} of Cu(II) (b). Inset (b): corresponding photographs of the paper-based sensor at the colorimetric detection zone after the addition of Cu(II) with various common metal ions.

3.7.5 Analytical performance of μPAD coupled dual electrochemical and colorimetric detection

Calibration curves for the simultaneous determination of Pb(II), Cd(II) and Cu(II) were achieved by μPAD with dual electrochemical and colorimetric detection in optimal conditions. For electrochemical detection, the anodic stripping voltammetry (ASV) of the different concentrations of Pb(II) and Cd(II) are shown in Figure 3.16. The resulting calibration plots are linear over the concentration range from 0.5 to 70 ng mL^{-1} for both Pb(II) and Cd(II). The detection limit of Pb(II) and Cd(II), which was calculated based on three times the signal of the background noise (3S/N), were 0.1 ng L^{-1} (Pb(II)=0.48 nM and Cd(II)=0.89 nM) for both target metals. The relative standard deviation (RSD) for the electrochemical detection was 4.13% and 4.22% for Pb(II) and Cd(II), respectively. For colorimetric detection, the increasing concentrations of Cu(II) in the range of 0 - 450 ng mL^{-1}, the color of the modified AuNPls on μPADs gradually changed from pinkish violet to colorless (Figure 3.17). A linear correlation between ΔI and the concentration of Cu(II) was observed in the range from 10 to 350 ng mL^{-1} (as shown in inset). The method can probably discriminate the concentration of Cu(II) using the naked eye compared with the reference color zone. The detection limit of the colorimetric detection was calculated based on 3*sd*/slope, where *sd* is the standard deviation of the blank samples and the slope was obtained from the standard correlation curve between the intensity of the signals and the concentration of Cu(II). The statistical analysis revealed that the detection limit of Cu(II) was 4.12 ng mL^{-1} or 64.8 nM, which is significantly lower than the maximum allowable levels of ~20 μM in the United States, ~30 μM in the European Union, and ~31 μM in Thailand [108].

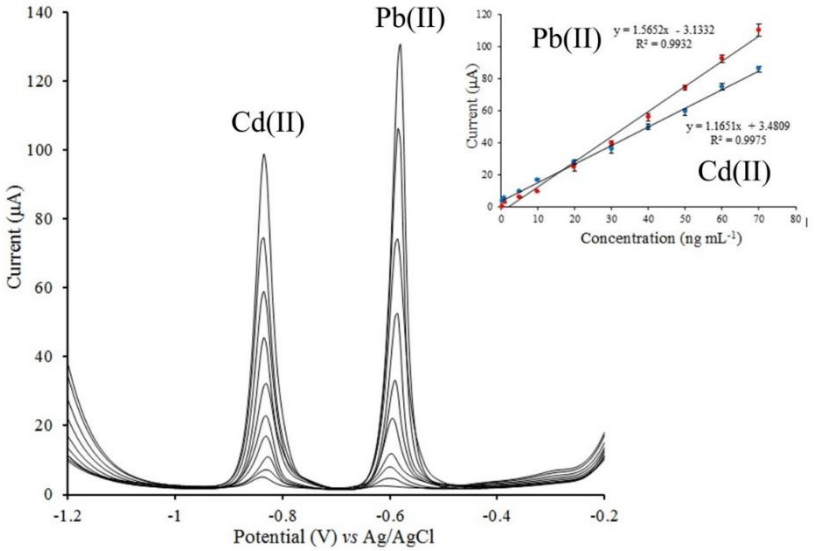

Figure 3.16 Anodic stripping voltammograms and respective calibration curves or increasing concentration of Pb(II) and Cd(II) (0.5 to 70 ng mL^{-1}) in 0.2 M NaCl solution at Bi-BDDE.

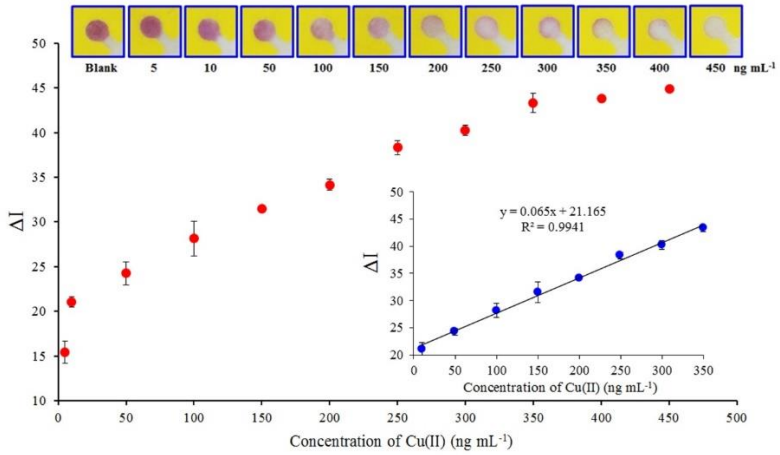

Figure 3.17 Photographs of the paper-based sensor at the colorimetric detection zone for the detection of Cu(II) at various concentrations (a). The plot of the mean intensity of the color of the AgNPls determined by photograph analysis using NIH ImageJ vs. Cu(II) concentration (0-450 ng mL^{-1})(b). Inset: linear regression analysis and best-fit line in the concentration range of 10 to 350 ng mL^{-1}.

3.7.6 Analytical application

A μPAD was successfully applied for the simultaneous determination of Pb(II), Cd(II) and Cu(II) in several samples, such as groundwater, stream water, fish and rice samples. The results are summarized in Table 3.5; the % recovery of the spiked Pb(II), Cd(II) and Cu(II) were 82.2-102.6%, 81.6-102.9% and 71.7-96.9%, respectively. The excellent average recoveries suggest that the proposed method offers benefits for various samples that contain Pb(II), Cd(II) and Cu(II). To validate the accuracy of this method, the results from μPAD were compared with the results obtained by inductively coupled plasma optical emission spectrometry (ICP – OES). A paired t-test at the 95% confidence level was performed; the statistics revealed that the $t_{calculated}$ of Pb(II) and Cd(II) were below $t_{critical}$ (4.30), which suggests no significant difference between the two methods and indicates the applicability and reliability of the proposed method.

Table 3.5 Simultaneous determination of Pb(II), Cd(II) and Cu(II) in real samples

Samples	Electrochemical detection								Colorimetric detection			
	Cadmium				Lead				Copper			
	Concentration of Cd (II) (ng mL^{-1})		Mean %Recovery ($\bar{X} \pm SD$)	RSD (%)	Concentration of Pb (II) (ng mL^{-1})		Mean %Recovery ($\bar{X} \pm SD$)	RSD (%)	Concentration of Cu (II) (ng mL^{-1})		Mean %Recovery ($\bar{X} \pm SD$)	RSD (%)
	Amount of added	Amount of found			Amount of added	Amount of found			Amount of added	Amount of found		
Ground water	0	*ND*	-	-	0	*ND*	-	-	0	30.93	-	-
	5	4.24	84.82 ± 2.84	3.34	5	4.74	94.70 ± 4.37	4.62	10	38.23	73.01 ± 4.59	6.29
	30	26.37	87.91 ± 1.94	2.21	30	24.66	82.20 ± 5.21	6.34	50	75.98	90.12 ± 4.23	4.69
	60	55.68	92.79 ± 1.52	1.64	60	61.59	102.64 ± 3.69	3.60	100	123.43	92.53 ± 3.21	3.47
Stream water	0	*ND*	-	-	0	*ND*	-	-	0	43.22	-	-
	5	4.08	81.68 ± 2.53	3.09	5	4.62	92.34 ± 5.06	5.48	10	50.39	71.71 ± 3.93	5.48
	30	28.23	94.12 ± 4.60	4.89	30	25.81	86.04 ± 4.38	5.09	50	89.05	91.66 ± 4.23	4.61
	60	58.82	98.04 ± 1.89	1.93	60	59.06	98.43 ± 2.10	2.13	100	139.64	96.42 ± 3.12	3.24
Rice	0	*ND*	-	-	0	*ND*	-	-	0	47.74	-	-
	5	4.27	85.35 ± 4.26	4.99	5	4.28	85.50 ± 0.96	1.12	10	55.83	80.94 ± 3.84	4.74
	30	28.52	95.07 ± 8.77	9.22	30	26.09	86.96 ± 5.73	6.59	50	92.45	89.42 ± 2.12	2.37
	60	58.39	97.32 ± 6.59	6.77	60	58.28	97.14 ± 3.61	3.71	100	143.22	95.48 ± 1.34	1.40
Fish	0	*ND*	-	-	0	*ND*	-	-	0	18.86	-	-
	5	4.77	95.31 ± 1.39	1.46	5	4.72	94.31 ± 3.01	3.19	10	26.23	73.72 ± 3.63	4.92
	30	30.22	100.72 ± 1.54	1.53	30	28.95	96.50 ± 3.65	3.78	50	67.32	96.92 ± 3.42	3.53
	60	61.77	102.94 ± 1.82	1.76	60	59.22	98.70 ± 3.95	4.00	100	111.96	93.13 ± 1.99	2.14

ND = Not detection

3.8 Conclusions

A new microfluidic paper-based analytical device that combines electrochemical and colorimetric detection was developed for the simultaneous determination of Pb(II), Cd(II) and Cu(II). The bismuth-modified boron doped diamond electrode was employed as a working electrode for the highly sensitive determination of Pb(II) and Cd(II). The specific determination of Cu(II) is based on colorimetric detection using the catalytic etching of silver nanoplates by thiosulfate. In optimal conditions, the minimum detection limits of 0.1 ng L^{-1} for both Pb(II) and Cd(II) were achieved by electrochemical detection, and the minimum detection limits of 4.12 ng mL^{-1} of Cu(II) were achieved by colorimetric detection. The ability of the microfluidic paper-based analytical device for the simultaneous determination of Pb(II), Cd(II) and Cu(II) in several samples was demonstrated. The results were validated using the ICP-OES method, which confirmed the accuracy and reliability of the approach. Therefore, the benefits of these devices are cost-effective and simple for the simultaneous determination of Pb(II), Cd(II) and Cu(II) without the need for complicated instrumentation, which could be very useful for food and environmental analysis.

CHAPTER IV

DEVELOPMENT OF ELECTROCHEMICAL SENSORS FOR HEAVY METAL DETECTION

This Chapter is the development of electrochemical sensors using a nafion/ionic liquid/graphene composite modified screen-printed carbon electrode for the simultaneous determination of heavy metals.

Electrochemical sensors for the simultaneous determination of zinc, cadmium and lead using a nafion/ionic liquid/graphene composite modified screen-printed carbon electrode

Sudkate Chaiyo[a], Eda Mehmeti[b], Kristina Žagar[c], Weena Siangproh[d]***, Orawon Chailapakul[a],[e]**, Kurt Kalcher[b]*

[a]Electrochemistry and Optical Spectroscopy Research Unit, Department of Chemistry, Faculty of Science, Chulalongkorn University, 254 Phayathai Road, Pathumwan, Bangkok 10330, Thailand

[b]Institute of Chemistry, Department of Analytical Chemistry, Karl-Franzens University, Universitätsplatz 1, Graz A-8010, Austria

[c]Department for Nanostructured Materials, Jozef Stefan Institute, Ljubljana, Slovenia

[d]Department of Chemistry, Faculty of Science, Srinakharinwirot University, Sukhumvit 23, Wattanna, Bangkok 10110, Thailand

[e]Center for Petroleum, Petrochemicals and Advanced Materials, Chulalongkorn University, 254 Phayathai Road, Pathumwan, Bangkok 10330, Thailand

*** Co-corresponding author

** Co-corresponding author

* Corresponding author

Analytica Chimica Acta 918 (2016): 26-34.

Abstract

A simple, low cost, and highly sensitive electrochemical sensor, based on a Nafion/ionic liquid/graphene composite modified screen-printed carbon electrode (N/IL/G/SPCE) was developed to determine zinc (Zn(II)), cadmium (Cd(II)), and lead (Pb(II)) simultaneously. This disposable electrode shows excellent conductivity and fast electron transfer kinetics. By *in situ* plating with a bismuth film (BiF), the developed electrode exhibited well-defined and separate peaks for Zn(II), Cd(II), and Pb(II) by square wave anodic stripping voltammetry (SWASV). Analytical characteristics of the BiF/N/IL/G/SPCE were explored with calibration curves which were found to be linear for Zn(II), Cd(II), and Pb(II) concentrations over the range from 0.1 to 100.0 ng mL^{-1}. With an accumulation period of 120 s detection limits of 0.09 ng mL^{-1}, 0.06 ng mL^{-1} and 0.08 ng mL^{-1} were obtained for Zn(II), Cd(II) and Pb(II), respectively, using the BiF/N/IL/G/SPCE sensor, calculated as 3σ value of the blank. In addition, the developed electrode displayed a good repeatability and reproducibility. The interference from other common ions associated with Zn(II), Cd(II) and Pb(II) detection could be effectively avoided. Finally, the proposed analytical procedure was applied to detect the trace metal ions in drinking water samples with satisfactory results which demonstrates the suitability of the BiF/N/IL/G/SPCE to detect heavy metals in water samples and the results agreed well with those obtained by inductively coupled plasma mass spectrometry.

Keywords: nafion/ionic liquid/graphene composite, screen-printed carbon electrode, bismuth film, zinc, cadmium, lead

4.1 Introduction

Trace and toxic elements, such as zinc (Zn(II)), cadmium (Cd(II)) and lead (Pb(II)) in various matrices, like environmental, food and biological samples have been of great interest due to several hazardous effects that these elements could provide to humans [109, 110]. Therefore, the determination of heavy metals in environmental, food and biological samples has drawn significant attention due to the toxic and nutritional effects of these elements [111]. Several analytical techniques such as atomic absorption spectrometry (AAS) [17], inductively coupled plasma atomic emission spectrometry (ICP-AES) [112] and inductively coupled plasma mass spectrometry (ICP-MS) [113] are available for the determination of trace heavy metals with sufficient sensitivity for most of applications. Usually, these methods are more expensive and time-consuming as compared to electrochemical methods.

Electrochemical methods, especially electrochemical stripping analysis, have been widely recognized as a powerful tool for determination of heavy metals due to its low cost, easy operation, good specificity, excellent stability, high sensitivity and low limit of detection [114, 115]. Mercury-based electrodes, such as mercury film electrodes (MFE) [116, 117] and hanging mercury drop electrodes (HMDE) [118], have traditionally been used in stripping techniques because of their advantages, like high sensitivity, reproducibility, purity of the surface, high hydrogen overpotential, and possibility of amalgam formation [116-118]. However, the toxicity of mercury restricts the use of these electrodes in today's ecologically oriented analysis [119]. Numerous attempts have consequently been made to replace mercury electrodes by alternative electrode materials with good analytical performance and environment friendly characteristics. The bismuth-film electrode (BiFE) was introduced around the year 2000 as an alternative to mercury electrodes due to its stripping behaviors similar to those of mercury electrodes and the environmentally friendly nature of bismuth [120]. The ability of bismuth to form intermetallic alloys with heavy metals, as well as its insensitivity towards dissolved oxygen are just some of remarkable electrochemical features of bismuth-based electrodes that stay behind their widespread use [121, 122]. The bismuth film can be constructed by electrodeposition on substrates including

glassy carbon electrodes (GCE) [123], carbon paste electrodes (CPE) [124], boron doped diamond electrode (BDDE) [96] and screen-printed carbon electrodes (SPCE) [92, 94]. SPCE was chosen as the electrode material in this research because screen printed technology is a rapid and cost-reducing way to fabricate robust and solid electrodes. It offers several advantages, among which the versatility of the design, reproducibility in the sensor preparation and low cost production are notable, which permits the sensors to be disposed after a single use [125, 126].

Graphene (G) has attracted attention among researchers for its properties like extremely high thermal conductivity, good mechanical strength, high mobility of charge carriers, large specific surface area and outstanding electrical properties [127, 128]. Ionic liquid (IL) is a promising material adopted in the field of electrochemistry. Due to the high ionic conductivity and wide electrochemical window, it has been widely used as electrochemical solvents and electrode modifiers for the fabrication of sensors [129, 130]. Recently, a synergistic effect of G and IL composite modified SPCE can enable a sensitive determination of heavy metals [131, 132]. To enhance the detection sensitivity towards heavy metals, Nafion (N), a perfluorinated sulphonated cation exchanger with properties of excellent antifouling capacity, chemical inertness, and high permeability to cations, has been extensively employed as an electrode modifier for organic molecules [103, 133]. The integration of G, IL and N could elicit synergistic effects in the electrochemical applications. Thus, G, IL and N composite could be used as a kind of robust and advanced electrode material for the determination of heavy metals.

In the present work, a graphene, ionic liquid (1-butyl-2, 3-dimethylimidazolium tetrafluoroborate) (IL) and Nafion composite and bismuth film-modified screen-printed carbon electrode, was developed. Tetrafluoroborates usually show good combined properties of high electric conductivity and electrochemical stability; for this reason 1-butyl-2,3-dimethylimidazolium tetrafluoroborate was chosen as a proper candidate for our studies whose moderate lipophilic properties should cope well with graphene [134]. After in situ deposition of the bismuth film, the sensor was applied to determine traces of Zn(II), Cd(II) and Pb(II) by square wave anodic stripping voltammetry (SWASV).

Finally, this highly sensitive, simple and low-cost sensor was applied to the determination of Zn(II), Cd(II) and Pb(II) in drinking water samples.

4.2 Experimental

4.2.1 Apparatus

Voltammetric experiments were performed using an Autolab electrochemical system with a potentiostat PGSTAT 128 (EcoChemie, Utrecht, Netherlands) controlled by the NOVA 10.1 software. The three-electrode system consisted of a Nafion/ionic liquid/graphene/screen-printed carbon electrode (N/IL/G/SPCE) as the working electrode, an Ag/AgCl/sat.KCl electrode as the reference and a platinum wire as the auxiliary electrode.

4.2.2 Reagents

Industrial-quality graphene was obtained from ACS Material, LLC (Medford, USA). The ionic liquid 1-butyl-2, 3-dimethylimidazolium tetrafluoroborate, Nafion (5 % in lower alcohols), N,N-dimethylformamide (DMF) and sodium acetate (CH_3COONa) were purchased from Sigma–Aldrich (Buchs, Switzerland). Stock solutions of Zn(II), Cd(II), Pb(II), phosphate (PO_4^{3-}), chloride (Cl^-), sulphate (SO_4^{2-}), fluoride (F^-), calcium (Ca(II)), potassium (K(I)) , magnesium (Mg(II)), iron (Fe(III)), arsenic (As(III)), mercury (Hg(II), copper (Cu(II)), cobalt (Co(II)), and nickel (Ni(II)) in concentrations 1000 mg L^{-1} were purchased from Carl Roth GmbH + Co. KG (Austria). The stock solutions of bismuth (Bi(III)) and manganese (Mn(II)) (1000 mg L^{-1}) were obtained from CPI International (USA). Acetic acid was purchased from Merck (Darmstadt, Germany). All reagents were of analytical grade, and were used without further purification. All solutions were prepared using ultra-purified water (>18 MΩ cm) refined by a cartridge purification system (Millipore, UK).

4.2.3 Preparation of the N/IL/G casting solution and fabrication of the modified electrode

To prepare the N/IL/G composite, 1.0 mg of the graphene was dispersed in 1.0 mL of DMF by ultrasonic agitation for about 2 h. Next, 0.5 % (m:v) of the ionic liquid and 0.1 % (v:v) of the Nafion solution were added to the graphene dispersion and sonicated for further 30 min. The N/G composite and the IL/G composite were prepared under the same experimental conditions but without adding the IL and N, respectively.

SPCEs were prepared by printing carbon ink (Acheson, USA) onto a ceramic substrate (Coors Ceramic, Chattanooga, TN, USA). The printed electrode was allowed to dry in an oven at 55 °C for 1 h. After that, 5 mm diameter-punched adhesive tape was attached to the working electrode for the fit surface area of sensor (area = 0.196 cm^2) (Figure 5.1). For the electrode modification by drop-casting, 1.0 µL of the N/IL/G composite solution was dropped onto the working electrode and allowed to dry completely at room temperature for approximately 10 min.

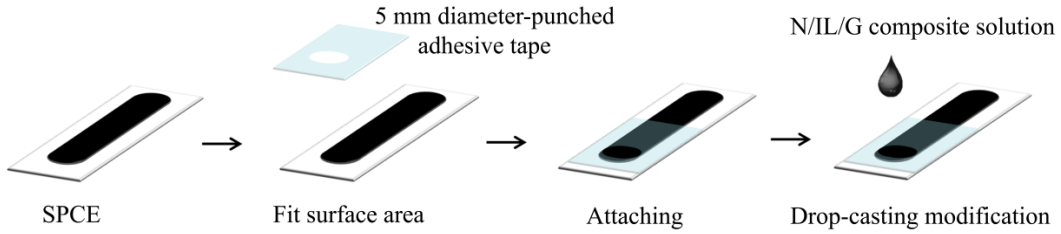

Figure 4.1 Schematic drawing of the electrochemical sensor fabrication and drop-casting modification

4.2.4 Electrochemical measurements

Cyclic voltammetry (CV) and square wave anodic stripping voltammetry (SWASV) were carried out in a 10 mL electrochemical cell. For the determination of Zn(II), Cd(II) and Pb(II) square wave voltammograms were recorded in 0.1 M acetate buffer solutions pH 4.5 in the presence of 200.0 ng mL^{-1} Bi(III). Standard solutions of

Zn(II), Cd(II) and Pb(II) were added to the cell and the mixed solution was stirred at a potential of -1.4 V for 120 s. Following the preconcentration step, the stirring was stopped. After 5 s of quiescence time, square wave stripping voltammetric measurement was performed by a potential scan from -1.4 V to +0.2 V with a frequency 25 Hz, a pulse amplitude 20 mV and a potential step of 5 mV. To obtain reproducible results the electrode was regenerated by polarizing the electrode at +0.3 V for 60 s prior to the next cycle.

4.2.5 Sample preparation

Drinking water samples were bought from a local supermarket (Graz, Austria). These samples were filtered through a 0.45 μm filter. Generally, 2.0 mL of drinking water sample was mixed with 8.0 mL of 0.1 M acetate buffer (pH 4.5) and then analysed by the optimized square wave anodic stripping voltammetry (SWASV) method.

4.3 Results and discussion

4.3.1 SEM characterization of the prepared electrodes

The scanning electron microscopy (SEM) of SPCE, G/SPCE and N/IL/G/SPCE are shown in Figure 4.2. The surface of the SPCE was predominated by isolated and irregularly shaped graphite flakes and separated layers were seen (Figure 4.2a). Therefore, the charges could not be transferred along the vertical direction of planes because of the block of non-conductive binder. The SEM image of N/IL/G/SPCE showed more uniform surface (Figure 4.2b). As a liquid with good conductivity and high viscosity, IL and N are capable of better dispersing the G in the paste than the conditional paraffin, thus, could better bridge the G sheets together. Thus, the conductive performance of the N/IL/G/SPCE was notably improved due to a mixed carbon-ionic contribution.

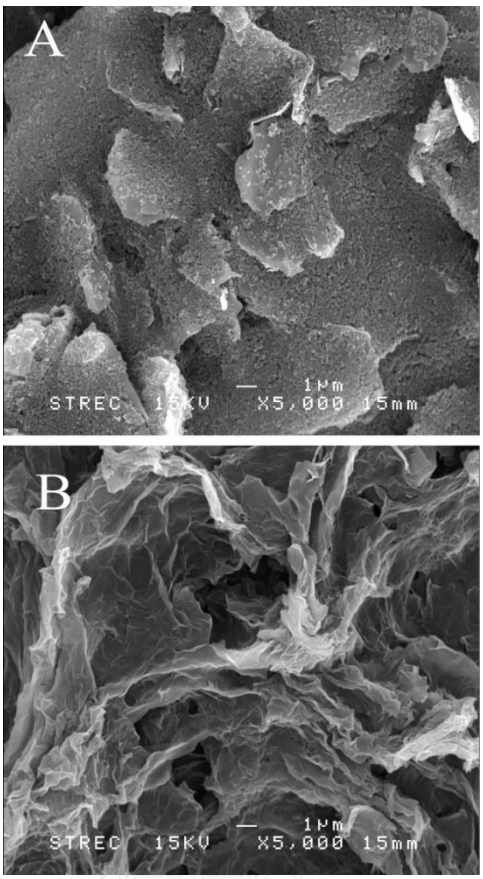

Figure 4.2 SEM images of surface morphologies of SPCE (b) and N/IL/G/SPCE (b)

4.3.2 Electrochemical characterization of the prepared electrodes

Cyclic voltammetry can provide interface information of the electrode surface in dependence of the modification process. The cyclic voltammetric behaviors of 1.0 mM $K_3(Fe(CN)_6]$ containing 0.1 M KCl at different electrodes were studied at a potential scan rate of 100 V s^{-1} (Figure 4.3a). On the bare SPCE (curve a), a pair of weak redox peaks with the peak-to-peak separation (*ΔEp*) of 0.31 V was observed, indicating the lethargic electron transfer rate at the interface. On the G/SPCE (curve b), a pair of well-defined peaks appeared with a peak potential separation *ΔEp* of 0.28 V. On the N/G/CPE (curve c), a higher peak current than that on both SPCE and G/SPCE was observed, but *ΔEp* extended to 0.39 V which is due to the presence of a membrane which deteriorates the diffusion process. The presence of the ionic liquid in IL/G/SPCE (curve d) causes well-defined and enhanced redox peaks with a small *ΔEp* of 0.22 V,

which could be ascribed to the high ionic conductivity and maybe an electrocatalytic activity of the IL. After N was added to the IL/G/SPCE, the anodic and cathodic peaks current even improved showing a ΔEp of 0.20 V, indicating that the ionic liquid slightly overcompensates and synergically improves the otherwise negative influence of the Nafion membrane in the N/IL/G/SPCE (curve e).

The relative peak separations, $\chi^0 = (E_{pa}-E_{pc})/0.058$, and anodic to cathodic peak current density ratios (I_{pa}/I_{pc}) are given in Table 4.1. The theoretical χ^0-values for this redox reaction is 1. The closer the χ^0-values are to the theoretical value, the faster the electron transfer kinetics on the electrode [135, 136]. The N/IL/G/SPCE electrodes showed a value of 3.45, which is closer to the theoretical value and much smaller than 5.34 for the bare SPCE.

The effective surface area of the N/IL/G/SPCE was evaluated using $K_3(Fe(CN)_6]$ as a probe based on the Randles–Sevcik equation. The experiment was performed with a 1.0 mM $K_3(Fe(CN)_6]$ solution at various scan rates (Figure 4.3b). For a reversible process, the following equation can be utilized [137]:

$$I_{pc} = 2.69 \times 10^5 \times (D_0) \cdot A \cdot \nu^{1/2} \cdot n^{3/2} \cdot C_0 \qquad \text{eq. 4.1}$$

where I_{pc} is the reduction peak current, D_0 is the diffusion coefficient of $K_3(Fe(CN)_6]$ ($cm^2\ s^{-1}$), A is the apparent electrode area (cm^2), ν is the scan rate ($V\ s^{-1}$), n is the electron transfer number and C_0 is the concentration for $K_3(Fe(CN)_6]$ ($mol\ cm^{-3}$), in consequence, the calculated effective surface area of the modified electrode is estimated as 0.648 cm^2. This surface is about 2.9 times that of the bare SPCE assuming that the diffusion coefficient is unaltered by the ionic liquid and the membrane.

Table 4.1 Influence of the modifiers on the characteristics of the electrode

Electrode	ΔE_p (V)	χ^0	I_{pa}/I_{pc}
SPCE	0.31	5.34	1.12
G/SPCE	0.28	4.83	1.17
N/G/SPCE	0.39	6.72	1.28
IL/G/SPCE	0.22	3.79	1.15
N/IL/G/SPCE	0.20	3.45	1.08

Figure 4.3b shows the cyclic voltammogram of the N/IL/G modified SPCE at different scan rates (20-200 mV s^{-1}). The oxidation and reduction peak current increases with the increasing scan rates. Further, the oxidation and reduction peak current exhibits a linear dependence on the square root of the scan rate (Figure 4.3b inset) in the range of 20-200 mV s^{-1}. The result suggests that the kinetics of the overall process is mainly controlled by diffusion.

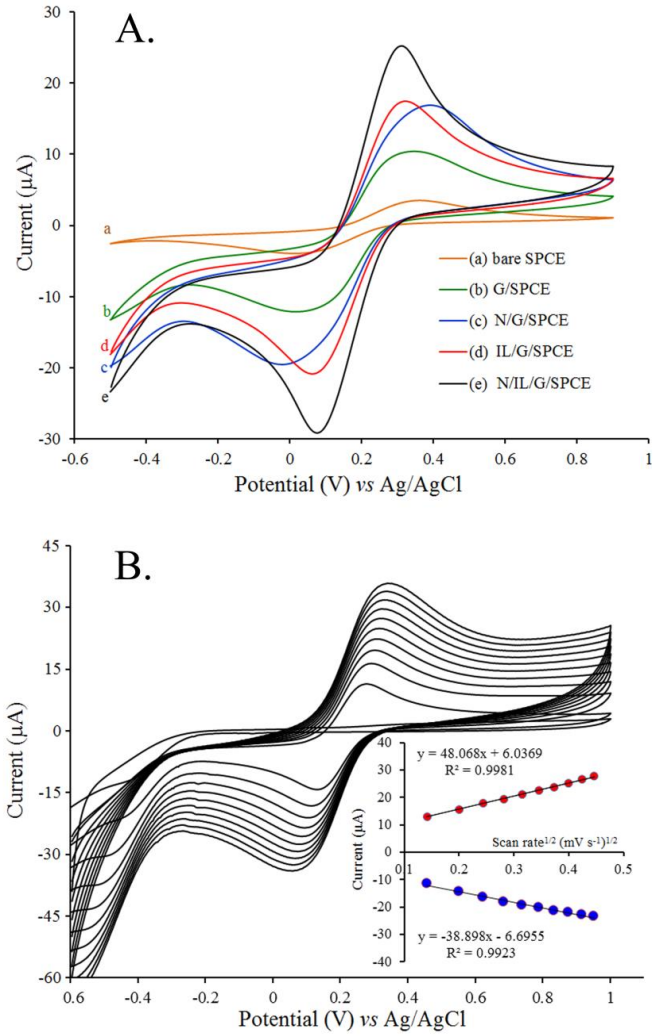

Figure 4.3 Cyclic voltammograms for 2 mM $K_3(Fe(CN)_6]$ in 0.1 M KCl (a) obtained with a (curve a) bare SPCE, (curve b) G/SPCE, (curve c) IL/G/SPCE, (curve d) N/G/SPCE and (curve e) N/IL/G/SPCE with a scan rate of 100 mV s^{-1}.; (b) at scan rates of 20 to 200 mV s^{-1} on a N/IL/G/SPCE. Inset: dependence of the peak current on the square root of the scan rate.

4.3.3 Electrochemical detection of Zn(II), Cd(II), and Pb(II)

Figure 4.4 shows the square wave anodic stripping voltammograms (SWASVs) of 50 ng L^{-1} Zn(II), Cd(II) and Pb(II) at the bare SPCE, bare bismuth film-modified SPCE (BiF/SPCE), N/IL/G/SPCE and bismuth film-modified N/IL/G/SPCE (BiF/N/IL/G/SPCE) in 0.1 M acetate buffer solution pH 4.5. As shown, relatively small stripping current responses are observed on the bare SPCE (curve a) due to the difficulty to deposit target metals onto the bare SPCE surface. The BiF/SPCE (curve b) yielded peak currents higher than those obtained with the bare SPCE, which is due to the bismuth providing an increased surface and facilitating a better deposition due to the formation of "fused" alloys with lead, cadmium and zinc. If graphene, Nafion or the ionic liquid were individually spread on the electrode surface only slight increases of the signal could be observed (not shown). An obvious increase in stripping currents could be detected upon casting Nafion, graphene and the ionic liquid to the bare electrode surface. (N/IL/G/SPCE, curve c); the improvement can be attributed to the high ionic conductivity and ion exchange properties of the polymer and IL as well as to the surface area increase and electric conductivity of graphene. If this electrode was combined with in situ bismuth fil formation, the highest stripping peaks were observed (BiF/N/IL/G/SPCE, curve d). The stripping voltammograms clearly demonstrate that the bismuth film in combination with the N/IL/G composite possesses very attractive electrochemical characteristics with highest sensitivity, compared with other electrodes studied in this work.

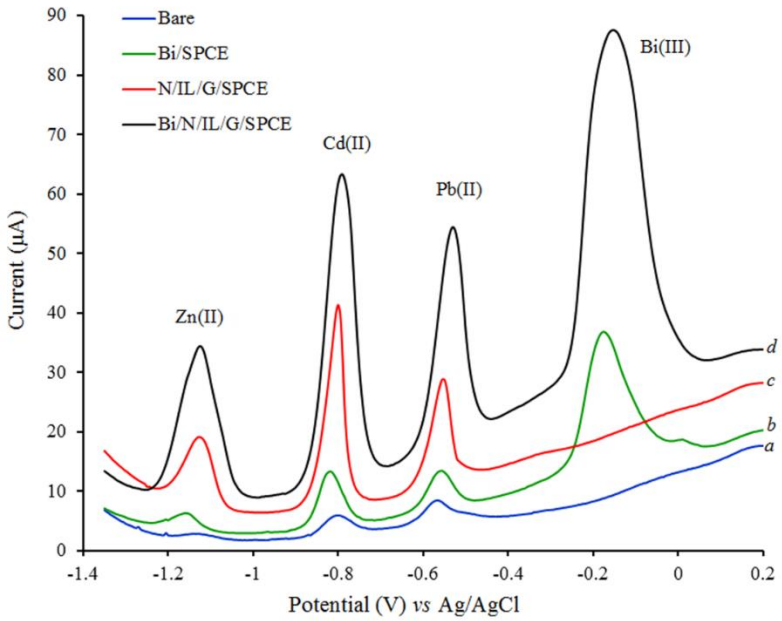

Figure 4.4 SWASVs of 50 ng mL^{-1} Zn(II), Cd(II) and Pb(II) in 0.1 M acetate buffer solution (pH 4.5) on the (a) bare SPCE, (b) Bi(III) film-modified SPCE, (c) N/IL/G/SPCE and (d) Bi(III) film-modified N/IL/G/SPCE. Deposition time: 120 s. Deposition potential: -1.4 V. Concentration of Bi(III): 200 ng mL^{-1}.

4.3.4 Optimization of experimental parameters

4.3.4.1 Effect of concentration of G, IL and N

Different concentrations of G, IL and N that benefited the electrochemical performance of Zn(II), Cd(II) and Pb(II) were dropped on the surface of SPCE, leading to various electrocatalytic actions. Figure 4.5 shows the stripping currents variations of 50.0 ng mL^{-1} Zn(II), Cd(II) and Pb(II) with 1 μL of casting solution at different concentrations. The stripping currents of Zn(II), Cd(II) and Pb(II) first gradually increased with rising concentration of G, IL and N casting-solution from 0.1 to 1.0 mg mL^{-1}, 0.05 to 0.5 % (m:m) and 0.01 to 0.1 % (m:v), respectively, and decreased thereafter. The film formed by N/IL/G composite, if too thick, probably weakens the plane structure of the N/IL/G composite and reduces the electrical conductivity. Taking all these into

consideration, 1.0 mg mL^{-1} of G, 0.5 % of IL and 0.1 % of N composites were used to modify the surface of SPCE. Concerning the cast volume one microliter per 0.2 cm^2 seemed optimal.

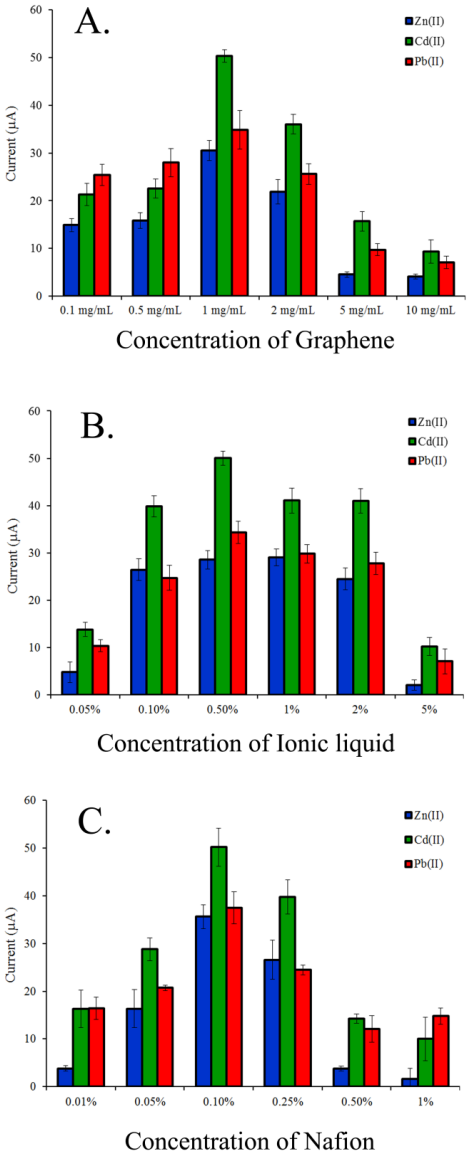

Figure 4.5 Effects of (a) concentration of graphene, (b) concentration of ionic liquid and (c) concentration of Nafion on the stripping peaks current of 50 ng mL^{-1} Zn(II), Cd(II) and Pb(II) in 0.1 M acetate buffer solution (pH 4.5). Error bar: n = 3.

4.3.4.2 Effect of pH, deposition potential, deposition time and concentration of Bi(III)

SWASV was used to study the effect of pH of the supporting electrolyte, deposition potential, deposition time and concentration of Bi(III) on the stripping peak current of 50.0 ng mL^{-1} Zn(II), Cd(II) and Pb(II) (Figure 5.6). Different pH of 0.1 M acetate buffer were tested in the range of 2.5 to 6.5. It was found that a pH of 4.5 produced the highest stripping currents (Figure 4.6a). Thus, for further studies, 0.1 M acetate buffer at pH 4.5 was chosen as the supporting electrolyte. A pH of 4.5 seems to be an optimum for the deposition of bismuth and is in accordance with other literature data [132, 138].

The effect of deposition potential on the stripping peak current of Zn(II), Cd(II) and Pb(II) was evaluated over the potential range from -1.0 to -1.6 V (Figure 4.6b). As can be seen, the current increased by applying the potential from -1.0 to -1.4 V (vs. Ag/AgCl), and then dramatically decreased due to hydrogen formation. Therefore, a deposition potential of -1.4 V was choden to record the voltammograms. The deposition time is other important parameters in stripping procedures that has a pronounced effect on both sensitivity and the dynamic range. The results showed that Zn(II), Cd(II) and Pb(II) were accumulated on the modified electrode surface within 120 s and further time did not improve the peak current (Figure 4.6c). In order to achieve high sensitivity within relatively short analysis time, a deposition time of 120 s was chosen.

The stripping peaks are affected by the thickness of the bismuth film, which can be controlled by varying the concentration of Bi(III) in the plating solution. The effect of the concentration of the Bi(III) was examined in the range from 10 to 1000 ng mL^{-1} (Figure 4.6d). The results show that even at very low concentrations of bismuth, the response of the modified electrode towards Zn(II), Cd(II) and Pb(II) was very sensitive. As the Bi(III) concentration increased, the stripping peaks became more prominent, and the stripping peak currents of Zn(II), Cd(II) and Pb(II) increased only slightly when increasing the concentration above 200 ng mL^{-1} Bi(III). Therefore, the

Bi(III) concentration of 200 ng mL^{-1} was chosen for the simultaneous determinations of Zn(II), Cd(II) and Pb(II).

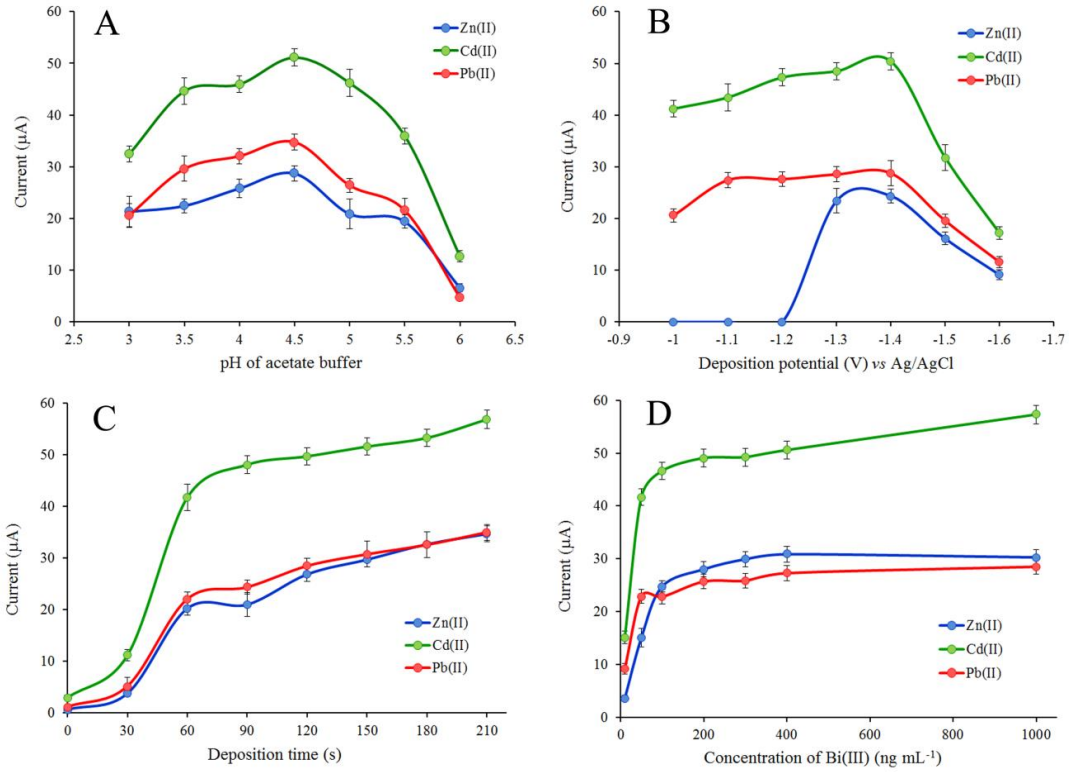

Figure 4.6 Effects of (a) pH, (b) deposition potential, (c) deposition time and (d) concentration of Bi(III) on the stripping peaks current of 50 ng mL^{-1} Zn(II), Cd(II) and Pb(II). Error bar: n = 3.

4.3.5 Analytical performance of BiF/N/IL/G/SPCE

The analytical performance of the BiF/N/IL/G/SPCE for the determination of Zn(II), Cd(II), and Pb(II) was evaluated with SWASV under the optimized experimental conditions, and the results are shown in Figure 4.7. It can be seen that an increase in target metals concentration is accompanied by an increase in stripping peak current. The sensor exhibits excellent linear concentration ranges of 0.1 to 100 ng mL^{-1} for Zn(II), Cd(II) and Pb(II). Beyond these concentrations the graphs level off. The limits of detection based on 3σ value of the blank are 0.09 ng mL^{-1}, 0.06 ng mL^{-1} and 0.08 ng mL^{-1} for Zn(II), Cd(II) and Pb(II), respectively. The obtained detection limits are very

low and more sensitive than for the previously reported methods. Table 4.2 summarizes the linear range and the detection limits of Zn(II), Cd(II) and Pb(II) by various modified electrodes. The detection limit and linear range of the proposed electrode are comparable with and even better than those obtained by other modified electrodes.

The repeatability estimated in terms of the relative standard deviation (RSD %) for ten repetitive measurements of 5.0, 30.0 and 60.0 ng mL^{-1} of Zn(II), Cd(II) and Pb(II) were less than 8.0 %. The reproducibility with different BiF/N/IL/G/SPCE (n = 10 sensorswas always lower than 12%. These results indicate that this sensor can be successfully applied to the simultaneous determination of heavy metal ions with excellent sensitivity and repeatability.

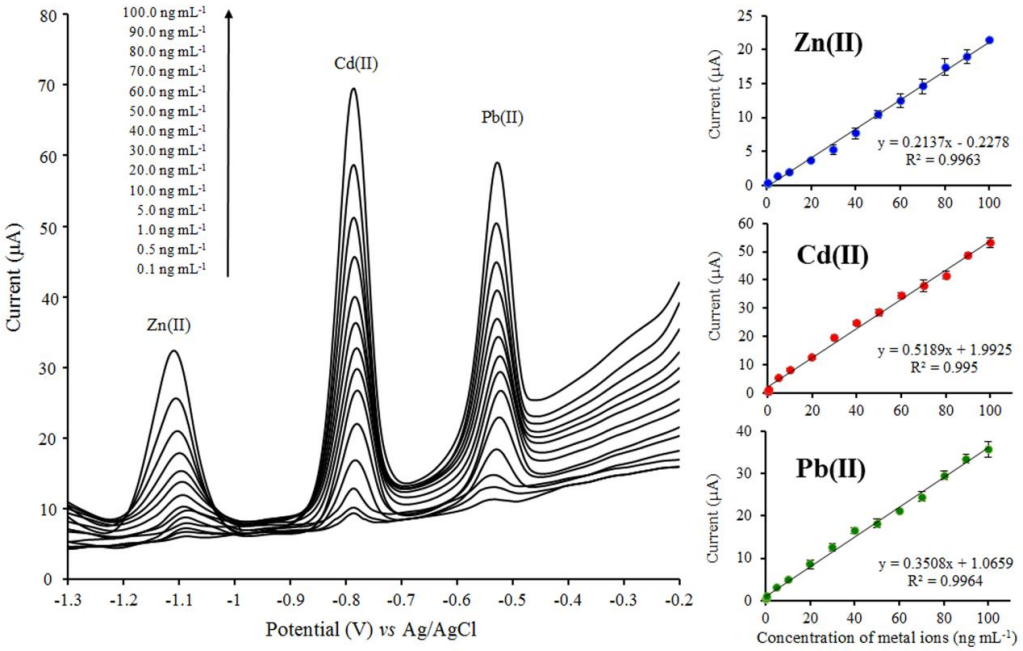

Figure 4.7 SWASVs of Zn(II), Cd(II) and Pb(II); concentrations of Zn(II), Cd(II) and Pb(II) 0.1, 0.5, 1.0, 5.0, 10.0, 20.0, 40.0, 60.0, 80.0 and 100.0 ng mL^{-1}. Other conditions are the same as in Figure 4.3. The insets show the calibration curves.

Table 4.2 Comparison of this method for the determination of Zn(II), Cd(II) and Pb(II) with other stripping techniques at modified electrodes

Electrodes	Method	Linear range (ng mL^{-1})			Detection limit (ng mL^{-1})			Ref.
		Zn(II)	Cd(II)	Pb(II)	Zn(II)	Cd(II)	Pb(II)	
Mercury film/SPCE	SWASV	*N.M.*	1-1000	1-1000	*N.M.*	1.0	0.3	[139]
Bismuth film/SPCE	SWASV	*N.M.*	0-70	0-70	*N.M.*	0.69	0.89	[92]
Bismuth film /carbon nanotubes/SPCE	SWASV	12-100	2-100	2-100	11	0.8	0.2	[94]
Bismuth film /carbon nanotubes/N/SPCE	DPASV	0.5–100	0.5-80	0.5-100	0.3	0.1	0.07	[140]
Bismuth film/G/IL/SPCE	SWASV	*N.M.*	1-80	1-80	*N.M.*	0.08	0.1	[131]
IL/G/CPE	SWASV	*N.M.*	*N.M.*	2.6-41.4	*N.M.*	*N.M.*	0.09	[132]
Bismuth film /N/G/ polyaniline nanocomposite/SPCE	SWASV	1-300	1-300	1-300	1	0.1	0.1	[141]
Hydroxyapatite/IL/CPE	SWASV	*N.M.*	0.1-11.2	0.2-20.8	*N.M.*	0.06	0.04	[142]
IL mediated hollow fiber/CPE	SWASV	*N.M.*	2–13000	0.6-6500	*N.M.*	0.61	0.19	[143]

Table 4.2 Comparison of this method for the determination of Zn(II), Cd(II) and Pb(II) with other stripping techniques at modified electrodes **(continuous)**

Electrodes	Method	Linear range (ng mL^{-1})			Detection limit (ng mL^{-1})			Ref.
		Zn(II)	Cd(II)	Pb(II)	Zn(II)	Cd(II)	Pb(II)	
Mercury Film/N/IL/ Electrode	AdSV	*N.M.*	0.1-16.0	1.0-16.0	*N.M.*	0.13	0.12	[114]
IL/Mesoporous Silica/CPE	DPASV	*N.M.*	67.5-3372.3	82.9-18648	*N.M.*	9.0	8.3	[144]
Bismuthfilm/G/polyaniline/ polystyrene nanoporous fibers/SPCE	SWASV	*N.M.*	10-500	10-500	*N.M.*	4.43	3.30	[145]
Bismuth film/N/IL/G/SPCE	SWASV	0.1-100	0.1-100	0.1-100	0.09	0.06	0.08	This work

SPCE: Screen-Printed Carbon Electrode; NA: Nafion; G: Graphene; IL: Ionic Liquid; CPE: Carbon Paste Electrode; DPASV: Differential Pulse Anodic Stripping Voltammetry; AdSV: Adsorptive stripping voltammetry; *N.M.*: Not Measured

4.3.6 Interference study

The effect of some possible interferents was investigated by adding them to a solution containing 50.0 ng mL^{-1} of Zn(II), Cd(II) and Pb(II) in 0.1 M acetate butter pH 4.5. The tolerance limit is estimated to be less than 5 % of the error. The experimental results reveal that 1000-fold mass ratios of PO_4^{3-}, Cl^-, SO_4^{2-}, F^-, Ca^{2+}, K^+ , Mg^{2+} and Mn^{2+}; 500-fold mass ratios of Fe^{3+}, As^{3+} and Hg^{2+} 200-fold mass ratio of Zn^{2+}, Cd^{2+} and Pb^{2+} and 10-fold mass ratios of Cu^{2+}, Co^{2+} and Ni^{2+}did not interfere with the analysis of Zn(II), Cd(II) and Pb(II) (Table 4.3). Hence determination of Zn(II), Cd(II) and Pb(II) was not considerably affected by common interfering species, which shows that the method is more selective toward three target metals.

Table 4.3 Tolerance ratio of interfering ions in the electrochemical determination of 50 ng mL^{-1} of Zn(II), Cd(II) and Pb(II) on BiF/N/IL/G/SPCE.

	5 % tolerance ratio ($W_{ions}/W_{target\ metals}$)		
Common ions	Zn(II)	Cd(II)	Pb(II)
PO_4^{3-}, Cl^-, SO_4^{2-}, F^-, Ca^{2+}, K^+ , Mg^{2+}, Mn^{2+}	>1000	>1000	>1000
Fe^{3+}, As^{3+}, Hg^{2+}	500	500	500
Cu^{2+}, Co^{2+}, Ni^{2+}	25	25	25
Pb^{2+}	200	200	-
Cd^{2+}	200	-	200
Zn^{2+}	-	200	200

4.3.7 Sample analysis

The BiF/N/IL/G/SPCE sensor was applied on treated drinking water samples using the standard addition method. Recovery studies were carried out by spiking Zn(II), Cd(II) and Pb(II) to the drinking water samples (with analyte concentrations below

the detection limit) at three concentration levels of 5.0, 30.0 and 60.0 ng mL^{-1}. The obtained recoveries of Zn(II), Cd(II) and Pb(II) were in the range of 90.3 - 112.5 % (Table 5.4). The recoveries were satisfactory reasonable, which indicated the capability of the method for determination of Zn(II), Cd(II) and Pb(II) in such samples. Commercially available drinking waters were analyzed, the results obtained by BiF/N/IL/G/SPCE were compared with those from inductively coupled plasma-mass spectrometry (ICP-MS) (Table 5.5). The applicability of the method to natural water matrices was additionally confirmed with the analysis of a reference material (NIST standard reference material 1640 a, "Trace Elements in Natural Water"). The significance of the developed method was also tested. The results thus obtained clearly reveal that the concentrations of Zn(II), Cd(II) and Pb(II) in the drinking samples obtained by the proposed stripping voltammetry are in satisfactory agreement with those determined by ICP-MS and the proposed stripping sensor has promising feasibility for trace-level determination of Zn(II), Cd(II) and Pb(II) in even more complex samples.

Table 4.4 Recovery for the determination of Zn(II), Cd(II) and Pb(II) in drinking water samples (n=3).

Samples	Added	% Recovery			% RSD		
	($ng\ mL^{-1}$)	Zn(II)	Cd(II)	Pb(II)	Zn(II)	Cd(II)	Pb(II)
Drinking water 1	5.0	94.7 ± 3.5	90.3 ± 2.9	110.4 ± 1.7	3.7	3.2	1.6
	30.0	101.6 ± 5.8	103.0 ± 4.2	96.8 ± 3.6	5.7	4.1	3.7
	60.0	99.6 ± 3.0	99.3 ± 2.3	100.7 ± 2.3	3.0	2.3	2.3
Drinking water 2	5.0	96.2 ± 4.3	93.0 ± 2.3	105.4 ± 5.7	4.5	2.4	4.6
	30.0	101.2 ± 0.9	102.2 ± 5.3	101.4 ± 1.2	0.9	5.2	1.2
	60.0	99.8 ± 4.1	99.5 ± 3.2	102.1 ± 5.1	4.1	3.2	5.0
Drinking water 3	5.0	105.3 ± 9.8	91.9 ± 5.6	112.5 ± 1.9	9.3	6.1	1.7
	30.0	98.4 ± 2.0	107.2 ± 4.8	93.4 ± 2.0	2.0	4.4	2.1
	60.0	100.4 ± 7.1	98.4 ± 6.6	101.5 ± 7.6	7.1	6.7	7.5

Table 4.5 The comparison of the proposed method and standard method for the determination of Zn(II), Cd(II) and Pb(II) in drinking water samples (n=3).

Samples	Found (ng mL^{-1})					
	Proposed method			ICP-MS		
	Zn(II)	Cd(II)	Pb(II)	Zn(II)	Cd(II)	Pb(II)
Drinking water 1	7.6 ± 0.4	3.0 ± 0.5	8.7 ± 0.4	8.0 ± 0.8	3.2 ± 0.4	9.2 ± 0.4
Drinking water 2	24.9 ± 0.9	2.5 ± 0.6	8.6 ± 0.3	25.3 ± 1.2	2.1 ± 0.3	8.8 ± 0.4
Drinking water 3	13.5± 0.4	<1.0	6.3 ± 0.3	13.8 ± 1.5	< 2.0	6.6 ± 0.2
Drinking water 4	9.6 ± 0.5	<1.0	<1.0	9.9 ± 1.4	< 2.0	< 2.0
NIST SRM 1640a	56.0± 1.3	4.1 ± 0.5	12.5 ± 0.6	55.64 ± 0.35*	3.992 ± 0.074*	12.101 ± 0.050*

* certified value

4.4 Conclusions

In this study, a Nafion/ionic liquid/graphene composite and bismuth film-modified screen-printed carbon electrode (BiF/N/IL/G/SPCE) was developed and used for the simultaneous determination of Zn(II), Cd(II) and Pb(II) by square wave anodic stripping voltammetry (SWASV). To the best of our knowledge, such a multiple composite - bismuth film electrode was used for the first time as a working electrode. The modified electrode exhibited greatly improved stripping performance for the determination of Zn(II), Cd(II) and Pb(II). This was attributed to the increased surface area, improved conductivity and mass transfer on the electrode surface due to the incorporation of Nafion, ionic liquid and graphene. Under optimized conditions, the relevant calibration curves were linear in the range of 0.1 to 100 ng mL^{-1} for three metal ions, with a detection limit of 0.09 ng mL^{-1}, 0.06 ng mL-^{1} and 0.08 ng mL^{-1} for Zn(II), Cd(II) and Pb(II), respectively, with 120 s deposition time. Good repeatability and reproducibility of the voltammetric responses was achieved. Compared to approaches with carbon nanotubes (21] the new type of sensor shows significantly lower detection limits, improved baseline and signal characteristics particularly for zinc, but also for the other analytes, and may be used simply in batch stripping analysis without sequential injection at very low concentration levels which will favor its application to matrices with low contents of the analytes, such as rain water. The reason for this drastic improvement can be found in many characteristics of graphene which are superior to CNTs, such as electric conductivity and surface area [146-149].

Furthermore, the utility of the proposed method was successfully tested by the determination of heavy metals in drinking water samples and the results were in satisfactory agreement with ICP-MS determination. This sensor can be used as an excellent alternative to more expensive spectroscopic methods for the determination of heavy metals in real sample.

CHAPTER V

CONCLUSIONS AND FUTURE WORKS

5.1 Conclusions

The main aim of this research is to develop microfluidic analytical device combined with colorimetric and/or electrochemical detection for determination of heavy metals in food, environmental and clinical applications. The conclusion of this study has been separated into 3 parts as follows:

Part I: Highly selective and sensitive paper-based colorimetric sensor using thiosulfate catalytic etching of silver nanoplates for trace determination of copper ions

Novel μPADs were developed for the determination of copper based on the catalytic etching of silver nanoplates by thiosulfate. This device shows highly sensitive and selective detection of copper in the presence of common interfering ions. Under optimized conditions, the limit of detection was found to be 1.0 ng mL^{-1} by visual detection, and the sensor was exhibited an acceptable linear range of 0.5–200 ng mL^{-1} with detection limits of 0.3 ng mL^{-1} by image processing. Lastly, the proposed method was successfully applied for the quantitative determination of copper in food, water and blood samples.

Part II: High sensitivity and specificity simultaneous determination of lead, cadmium and copper using μPAD with dual electrochemical and colorimetric detection

New μPAD coupled with dual electrochemical and colorimetric detection were developed high sensitivity and specificity for the determination of heavy metal ions. Electrochemical detection on μPAD was applied for the determination of lead and

cadmium using a bismuth-modified boron-doped diamond electrode (Bi-BDDE). The limit of detection was 0.1 ng mL^{-1} for lead and cadmium. For determination of copper, colorimetric detection was uesd for the determination of copper based on the catalytic etching of silver nanoplates by thiosulfate. The color of AgNPls on μPAD changed from pinkish violet to colorless after the addition of copper. 5 ng mL^{-1} is the limits of detection of copper by naked eyes. This device showed simplicity, high sensitivity, good specificity and excellent reproducibility for simultaneous determination of these three metals in real samples. The obtained results are promising and corresponding to results obtained from standard methods.

Part III: Electrochemical sensors for the simultaneous determination of zinc, cadmium and lead using a nafion/ionic liquid/graphene composite modified screen-printed carbon electrode

The bismuth film on nafion/ionic liquid/graphene composite modified screen-printed carbon electrode (BiF/N/IL/G/SPCE) was developed for determination of heavy metal ions. This method exhibited a simple, low cost, and highly sensitive for simultaneous of zinc, cadmium and lead. The linear calibration curves ranged from 0.1 to 100 ng mL^{-1} for zinc, cadmium and lead. The detection limits were 0.09 ng mL^{-1} for zinc, 0.06 ng mL^{-1} for cadmium and 0.08 ng mL^{-1} for lead. Additionally, the results showed a highly reproducible procedure having a relative standard deviation of 8.0 % for 10 replicate measurements. Furthermore, the method was successfully applied to determine these heavy metal ions in various real samples. The results were in a good agreement with those obtained by inductively coupled plasma mass spectrometry. In future works, the proposed sensors can be applied to be a detector for microfluidic analytical system to obtain the portable device for field analysis.

5.2 Future works

The proposed sensors in part III of this research is very interesting for microfluidic analytical device because it exhibited high sensitivity and low limits of

detection for determination of heavy metal ions. Therefore, future works is the combination it to microfluidic analytical device for simultaneous determination of zinc, cadmium and lead due to high sensitivity and selectivity to obtain portability, ease of use, small samples volume requirement, and inexpensiveness assay.

REFERENCES

[1] Agency, U.S.E.P. EPA's Report on the Environment [Online]. 2016. Available from: https://cfpub.epa.gov/roe/index.cfm

[2] Organization, W.H. Food safety [Online]. 2016. Available from: http://www.who.int/mediacentre/factsheets/fs399/en/

[3] Department, P.C. Water Quality Standards [Online]. 2016. Available from: http://www.pcd.go.th/info_serv/en_reg_std_water04.html

[4] Järup, L. Hazards of heavy metal contamination. British Medical Bulletin 68(1) (2003): 167-182.

[5] Park, G.J., You, G.R., Choi, Y.W., and Kim, C. A naked-eye chemosensor for simultaneous detection of iron and copper ions and its copper complex for colorimetric/fluorescent sensing of cyanide. Sensors and Actuators B: Chemical 229 (2016): 257-271.

[6] Xu, D., et al. Simultaneous determination of traces amounts of cadmium, zinc, and cobalt based on UV–Vis spectrometry combined with wavelength selection and partial least squares regression. Spectrochimica Acta Part A: Molecular and Biomolecular Spectroscopy 123 (2014): 430-435.

[7] She, P., et al. A competitive immunoassay for ultrasensitive detection of Hg2+ in water, human serum and urine samples using immunochromatographic test based on surface-enhanced Raman scattering. Analytica Chimica Acta 906 (2016): 139-147.

[8] Zhong, W.-S., Ren, T., and Zhao, L.-J. Determination of Pb (Lead), Cd (Cadmium), Cr (Chromium), Cu (Copper), and Ni (Nickel) in Chinese tea with high-resolution continuum source graphite furnace atomic absorption spectrometry. Journal of Food and Drug Analysis 24(1) (2016): 46-55.

[9] Zeng, C., Jia, Y., Lee, Y.-I., Hou, X., and Wu, L. Ultrasensitive determination of cobalt and nickel by atomic fluorescence spectrometry using APDC enhanced chemical vapor generation. Microchemical Journal 104 (2012): 33-37.

[10] McGillicuddy, N., Nesterenko, E.P., Nesterenko, P.N., Jones, P., and Paull, B. Chelation ion chromatography of alkaline earth and transition metals a using monolithic silica column with bonded N-hydroxyethyliminodiacetic acid functional groups. Journal of Chromatography A 1276 (2013): 102-111.

[11] Li, Y., et al. Determination of ultra-trace rare earth elements in high-salt groundwater using aerosol dilution inductively coupled plasma-mass spectrometry (ICP-MS) after iron hydroxide co-precipitation. Microchemical Journal 126 (2016): 194-199.

[12] Nunes, A.M., et al. Fast determination of Fe, Mg, Mn, P and Zn in meat samples by inductively coupled plasma optical emission spectrometry after alkaline solubilization. Journal of Food Composition and Analysis 32(1) (2013): 1-5.

[13] Date, Y., et al. Microfluidic heavy metal immunoassay based on absorbance measurement. Biosensors and Bioelectronics 33(1) (2012): 106-112.

[14] Guo, L., Feng, J., Fang, Z., Xu, J., and Lu, X. Application of microfluidic "lab-on-a-chip" for the detection of mycotoxins in foods. Trends in Food Science & Technology 46(2, Part A) (2015): 252-263.

[15] Martinez, A.W., Phillips, S.T., Butte, M.J., and Whitesides, G.M. Patterned paper as a platform for inexpensive, low-volume, portable bioassays. Angewandte Chemie International Edition 46(8) (2007): 1318-1320.

[16] Müller, R.H. and Clegg, D.L. Automatic Paper Chromatography. Analytical Chemistry 21(9) (1949): 1123-1125.

[17] Alkasir, R.S.J., Ornatska, M., and Andreescu, S. Colorimetric paper bioassay for the detection of phenolic compounds. Analytical Chemistry 84(22) (2012): 9729-9737.

[18] Dungchai, W., Chailapakul, O., and Henry, C.S. Electrochemical detection for paper-based microfluidics. Analytical Chemistry 81(14) (2009): 5821-5826.

[19] He, M. and Liu, Z. Paper-Based Microfluidic device with upconversion fluorescence assay. Analytical Chemistry 85(24) (2013): 11691-11694.

[20] Delaney, J.L., Hogan, C.F., Tian, J., and Shen, W. Electrogenerated chemiluminescence detection in paper-based microfluidic sensors. Analytical Chemistry 83(4) (2011): 1300-1306.

[21] Shi, C.-G., et al. Quantum dot (QD)-modified carbon tape electrodes for reproducible electrochemiluminescence (ECL) emission on a paper-based platform. Analytical Chemistry 84(6) (2012): 3033-3038.

[22] Liana, D.D., Raguse, B., Gooding, J.J., and Chow, E. Toward paper-based sensors: turning electrical signals into an optical readout system. ACS Applied Materials & Interfaces 7(34) (2015): 19201-19209.

[23] Liang, L., Ge, S., Li, L., Liu, F., and Yu, J. Microfluidic paper-based multiplex colorimetric immunodevice based on the catalytic effect of Pd/Fe3O4@C peroxidase mimetics on multiple chromogenic reactions. Analytica Chimica Acta 862 (2015): 70-76.

[24] Cinti, S., Talarico, D., Palleschi, G., Moscone, D., and Arduini, F. Novel reagentless paper-based screen-printed electrochemical sensor to detect phosphate. Analytica Chimica Acta 919 (2016): 78-84.

[25] Santhiago, M., Henry, C.S., and Kubota, L.T. Low cost, simple three dimensional electrochemical paper-based analytical device for determination of p-nitrophenol. Electrochimica Acta 130 (2014): 771-777.

[26] Wagesho, Y. and Chandravanshi, B.S. Levels of essential and non-essential metals in ginger (Zingiber officinale) cultivated in Ethiopia. SpringerPlus 4(1) (2015): 1-13.

[27] Panebianco, M.V., Negri, M.F., Botte, S.E., Marcovecchio, J.E., and Cappozzo, H.L. Essential and non-essential heavy metals in skin and muscle tissues of franciscana dolphins (Pontoporia blainvillei) from the southern Argentina coast. Chemistry and Ecology 29(6) (2013): 511-518.

[28] Leavitt, S.W., Dueser, R.D., and Goodell, H.G. Plant regulation of essential and non-essential heavy metals. Journal of Applied Ecology 16(1) (1979): 203-212.

[29] Terry, S.C., Jerman, J.H., and Angell, J.B. A gas chromatographic air analyzer fabricated on a silicon wafer. IEEE Transactions on Electron Devices 26(12) (1979): 1880-1886.

[30] Reyes, D.R., Iossifidis, D., Auroux, P.-A., and Manz, A. Micro total analysis systems. 1. introduction, theory, and technology. Analytical Chemistry 74(12) (2002): 2623-2636.

[31] Manz, A., Miyahara, Y., Miura, J., Watanabe, Y., Miyagi, H., and Sato, K. Design of an open-tubular column liquid chromatograph using silicon chip technology. Sensors and Actuators B: Chemical 1(1) (1990): 249-255.

[32] Manz, A., Graber, N., and Widmer, H.M. Miniaturized total chemical analysis systems: A novel concept for chemical sensing. Sensors and Actuators B: Chemical 1(1) (1990): 244-248.

[33] Whitesides, G.M. The origins and the future of microfluidics. Nature 442(7101) (2006): 368-373.

[34] Sharma, H., Nguyen, D., Chen, A., Lew, V., and Khine, M. Unconventional low-cost fabrication and patterning techniques for point of care diagnostics. Annals of Biomedical Engineering 39(4) (2011): 1313-1327.

[35] Auroux, P.-A., Iossifidis, D., Reyes, D.R., and Manz, A. Micro total analysis systems. 2. analytical standard operations and applications. Analytical Chemistry 74(12) (2002): 2637-2652.

[36] Asano, H. and Shiraishi, Y. Development of paper-based microfluidic analytical device for iron assay using photomask printed with 3D printer for fabrication of hydrophilic and hydrophobic zones on paper by photolithography. Analytica Chimica Acta 883 (2015): 55-60.

[37] Tsai, S.-W., Chen, P.-Y., Huang, S.-R., and Lee, Y.-C. Fabrication of seamless roller mold with 3D micropatterns using inner curved surface photolithography. Microelectronic Engineering 150 (2016): 19-25.

[38] Xia, Y., Si, J., and Li, Z. Fabrication techniques for microfluidic paper-based analytical devices and their applications for biological testing: A review. Biosensors and Bioelectronics 77 (2016): 774-789.

[39] Yetisen, A.K., Akram, M.S., and Lowe, C.R. Paper-based microfluidic point-of-care diagnostic devices. Lab on a Chip 13(12) (2013): 2210-2251.

[40] Carrilho, E., Martinez, A.W., and Whitesides, G.M. Understanding wax printing: a simple micropatterning process for paper-based microfluidics. Analytical Chemistry 81(16) (2009): 7091-7095.

[41] Hossain, S.M.Z. and Brennan, J.D. β-Galactosidase-based colorimetric paper sensor for determination of heavy metals. Analytical Chemistry 83(22) (2011): 8772-8778.

[42] Carvalhal, R.F., Simão Kfouri, M., de Oliveira Piazetta, M.H., Gobbi, A.L., and Kubota, L.T. Electrochemical detection in a paper-based separation device. Analytical Chemistry 82(3) (2010): 1162-1165.

[43] Liang, L., et al. Aptamer-based fluorescent and visual biosensor for multiplexed monitoring of cancer cells in microfluidic paper-based analytical devices. Sensors and Actuators B: Chemical 229 (2016): 347-354.

[44] Liu, W., et al. A molecularly imprinted polymer based a lab-on-paper chemiluminescence device for the detection of dichlorvos. Spectrochimica Acta Part A: Molecular and Biomolecular Spectroscopy 141 (2015): 51-57.

[45] Liu, F. and Zhang, C. A novel paper-based microfluidic enhanced chemiluminescence biosensor for facile, reliable and highly-sensitive gene detection of Listeria monocytogenes. Sensors and Actuators B: Chemical 209 (2015): 399-406.

[46] Wu, L., Ma, C., Zheng, X., Liu, H., and Yu, J. Paper-based electrochemiluminescence origami device for protein detection using assembled cascade DNA–carbon dots nanotags based on rolling circle amplification. Biosensors and Bioelectronics 68 (2015): 413-420.

[47] Siegel, A.C., Phillips, S.T., Wiley, B.J., and Whitesides, G.M. Thin, lightweight, foldable thermochromic displays on paper. Lab on a Chip 9(19) (2009): 2775-2781.

[48] Cai, W., Lai, T., Du, H., and Ye, J. Electrochemical determination of ascorbic acid, dopamine and uric acid based on an exfoliated graphite paper electrode: A high performance flexible sensor. Sensors and Actuators B: Chemical 193 (2014): 492-500.

[49] Bakker, E. and Qin, Y. Electrochemical Sensors. Analytical chemistry 78(12) (2006): 3965-3984.

[50] Laborda, E., González, J., and Molina, Á. Recent advances on the theory of pulse techniques: A mini review. Electrochemistry Communications 43 (2014): 25-30.

[51] Nikolic, J., Expósito, E., Iniesta, J., González-Garcia, J., and Montiel, V. Theoretical concepts and applications of a rotating disk electrode. Journal of Chemical Education 77(9) (2000): 1191.

[52] Climent, V. and Feliu, J.M. Cyclic voltammetry. in Reference Module in Chemistry, Molecular Sciences and Chemical Engineering: Elsevier, 2015.

[53] Lovrić, M. and Komorsky-Lovrić, Š. Theory of square wave voltammetry of three step electrode reaction. Journal of Electroanalytical Chemistry 735 (2014): 90-94.

[54] Ball, J.C., Compton, R.G., and Brett, C.M.A. Theory of anodic stripping voltammetry at wall-jet electrodes. simulation of spatially differential stripping and redeposition phenomena. The Journal of Physical Chemistry B 102(1) (1998): 162-166.

[55] Gholivand, M.B., Sohrabi, A., and Abbasi, S. Determination of copper by adsorptive stripping voltammetry in the presence of calcein blue. Electroanalysis 19(15) (2007): 1609-1615.

[56] Reddy, S.A., Reddy, K.J., Narayana, S.L., and Reddy, A.V. Analytical applications of 2,6-diacetylpyridine bis-4-phenyl-3-thiosemicarbazone and determination of Cu(II) in food samples. Food Chemistry 109(3) (2008): 654-659.

[57] Aguilar F., C.U.R., Dusemund B., Galtie.r P, Gilbert J., Gott D.M., Grilli S., , Guertler R., K.G.E.N., Koenig J., Lambré C., Larsen J-C., Leblanc J-C., Mortensen A., , Parent-Massin D., P.I., Rietjens I.M.C.M., Stankovic I., Tobback P., Verguieva T., , and R.A., W. Copper(II) oxide as a source of copper added for nutritional purposes to food supplements. European Food Safety Authority 1089 (2009): 1-15.

[58] Pourreza, N. and Hoveizavi, R. Simultaneous preconcentration of Cu, Fe and Pb as methylthymol blue complexes on naphthalene adsorbent and flame atomic absorption determination. Analytica Chimica Acta 549(1–2) (2005): 124-128.

[59] Atanassova, D., Stefanova, V., and Russeva, E. Co-precipitative pre-concentration with sodium diethyldithiocarbamate and ICP-AES determination of Se, Cu, Pb, Zn, Fe, Co, Ni, Mn, Cr and Cd in water. Talanta 47(5) (1998): 1237-1243.

[60] Zhu, Y., Inagaki, K., and Chiba, K. Determination of Fe, Cu, Ni, and Zn in seawater by ID-ICP-MS after preconcentration using a syringe-driven chelating column. Journal of Analytical Atomic Spectrometry 24(9) (2009): 1179-1183.

[61] Chaiyo, S., Chailapakul, O., Sakai, T., Teshima, N., and Siangproh, W. Highly sensitive determination of trace copper in food by adsorptive stripping voltammetry in the presence of 1,10-phenanthroline. Talanta 108 (2013): 1-6.

[62] Zhang, S., et al. Highly sensitive and selective fluorescence detection of copper (II) ion based on multi-ligand metal chelation. Talanta 126 (2014): 185-190.

[63] Weng, Z., et al. Self-assembly of core-satellite gold nanoparticles for colorimetric detection of copper ions. Analytica Chimica Acta 803 (2013): 128-134.

[64] Zhou, Y., Zhao, H., He, Y., Ding, N., and Cao, Q. Colorimetric detection of Cu2+ using 4-mercaptobenzoic acid modified silver nanoparticles. Colloids and Surfaces A: Physicochemical and Engineering Aspects 391(1–3) (2011): 179-183.

[65] Jiang, X.C. and Yu, A.B. Silver Nanoplates: A Highly Sensitive Material toward Inorganic Anions. Langmuir 24(8) (2008): 4300-4309.

[66] Miao, L.-J., Xin, J.-W., Shen, Z.-Y., Zhang, Y.-J., Wang, H.-Y., and Wu, A.-G. Exploring a new rapid colorimetric detection method of Cu2+ with high sensitivity and selectivity. Sensors and Actuators B: Chemical 176 (2013): 906-912.

[67] Ratnarathorn, N., Chailapakul, O., Henry, C.S., and Dungchai, W. Simple silver nanoparticle colorimetric sensing for copper by paper-based devices. Talanta 99 (2012): 552-557.

[68] Lou, T., Chen, L., Chen, Z., Wang, Y., Chen, L., and Li, J. Colorimetric detection of trace copper ions based on catalytic leaching of silver-coated gold nanoparticles. ACS Applied Materials & Interfaces 3(11) (2011): 4215-4220.

[69] Liu, R., Chen, Z., Wang, S., Qu, C., Chen, L., and Wang, Z. Colorimetric sensing of copper(II) based on catalytic etching of gold nanoparticles. Talanta 112 (2013): 37-42.

[70] Zhao, W. and Van Den Berg, A. Lab on paper. Lab on a Chip - Miniaturisation for Chemistry and Biology 8(12) (2008): 1988-1991.

[71] Apilux, A., Dungchai, W., Siangproh, W., Praphairaksit, N., Henry, C.S., and Chailapakul, O. Lab-on-paper with dual electrochemical/colorimetric detection for simultaneous determination of gold and iron. Analytical Chemistry 82(5) (2010): 1727-1732.

[72] Abe, K., Suzuki, K., and Citterio, D. Inkjet-printed microfluidic multianalyte chemical sensing paper. Analytical Chemistry 80(18) (2008): 6928-6934.

[73] Bruzewicz, D.A., Reches, M., and Whitesides, G.M. Low-cost printing of poly(dimethylsiloxane) barriers to define microchannels in paper. Analytical Chemistry 80(9) (2008): 3387-3392.

[74] Li, X., Tian, J., Nguyen, T., and Shen, W. Paper-based microfluidic devices by plasma treatment. Analytical Chemistry 80(23) (2008): 9131-9134.

[75] Dungchai, W., Chailapakul, O., and Henry, C.S. A low-cost, simple, and rapid fabrication method for paper-based microfluidics using wax screen-printing. Analyst 136(1) (2011): 77-82.

[76] Parnklang, T., Lertvachirapaiboon, C., Pienpinijtham, P., Wongravee, K., Thammacharoen, C., and Ekgasit, S. H_2O_2-triggered shape transformation of silver nanospheres to nanoprisms with controllable longitudinal LSPR wavelengths. RSC Advances 3(31) (2013): 12886-12894.

[77] Abbasi, S., Khani, H., and Tabaraki, R. Determination of ultra trace levels of copper in food samples by a highly sensitive adsorptive stripping voltammetric method. Food Chemistry 123(2) (2010): 507-512.

[78] Ye, Q.-y., Li, Y., Jiang, Y., and Yan, X.-p. Determination of trace cadmium in rice by flow injection on-line filterless precipitation–dissolution preconcentration coupled with flame atomic absorption spectrometry. Journal of Agricultural and Food Chemistry 51(8) (2003): 2111-2114.

[79] Tarik, A., Harek Yahia, and Lahcen, L. Determination of ultra trace levels of copper in whole blood by adsorptive stripping voltammetry. Journal of the Korean Chemical Society 57 (2013).

[80] Grosse, A.C., Dicinoski, G.W., Shaw, M.J., and Haddad, P.R. Leaching and recovery of gold using ammoniacal thiosulfate leach liquors (a review). Hydrometallurgy 69(1–3) (2003): 1-21.

[81] Hormozi-Nezhad, M.R. and Abbasi-Moayed, S. A sensitive and selective colorimetric method for detection of copper ions based on anti-aggregation of unmodified gold nanoparticles. Talanta 129 (2014): 227-232.

[82] Liu, J.-M., et al. Non-aggregation based label free colorimetric sensor for the detection of Cu2+ based on catalyzing etching of gold nanorods by dissolve oxygen. Talanta 117 (2013): 425-430.

[83] Wang, S., Chen, Z., Chen, L., Liu, R., and Chen, L. Label-free colorimetric sensing of copper(ii) ions based on accelerating decomposition of H_2O_2 using gold nanorods as an indicator. Analyst 138(7) (2013): 2080-2084.

[84] Sadollahkhani, A., Hatamie, A., Nur, O., Willander, M., Zargar, B., and Kazeminezhad, I. Colorimetric disposable paper coated with zno@zns core–shell nanoparticles for detection of copper ions in aqueous solutions. ACS Applied Materials & Interfaces 6(20) (2014): 17694-17701.

[85] Kemper, T. and Sommer, S. Estimate of heavy metal contamination in soils after a mining accident using reflectance spectroscopy. Environmental Science & Technology 36(12) (2002): 2742-2747.

[86] Mahmoud, M.E., Kenawy, I.M.M., Hafez, M.A.H., and Lashein, R.R. Removal, preconcentration and determination of trace heavy metal ions in water samples by AAS via chemically modified silica gel N-(1-carboxy-6-hydroxy) benzylidenepropylamine ion exchanger. Desalination 250(1) (2010): 62-70.

[87] Dai, B., et al. Schiff base-chitosan grafted multiwalled carbon nanotubes as a novel solid-phase extraction adsorbent for determination of heavy metal by ICP-MS. Journal of Hazardous Materials 219–220 (2012): 103-110.

[88] Jarić, I., et al. Determination of differential heavy metal and trace element accumulation in liver, gills, intestine and muscle of sterlet (Acipenser ruthenus)

from the Danube River in Serbia by ICP-OES. Microchemical Journal 98(1) (2011): 77-81.

[89] Huang, H., Chen, T., Liu, X., and Ma, H. Ultrasensitive and simultaneous detection of heavy metal ions based on three-dimensional graphene-carbon nanotubes hybrid electrode materials. Analytica Chimica Acta 852 (2014): 45-54.

[90] Rodrigues, J.A., et al. Increased sensitivity of anodic stripping voltammetry at the hanging mercury drop electrode by ultracathodic deposition. Analytica Chimica Acta 701(2) (2011): 152-156.

[91] Brett, C.M.A. and Fungaro, D.A. Poly(ester sulphonic acid) coated mercury thin film electrodes: characterization and application in batch injection analysis stripping voltammetry of heavy metal ions. Talanta 50(6) (2000): 1223-1231.

[92] Chuanuwatanakul, S., Dungchai, W., Chailapakul, O., and Motomizu, S. Determination of trace heavy metals by sequential injection-anodic stripping voltammetry using bismuth film screen-printed printed carbon electrode. Analytical Sciences 24(5) (2008): 589-594.

[93] Zhu, L., Xu, L., Huang, B., Jia, N., Tan, L., and Yao, S. Simultaneous determination of Cd(II) and Pb(II) using square wave anodic stripping voltammetry at a gold nanoparticle-graphene-cysteine composite modified bismuth film electrode. Electrochimica Acta 115 (2014): 471-477.

[94] Injang, U., Noyrod, P., Siangproh, W., Dungchai, W., Motomizu, S., and Chailapakul, O. Determination of trace heavy metals in herbs by sequential injection analysis-anodic stripping voltammetry using screen-printed carbon nanotubes electrodes. Analytica Chimica Acta 668(1) (2010): 54-60.

[95] Cao, L., Jia, J., and Wang, Z. Sensitive determination of Cd and Pb by differential pulse stripping voltammetry with in situ bismuth-modified zeolite doped carbon paste electrodes. Electrochimica Acta 53(5) (2008): 2177-2182.

[96] Toghill, K.E., Wildgoose, G.G., Moshar, A., Mulcahy, C., and Compton, R.G. The fabrication and characterization of a bismuth nanoparticle modified boron doped diamond electrode and its application to the simultaneous

determination of cadmium(II) and lead(II). Electroanalysis 20(16) (2008): 1731-1737.

[97] Pecková, K., Musilová, J., and Barek, J. Boron-doped diamond film electrodes—new tool for voltammetric determination of organic substances. Critical Reviews in Analytical Chemistry 39(3) (2009): 148-172.

[98] Yang, D., Wang, L., Chen, Z., Megharaj, M., and Naidu, R. Investigation of copper(II) interference on the anodic stripping voltammetry of lead(II) and cadmium(II) at bismuth film electrode. Electroanalysis 25(12) (2013): 2637-2644.

[99] Wang, J., Lu, J., Kirgöz, Ü.A., Hocevar, S.B., and Ogorevc, B. Insights into the anodic stripping voltammetric behavior of bismuth film electrodes. Analytica Chimica Acta 434(1) (2001): 29-34.

[100] Yu, J., Ge, L., Huang, J., Wang, S., and Ge, S. Microfluidic paper-based chemiluminescence biosensor for simultaneous determination of glucose and uric acid. Lab on a Chip 11(7) (2011): 1286-1291.

[101] Chaiyo, S., Siangproh, W., Apilux, A., and Chailapakul, O. Highly selective and sensitive paper-based colorimetric sensor using thiosulfate catalytic etching of silver nanoplates for trace determination of copper ions. Analytica Chimica Acta 866 (2015): 75-83.

[102] Brainina, K.Z., et al. Determination of heavy metals in wines by anodic stripping voltammetry with thick-film modified electrode. Analytica Chimica Acta 514(2) (2004): 227-234.

[103] Keawkim, K., Chuanuwatanakul, S., Chailapakul, O., and Motomizu, S. Determination of lead and cadmium in rice samples by sequential injection/anodic stripping voltammetry using a bismuth film/crown ether/Nafion modified screen-printed carbon electrode. Food Control 31(1) (2013): 14-21.

[104] Hočevar, S.B., Ogorevc, B., Wang, J., and Pihlar, B. A study on operational parameters for advanced use of bismuth film electrode in anodic stripping voltammetry. Electroanalysis 14(24) (2002): 1707-1712.

[105] Luo, J.H., Jiao, X.X., Li, N.B., and Luo, H.Q. Sensitive determination of Cd(II) by square wave anodic stripping voltammetry with in situ bismuth-modified multiwalled carbon nanotubes doped carbon paste electrodes. Journal of Electroanalytical Chemistry 689 (2013): 130-134.

[106] Li, Y., Sun, G., Zhang, Y., Ge, C., Bao, N., and Wang, Y. A glassy carbon electrode modified with bismuth nanotubes in a silsesquioxane framework for sensing of trace lead and cadmium by stripping voltammetry. Microchimica Acta 181(7) (2013): 751-757.

[107] Gerent, G.G., Gonçalves, C.Q., da Silva, P.S., and Spinelli, A. In situ bismuth-film electrode for square-wave cathodic voltammetric detection of pendimethalin at nanomolar level. Electrochimica Acta 168 (2015): 379-385.

[108] Wang, X., Chen, L., and Chen, L. Colorimetric determination of copper ions based on the catalytic leaching of silver from the shell of silver-coated gold nanorods. Microchimica Acta 181(1) (2013): 105-110.

[109] Hassanzadeh, R., Abbasnejad, A., and Hamzeh, M.A. Assessment of groundwater pollution in Kerman Urban areas. Journal of Environmental Studies 36(56) (2011): 101-110.

[110] Nriagu, J. Zinc Toxicity in Humans [Online]. 2007. Available from: http://www.extranet.elsevier.com/homepage_about/mrwd/nvrn/Zinc%20Toxicity%20in%20Humans.pdf

[111] Mandour, R.A. and Azab, Y.A. Toxic levels of some heavy metals in drinking groundwater in Dakahlyia Governorate, Egypt in the year 2010. International Journal of Occupational and Environmental Medicine 2(2) (2011): 112-117.

[112] Sreenivasa Rao, K., Balaji, T., Prasada Rao, T., Babu, Y., and Naidu, G.R.K. Determination of iron, cobalt, nickel, manganese, zinc, copper, cadmium and lead in human hair by inductively coupled plasma-atomic emission spectrometry. Spectrochimica Acta Part B: Atomic Spectroscopy 57(8) (2002): 1333-1338.

[113] Ammann, A.A. Speciation of heavy metals in environmental water by ion chromatography coupled to ICP–MS. Analytical and Bioanalytical Chemistry 372(3) (2001): 448-452.

[114] Nagles, E., Arancibia, V., Rojas, C., and Segura, R. Nafion–mercury coated film electrode for the adsorptive stripping voltammetric determination of lead and cadmium in the presence of pyrogallol red. Talanta 99 (2012): 119-124.

[115] Güell, R., Aragay, G., Fontàs, C., Anticó, E., and Merkoçi, A. Sensitive and stable monitoring of lead and cadmium in seawater using screen-printed electrode and electrochemical stripping analysis. Analytica Chimica Acta 627(2) (2008): 219-224.

[116] Oliveira, M.F., Saczk, A.A., Okumura, L.L., Fernandes, A.P., Moraes, M., and Stradiotto, N.R. Simultaneous determination of zinc, copper, lead, and cadmium in fuel ethanol by anodic stripping voltammetry using a glassy carbon–mercury-film electrode. Analytical and Bioanalytical Chemistry 380(1) (2004): 135-140.

[117] da Silva, L.C. and Masini, C.J. Determination of Cu, Pb, Cd, and Zn in river sediment extracts by sequential injection anodic stripping voltammetry with thin mercury film electrode. Fresenius' Journal of Analytical Chemistry 367(3): 284-290.

[118] Rojahn, T. Determination of copper, lead, cadmium and zinc in estuarine water by anodic-stripping alternating-current voltammetry on the hanging mercury drop electrode. Analytica Chimica Acta 62(2) (1972): 438-441.

[119] Wang, J. Real-time electrochemical monitoring: toward green analytical chemistry. Accounts of Chemical Research 35(9) (2002): 811-816.

[120] Wang, J., Lu, J., Hocevar, S.B., Farias, P.A.M., and Ogorevc, B. Bismuth-coated carbon electrodes for anodic stripping voltammetry. Analytical Chemistry 72(14) (2000): 3218-3222.

[121] Economou, A. Bismuth-film electrodes: recent developments and potentialities for electroanalysis. TrAC Trends in Analytical Chemistry 24(4) (2005): 334-340.

[122] Christos, K. and Anastasios, E. Stripping Analysis at Bismuth-Based Electrodes. Current Analytical Chemistry 4(3) (2008): 183-190.

[123] Kefala, G., Economou, A., Voulgaropoulos, A., and Sofoniou, M. A study of bismuth-film electrodes for the detection of trace metals by anodic stripping

voltammetry and their application to the determination of Pb and Zn in tapwater and human hair. Talanta 61(5) (2003): 603-610.

[124] Wonsawat, W., Chuanuwatanakul, S., Dungchai, W., Punrat, E., Motomizu, S., and Chailapakul, O. Graphene-carbon paste electrode for cadmium and lead ion monitoring in a flow-based system. Talanta 100 (2012): 282-289.

[125] Wei, H., et al. Enhanced electrochemical performance at screen-printed carbon electrodes by a new pretreating procedure. Analytica Chimica Acta 588(2) (2007): 297-303.

[126] Honeychurch, K.C., Hart, J.P., and Cowell, D.C. Voltammetric behavior and trace determination of lead at a mercury-free screen-printed carbon electrode. Electroanalysis 12(3) (2000): 171-177.

[127] Li, D. and Kaner, R.B. Graphene-based materials. Science 320(5880) (2008): 1170-1171.

[128] Guo, S. and Dong, S. Graphene and its derivative-based sensing materials for analytical devices. Journal of Materials Chemistry 21(46) (2011): 18503-18516.

[129] Armand, M., Endres, F., MacFarlane, D.R., Ohno, H., and Scrosati, B. Ionic-liquid materials for the electrochemical challenges of the future. Nat Mater 8(8) (2009): 621-629.

[130] Niu, X., Zhao, H., and Lan, M. Disposable screen-printed antimony film electrode modified with carbon nanotubes/ionic liquid for electrochemical stripping measurement. Electrochimica Acta 56(27) (2011): 9921-9925.

[131] Wang, Z., Wang, H., Zhang, Z., and Liu, G. Electrochemical determination of lead and cadmium in rice by a disposable bismuth/electrochemically reduced graphene/ionic liquid composite modified screen-printed electrode. Sensors and Actuators B: Chemical 199 (2014): 7-14.

[132] Bagheri, H., Afkhami, A., Khoshsafar, H., Rezaei, M., Sabounchei, S.J., and Sarlakifar, M. Simultaneous electrochemical sensing of thallium, lead and mercury using a novel ionic liquid/graphene modified electrode. Analytica Chimica Acta 870 (2015): 56-66.

[133] Amini, N., Gholivand, M.B., and Shamsipur, M. Electrocatalytic determination of traces of insulin using a novel silica nanoparticles-Nafion modified glassy carbon electrode. Journal of Electroanalytical Chemistry 714–715 (2014): 70-75.

[134] Bhat, M.A., Dutta, C.K., and Rather, G.M. Exploring physicochemical aspects of N-alkylimidazolium based ionic liquids. Journal of Molecular Liquids 181 (2013): 142-151.

[135] Kalcher, K., Švancara, I., Metelka, R., Vytřas, K., and Walcarius, A. Heterogeneous carbon electrochemical sensors. Encyclopedia of Sensors 4 (2006): 283–430.

[136] Svancara, I., Kalcher, K., Walcarius, A., and K, V. Electroanalysis with Carbon Paste Electrodes. Vol. 2012, 2012.

[137] Xu, F., Wang, F., Yang, D., Gao, Y., and Li, H. Electrochemical sensing platform for L-CySH based on nearly uniform Au nanoparticles decorated graphene nanosheets. Materials Science and Engineering: C 38 (2014): 292-298.

[138] Wang, J. Stripping Analysis at Bismuth Electrodes: A Review. Electroanalysis 17(15-16) (2005): 1341-1346.

[139] Palchetti, I., Laschi, S., and Mascini, M. Miniaturised stripping-based carbon modified sensor for in field analysis of heavy metals. Analytica Chimica Acta 530(1) (2005): 61-67.

[140] Fu, L., Li, X., Yu, J., and Ye, J. Facile and simultaneous stripping determination of zinc, cadmium and lead on disposable multiwalled carbon nanotubes modified screen-printed electrode. Electroanalysis 25(2) (2013): 567-572.

[141] Ruecha, N., Rodthongkum, N., Cate, D.M., Volckens, J., Chailapakul, O., and Henry, C.S. Sensitive electrochemical sensor using a graphene–polyaniline nanocomposite for simultaneous detection of Zn(II), Cd(II), and Pb(II). Analytica Chimica Acta 874 (2015): 40-48.

[142] Li, Y., et al. Simultaneous determination of ultra-trace lead and cadmium at a hydroxyapatite-modified carbon ionic liquid electrode by square-wave stripping voltammetry. Sensors and Actuators B: Chemical 139(2) (2009): 604-610.

[143] Es'haghi, Z., Heidari, T., and Mazloomi, E. In situ pre-concentration and voltammetric determination of trace lead and cadmium by a novel ionic liquid

mediated hollow fiber-graphite electrode and design of experiments via Taguchi method. Electrochimica Acta 147 (2014): 279-287.

[144] Zhang, P., Dong, S., Gu, G., and Huang, T. Simultaneous determination of Cd^{2+}, Pb^{2+}, Cu^{2+} and Hg^{2+} at a carbon paste electrode modified with ionic liquid-functionalized ordered mesoporous silica. Seoul, COREE, REPUBLIQUE DE: Korean Chemical Society, 30 (2010): 2949-2954.

[145] Promphet, N., Rattanarat, P., Rangkupan, R., Chailapakul, O., and Rodthongkum, N. An electrochemical sensor based on graphene/polyaniline/polystyrene nanoporous fibers modified electrode for simultaneous determination of lead and cadmium. Sensors and Actuators B: Chemical 207, Part A (2015): 526-534.

[146] Bose, S., Kuila, T., Mishra, A.K., Rajasekar, R., Kim, N.H., and Lee, J.H. Carbon-based nanostructured materials and their composites as supercapacitor electrodes. Journal of Materials Chemistry 22(3) (2012): 767-784.

[147] Aboutalebi, S.H., et al. Comparison of GO, GO/MWCNTs composite and MWCNTs as potential electrode materials for supercapacitors. Energy & Environmental Science 4(5) (2011): 1855-1865.

[148] Biswas, C. and Lee, Y.H. Graphene versus carbon nanotubes in electronic devices. Advanced Functional Materials 21(20) (2011): 3806-3826.

[149] Liu, C., Alwarappan, S., Chen, Z., Kong, X., and Li, C.-Z. Membraneless enzymatic biofuel cells based on graphene nanosheets. Biosensors and Bioelectronics 25(7) (2010): 1829-1833.

APPENDIX

VITA

Mr. Sudkate Chaiyo was born in Angthong, Thailand, on February 22, 1987. After completing his degree at Sriprachan methipramuk school, Suphanburi, Thailand, in 2005, he entered Suansunanta Rajabhat University, Bangkok, Thailand, receiving the degree of Bachelor of Science, majoring in Chemistry in December, 2008. He entered The Graduate School in the Department of Chemistry at Srinakarinwirot University, Bangkok, Thailand, in May 2009, receiving a Master's of Science degree in March 2012. In 2013, he received scholarship from Thailand through The Jubilee PhD, Program (RGJ-Ph.D.), he was a visiting scholar at Electroanalysis and Sensorics group, Analytical Chemistry Department, from Karl Franzens Universität Graz, Austria.